LEAN BURN AND STRATIFIED COMBUSTION STRATEGIES FOR SMALL UTILITY ENGINES

by

CHANDAN MAHATO

A DISSERTATION

Submitted in partial fulfillment of the requirements
for the degree of Doctor of Philosophy in the
Department of Mechanical Engineering
in the Graduate School of
The University of Alabama

TUSCALOOSA, ALABAMA

2010

ABSTRACT

The research presented in this thesis is an effort to improve small engine combustion through the application of lean combustion.

The first part of the research is focused on conducting an experimental investigation into the application of lean burn strategy on a single cylinder OHV utility engine to reduce engine-out emissions and at the same time maintain acceptable cyclic variability in combustion. The parameters of interest to investigate cyclic variability in combustion were spark plug variations, load control and charge stratification. The main findings showed that the spark discharge energy had a major influence on engine performance. It was also found that the engine can be operated at a high volumetric efficiency and very lean AFR at 75% and 50% load by the use of fuel injection. This is especially helpful for small engines operating on the EPA B-cycle.

The second part of the research deals with the study of a Flat head, also known as side valve (SV) engine platform. A novel approach to lean combustion in a flat head engine is proposed by directly injecting gasoline fuel into the combustion chamber. The main advantage of the direct injection flat head (DIFH) engine over the conventional OHV GDI engine is its simplicity in design, low cost and, greater flexibility in placement of key engine performance hardware in the cylinder head. To first understand the behavior of the in-cylinder air motion, the air-flow structure developing within the combustion

chamber was investigated using PIV techniques. The results show that squish is the dominant turbulence generating mean flow structure in the combustion chamber of the DIFH engine. Although the DIFH engine produced about 8 times more UHC emissions as compared to the conventional spark ignited OHV engines, it produced about 5 times less CO emissions as compared to the OHV engine and showed a 16% improvement in brake specific fuel consumption. The current combustion chamber has a dual chamber design exhibiting different combustion mechanisms in both the chambers, causing complex undesirable interactions between key engine performance parameters. Based on these fundamental studies a new combustion chamber design is presented for better performance.

DEDICATION

To my little buddy

Aarush Aritra

my wife and parents.

One should, perform karma with nonchalance without expecting the benefits because sooner or later one shall definitely get the fruits.

LIST OF ABBREVIATIONS AND SYMBOLS

A	Ampere
ABDC	After Bottom Dead Center
AC	Alternating Current
AFR	Air-Fuel Ratio
ATDC	After Top Dead Center
BTDC	Before Top Dead Center
C	Capacitance
CAD	Crank Angle Degrees
CARB	California Air Resource Board
CDI	Capacitive Discharge Ignition
CI	Compression Ignition
CO_2	Carbon dioxide
COV	Coefficient of Variation
COV_{IMEP}	Coefficient of Variation of indicated mean effective pressure
CO	Carbon Monoxide
CR	Compression Ratio
DOE	Design of Experiment
DIFH	Direct Injection Flat Head

d_p	Tracer particle diameter
EFI	Electronic Fuel Injection
EGR	Exhaust Gas Recirculation
EMS	Engine Management System
EPA	Environmental Protection Agency
E_{sp}	Spark Energy
GDI	Gasoline Direct Injection
HC	Hydrocarbon
hr	Hour
HWA	Hot Wire Anemometry
IC	Internal Combustion
IMEP	Indicated Mean Effective Pressure
I_{sp}	Measured current in the secondary coil
K	Kelvin
kV	Kilovolts
kW	Kilowatts
LDV	Laser Doppler Anemometry
L_I	Integral length scale
L_M	Taylor microscale
MBT	Minimum Advance for best Torque
mm	Millimeter
ms	Milliseconds
Nd-YAG	Neodymium-doped yttrium aluminium garnet; Nd:$Y_3Al_5O_{12}$

NIMEP	Net Indicated Mean Effective Pressure
NO	Nitric Oxide
NO_x	Oxides of Nitrogen
NO_2	Nitrogen dioxide
ns	Nanosecond
N_s	Stokes number
OEM	Original Equipment Manufacturer
OHV	Overhead Valve
PCT	Patent Cooperation Treaty
PFI	Port Fuel Injection
pF	Picofarad
PIV	Particle Image Velocimetry
PTV	Particle Tracking Velocimetry
P_{max}	Peak cylinder pressure
q	Normalized particle diameter
SA	Spark Advance
SI	Spark Ignition
SV	Side Valve
TC	Top center of piston travel
TTL	Transistor-Transistor Logic
u’	Turbulence intensity
UEGO	Universal Exhaust Gas Oxygen Sensor
UHC	Unburned Hydrocarbon

V	Volts
V_b	Breakdown voltage
V_{sp}	Voltage in the secondary coil
2S	Two Stroke
4S	Four Stroke
θ_{Pmax}	Crank angle at which peak pressure occurs
$(dP/d\theta)_{max}$	Maximum rate of pressure rise
$\theta_{(dP/d\theta)max}$	Crank angle at which maximum rate of pressure rise occurs
σ_{IMEP}	Standard deviation of indicated mean effective pressure
$\Delta\theta_d$	Ignition delay
Φ	Equivalence ratio (phi)
µs	Microseconds
ρ_p	Particle density
ρ_f	Fluid density
ν	Fluid kinematic viscosity
ω	Angular frequency of flow fluctuations
λ	Wavelength
µm	Micrometer
Δt	Time interval between two laser pulses
95% CI	95% Confidence Interval

ACKNOWLEDGEMENTS

I am pleased to have this opportunity to thank the many colleagues, friends, and faculty members who have helped me with this dissertation. I am most indebted to my advisor Dr. Clark Midkiff, for sharing his expertise and wisdom in engine research. He encouraged me to look into new ideas, the result of which was a patent on a novel engine design. I would like to take this opportunity to thank Dr. Paul Puzinauskas for co-advising me in my research. From him I learned many practical aspects of engine operation and design. I would also like to thank all of my committee members, Dr. John Baker, Dr. Marcus Ashford, and Dr. Nagy El-Kaddah for their invaluable input, inspiring questions, and support of both the dissertation and my academic progress.

Special thanks to Mr. Ken Dunn, Jim Edmonds, Sam Tingle and James Yarbrough in the machine shop for their time and invaluable advice during building my experimental setup. Mr. Barry Johnson, thank you for helping me build my experiments. I would also like to thank Ms. Pamelia Beddingfield, Ms. Lynn Hamric and, Ms. Betsy Singleton in the Mechanical engineering department and Ms. Sherry Barrow from the Center for Advanced Vehicle Technologies for all the help they extended during my research.

This research would not have been possible without the support of my friends and fellow graduate students. I would like to thank Dr. Sundar Rajan Krishnan, Dr. Kalyan Srinivasan, Mr. Raju Dantuluri, Jennifer Beasley Smelser, Drabo Mebougna, Siddharth Bhattacharya, Ravikiran Chaudhary and, Kendrick Gibson for their help during my experiments.

Last but not least, my family who never stopped encouraging me to persist. More than me it is my parent's dream come true that I have made such accomplishments. I cannot thank enough to my wife Simpla who provided unconditional support through all hard times. I would not do justice if I fail to mention her help in conducting my experiments during my research. My special thanks to my sister Seema and my brother in-law Niadri for their great encouragement and keen interest in my research. Also many thanks to all my family members and friends.

CONTENTS

ABSTRACT……ii

DEDICATION……iv

LIST OF ABBREVIATIONS AND SYMBOLS……v

ACKNOWLEDGEMENTS……ix

LIST OF TABLES……...xiii

LIST OF FIGURES…… ...xiv

1. INTRODUCTION……..….1

a. Overview……..…..1

b. Background on Lean Combustion…….....…3

I. Indicators of cyclic variability……3

II. Development of combustion process……..5

III. Factors affecting cyclic variability of combustion……11

i. Mixture composition……..11

ii. In-cylinder mixture motion……14

iii. Spark and spark plug effects……..20

c. Dissertation Organization…….....23

2. LEAN BURN OPTIMIZATION STRATEGIES IN SPARK IGNITED SMALL ENGINES ……..26

3. THE DIRECT INJECTION FLAT HEAD (DIFH) ENGINE – A NOVEL APPROACH TO LEAN COMBUSTION……..…63

4. EXPERIMENTAL INVESTIGATION OF THE DIRECT INJECTION FLAT HEAD (DIFH) COMBUSTION SYSTEM AND QUANTIFICATION OF IN-CYLINDER FLOW USING TWO DIMENSIONAL PARTICLE IMAGE VELOCIMETRY……..……83

5. SUMMARY AND CONCLUSIONS……136

a. Overview……..136

b. Summary……..136

c. Conclusions……..138

d. Future Work…….141

REFERENCES……143

LIST OF TABLES

1. Summary of modified test engine……..……..…..37

2. EPA/CARB 6-mode SORE test cycle……...…….38

3. Design of Experiment……38

4. Dwell table interpolated for all break points…….....….40

5. Spark plug specifications…….……..….40

6. Engine operating conditions……..……47

7. Strategies to optimize ($HC+NO_x$) and CO emissions…….……...60

8. Factors and levels for DOE……..103

LIST OF FIGURES

1. Current and voltage characteristics of the discharge from a typical coil ignition system [7]……..…….…..……..9

2. Reaction front speeds for different fuels [Young, 1981]……...13

3. Principles of flamelet assumption……...18

4. Smog formation mechanism……...…….....28

5a. Honda GX series cylinder head with inclined intake and exhaust valves……..…31

5b. Top view of cylinder head showing spark at the periphery of combustion chamber……..……...31

6. Throttle body with fuel injection system……...36

7. Schematic of experimental setup…….....38

8. J-type spark plugs with thick and thin electrodes……..……41

9. Interval plot of ignition energy vs. engine mode and spark plug type; 0.75 mm spark gap.. 43

10. Interval plot of ignition energy vs. electrode gap; engine mode 3, OEM spark plug.……...……...43

11. Interval plot of breakdown voltage vs. spark plug type and engine mode; 0.75 mm electrode gap.……...……....45

12. Interval plot of breakdown voltage vs. electrode gap; OEM spark plug……..…...…45

13. Interval plot of 0-10% burn duration vs. spark plug type and engine mode…….……..49

14. Interval plot of 0-10% burn duration vs. electrode gap and engine mode; OEM spark plug.……...……..……49

15. Interval plot of 10-90% burn duration vs. spark plug type and engine mode.……..50

16. Interval plot of 10-90% burn duration vs. electrode gap and engine mode; OEM spark plug.……..……..50

17. Interval plot of cov torque (%) vs. spark plug type and engine mode.…….……..51

18. Interval plot of cov torque (%) vs. electrode gap and engine mode; OEM spark plug.……..……...51

19. Interval plot of cylinder head temp (deg C) vs. engine mode.……...…54

20. Interval plot of air mass flow rate (lb/hr) vs. engine mode.……..…….54

21. Plot of injector fuel flow rate (lb/hr); OEM (low flow) vs. high flow.……..55

22. Plot of burn duration; OEM vs. high flow injector……55

23. Interval plot of ($HC+NO_x$) (g/kW) vs. spark plug type, electrode gap…….…….56

24. Interval plot of CO (g/kW) vs. spark plug type, electrode gap.……..……...56

25. Interval plot of cov torque (%) vs. spark plug type, electrode gap ….....57

26. Interval plot of ($HC+NO_x$)(g/kW) vs. injector type, electrode gap……...57

27. Interval plot of CO (g/kW) vs. injector type, electrode gap.…….58

28. Interval plot of cov torque (%) vs. injector type, electrode gap ……..……58

29. Interval plot of cov torque (%) vs. engine configuration, engine mode ...…….……..59

30. Cross sectional view of DIFH engine……..……..…80

31. Plan view of DIFH cylinder block…….…81

32. Plan view of DIFH cylinder head……..……82

33. Cross-section of the DIFH engine…….86

34. Schematic diagram of the DIFH cylinder head…….87

35. Evaluation of PIV recordings using auto-correlation [54]…….……93

36. Evaluation of PIV recordings using cross-correlation [54]…….……..93

37. Top view of the optical cylinder head……97

38. Experimental setup showing the engine, laser/camera system and, seeding system…….…….....98

39. Snapshot of PIV image and cylinder pressure measurement…….....99

40. Plane of interest at which PIV measurements are made…….....100

41. DIFH engine valve lift profile……..100

42. Velocity vector plot of 0^{o} ATDC intake stroke……...108

43. Velocity vector plot of 45^{o} ATDC intake stroke…….....109

44. Velocity vector plot of 90^{o} ATDC intake stroke……...……..110

45. Velocity vector plot of 135^{o} ATDC intake stroke……..…….111

46. Velocity vector plot of 180^{o} ATDC intake stroke (BDC compression)……112

47. Velocity vector plot of 45^{o} ABDC compression stroke……...113

48. Velocity vector plot of 90^{o} ABDC compression stroke……...…114

49. Velocity vector plot of 135^{o} ABDC compression stroke…….115

50. Velocity vector plot of 180^{o} ABDC compression stroke…….116

51. Interval plot of cov (nimep) vs. compression ratio, injector location, spark plug location……...117

52. Interval plot of 0-10% burn duration vs. compression ratio, injector location, spark plug location…….…..……117

53. Main effects plot (data means) for power, 8:1 compression ratio.…...……...118

54. Interaction plot (data means) for power, 8:1 compression ratio.…….121

55. Main effects plot (data means) for HC, 8:1 compression ratio.…….....121

56. Main effects plot (data means) for NO_x, 8:1 compression ratio.……122

57. Main effects plot (data means) for ($HC+NO_x$) ...……..…….122

58. Main effects plot (data means) for CO.…….……..123

59. Interval plot of HC vs fuel pressure. Error bars are one standard error from the mean…….....128

60. Interval plot of power, injector location over exhaust valve, spark plug location over exhaust valve……...…….128

61. Interval plot of power, injector location over exhaust valve, spark plug location over intake valve……..129

62. Interval plot of power, injector location over intake valve, spark plug location over exhaust valve……129

63. Interval plot of power, injector location over intake valve, spark plug location over intake valve……..130

64. Histogram of power.…….…...130

65. Interval plot of ($HC+NO_x$) vs engine configuration, optimized at modes 3, 4, and 5 power levels. Error bars are one standard error from the mean……...……..131

66. Interval plot of CO vs engine configuration, optimized at modes 3, 4, and 5 power levels. Error bars are one standard error from the mean.……131

67. Interval plot of bsfc vs engine configuration, optimized at modes 3, 4, and 5 power levels. Error bars are one standard error from the mean…….....132

68. Proposed DIFH combustion chamber design…….133

CHAPTER 1

INTRODUCTION

Overview

With the growing intensification of emissions regulations on energy derived from fossil fuels, small engines operating on gasoline have come under greater scrutiny in the recent years than before. Small engines can be classified as spark-ignition (SI) non-road engines rated below 25 horsepower (19 kW) used in household and commercial applications, including lawn and garden equipment, utility vehicles, generators, and a variety of other construction, farm, and industrial equipment. Engine sales for small engine powered utility equipment exceed car engine sales by about 100 to 1000 times. Although cars operate on an average about a 1000 times more number of hours than small engines, the latter are in total a greater source of regulated emissions than automotive engines [1].

Conventionally small engines have been manufactured based on the two stroke (2S) cycle, four stroke (4S) cycle with overhead valves (OHV) and 4S cycle with side valves (SV). The 2S engines are in the process of being replaced by 4S engines because of their higher engine-out emissions. The 4S-SV engines, though not as clean as the 4S-OHV engines in terms of engine-out emissions, are still currently produced because they have

lower manufacturing costs and a simpler design, however upcoming/current emission restrictions make long term prospects for these engines poor.

The recent attention to small engine emissions has created a new opportunity for researchers to investigate and incorporate new strategies for operating small engines, which forms the focus of this dissertation. This research is categorized by the three following chapters. The first chapter focuses on strategies for lean burn in a conventional 4S-OHV SI engine. In the next two chapters of the research a novel approach to apply direct injection of fuel into the combustion chamber of a 4S-SV SI engine is investigated. All of the research sections presented in this thesis are based on an effort to improve small engine combustion through the application of lean combustion. Because it forms a common thread to all parts of the research, information on lean combustion is presented in this first introductory chapter, and detailed discussions are presented in the individual chapters as appropriate. The three research chapters that follow this introductory chapter are as given below;

Chapter 2: Lean Burn Optimization Strategies in Spark Ignited Small Engines.

Chapter 3: The Direct Injection Flat Head (DIFH) engine – A novel approach to lean combustion.

Chapter 4: Experimental investigation of the Direct Injection Flat Head (DIFH) combustion system and quantification of in-cylinder flow using two dimensional Particle Image Velocimetry.

Finally, the dissertation is concluded with Chapter 5, which presents a summary of the research and some overall conclusions, as well as suggestions for future work.

Background on lean combustion

The focus of this work is to study the important parameters that affect lean combustion in internal combustion (IC) engines. Lean combustion in an IC engine increases the efficiency but is often limited by the onset of unacceptable cyclic variations in the overall combustion rate. As the equivalence ratio of homogeneous mixtures is moved lean of stoichiometric the associated changes in mixture property favor increased engine efficiency. However corresponding decrease in heat release rates cause large cycle to cycle variation in power output and ultimately, misfire overwhelms the advantage in lean mixture properties. The background discussion is mainly focused on three parts related to cyclic variability of combustion; indicators of cyclic variability, development of the combustion process, and factors affecting the cyclic variability of combustion. These are discussed in detail as follows.

Indicators of cyclic variability

One current focus of research in spark ignition engine technology is the lean burn strategy. It is widely recognized that cyclic variability is the defining parameter that limits the operating range of SI engines, particularly under highly diluted operating conditions obtained with either lean mixtures or through the use of EGR.

Cyclic variations are defined as intercyclic differences in the cylinder pressure history, and in the absence of mechanical malfunction are caused by cycle-to-cycle variations in the combustion process. Even during steady state operation, two consecutive cycles are not identical. They reveal random variations in the combustion process in terms of variations in peak pressure, indicated mean effective pressure (IMEP),

rate of heat release, ignition delay, etc. These variations are more noticeable under low load conditions and with the use of charge dilution by exhaust gas recirculation (EGR). Cyclic variations can lead to a situation where one cycle is fast burning while the next is very slow. The fast burning cycles can lead to very high in-cylinder peak pressures and engine knock tendency, imposing the lower limit for fuel octane number and upper limit for the compression ratio. The combustion may not proceed to completion before the exhaust valve opens in the slower burning cycles thereby leading to very low in-cylinder peak pressures and unburned hydrocarbon (UHC) emissions. This lowers the work output of that particular cycle and also increases the fuel consumption [2].

The parameters that can be used as indicators of cycle by cycle variation are; in-cylinder peak pressure (P_{max}), crank angle at which peak pressure (θ_{Pmax}) occurs and, indicated mean effective pressure (IMEP). They can all be directly obtained from the cylinder pressure data. The ease of measurement of cylinder pressure makes it and its related parameters the popular choice for studying cyclic variability. It has been shown in previous studies that P_{max} and θ_{Pmax} are both very sensitive to ignition timing and show little variation as the ignition timing approaches MBT (minimum spark timing advance for best torque). Similar results have been reported about variation in IMEP with respect to ignition timing and have been the point of debate whether IMEP or P_{max} is the best indicator of cyclic variability. From a practical standpoint the effect of cyclic variability in the combustion process is reflected in degraded engine smoothness, increased fuel consumption and engine-out emissions. A widely accepted method of measuring cyclic variability is through the coefficient of variation (COV) of the indicated mean effective pressure, expressed as [2];

$$COV_{IMEP} = \frac{\sigma_{IMEP}}{IMEP} \times 100\% \quad (1)$$

where σ is the standard deviation.

Other parameters that have been used as indicators of cyclic variability are related to the flame front during combustion. These parameters can be categorized as flame entrained volume at a specific crank position, the flame front position, time taken by the flame front to travel between two pre-specified locations in the cylinder, and flame kernel displacement from spark gap at different crank angles. Flame front related parameters are usually measured by either visual techniques or ionization gap techniques. By using these techniques, important information regarding the flame kernel development can be obtained such as flame kernel convection velocity and direction, the rate and extent of flame front wrinkling and the rate of flame kernel radius growth [2]. The effect of variations in flame front related parameters gain more significance in lean combustion and in combustion chamber shapes that induce turbulent in-cylinder fluid flows. Unfortunately, the techniques required to obtain these important pieces of information are complicated, expensive and, often limited by the extensive engine modifications required to provide the associated necessary access to the combustion chamber to implement them.

Development of combustion process

To understand limitations of lean combustion it is imperative to gain insight into the combustion development process. In a spark ignition engine the combustion process is comprised of four distinct stages. The first stage is the sparking and flame initiation stage followed by the initial flame kernel development stage. The third stage is the turbulent

flame propagation stage. The last stage of flame termination is not believed to have significant impact on the cyclic variability of the combustion process, therefore, can be discounted in the current discussion.

The sparking in the electrode gap of a spark plug is characterized by a rise in the voltage between the electrodes followed by an electrical breakdown in the spark gap. This leads to the development of a plasma kernel in the spark gap. The whole sparking process can be divided into three phases defined as the breakdown phase, the arc phase and the glow discharge phase, as shown in figure 1. The breakdown phase lasts for an extremely short period of time of the order of 10^{-8} s [3, 5]. The high energy transfer efficiency of the breakdown phase is what makes it better suited for ignition than the arc or the glow phase. Also, an increase in breakdown energy effectively increases the original flame size more than do the arc or glow phases [6]. The breakdown phase is characterized by a high electrical potential difference between the electrodes of the spark plug which causes the breakdown of the intermediate mixture between the spark plug electrodes. These ionizing streamers cross the path between the electrodes establishing the path for current flow. The duration of this phase lasts about 10 ns with a high voltage and peak current of about 10 kV and 200 A respectively. During this phase the plasma kernel, which is at a very high temperature of about 40,000 K and a very high pressure of a few hundred atmospheres, expands forming the shape of the initial flame kernel prior to flame propagation [5, 7]. Because the energy losses during this phase due to heat transfer to the electrodes are very small, most of the deposited energy is consumed for kernel growth. The plasma kernel creates a hot spot on the cathode (center electrode) which initiates the next phase i.e., the arc phase. This phase lasts for several hundred

microseconds and the temperature of the plasma drops due to expansion and heat transfer to the electrodes [3, 7]. At this stage the spark characteristics are affected by the external flow field such as the mean velocity in the vicinity of the spark gap and its direction. The discharge channel in the spark gap is stretched due to this flow field causing the spark duration to be shorter while depositing higher energy into the spark [8]. Although the current flow during the arc phase is still high, the voltage is very low, about 100 V. The arc phase lasts longer than the breakdown phase, depositing more energy than the latter, but can exist only till the hot spot on the cathode exits. Because of this, significant energy is lost to the electrodes. In this phase the outer surface of the flame kernel at a temperature range of 1000 to 5000 K provides a conducive environment for the active radicals to interact with the ignitable mixture through diffusion and initiate the combustion process, marking the beginning of the flame propagation phase. The glow phase is the last phase of the sparking process. Depending on the type of ignition system it may last from a few milliseconds (inductive spark) to almost negligible duration (capacitive discharge) [3]. Almost 90% of the total spark energy is deposited in this phase, although about 70% of the total spark energy is lost to the electrodes in this phase because of the cold cathode and higher surface area of the flame in contact with the spark plug electrodes [3].

The sparking and flame initiation stage is followed by the initial flame kernel development stage. During this stage about 1-2% of the mass fraction is burned. After spark breakdown the kernel formed is roughly spherical in shape with a smooth surface. While the size of the kernel is smaller than the smallest eddies, it preserves its surface smoothness and grows by expansion and mass burning that occurs close to the laminar

burning value [8, 9]. The cyclic variability of the combustion during this period is mainly due to the local fluctuations in the equivalence ratio of the mixture, the extent of air-fuel mixture dilution and the local thermodynamic conditions. As the kernel size increases, its interactions with the turbulent eddies begin to wrinkle the kernel surface thereby increasing its surface area. The interaction between laminar and turbulent characteristics during flame kernel development is illustrated by the ignition delay correlation proposed by [2];

$$\Delta\theta_d = C\left(\frac{L_I}{u'}\right)^{1/3}\left(\frac{L_M}{S_L}\right)^{2/3} \tag{2}$$

where L_I, u', L_M and S_L are the integral length scale, the turbulence intensity, the Taylor microscale and the laminar flame speed, respectively. As can be seen from equation (2) the influence of the turbulence intensity is less as compared to that of the laminar flame speed. Therefore, the influence of the turbulence intensity on the cyclic variability of combustion is secondary at this stage. Before the plasma kernel reaches the size of the largest eddies, the kernel can be convected as a whole from the electrodes by the mean flow and the large scale fluctuations, and still not get detached from the electrodes. This movement of the kernel determines the instantaneous fraction of the kernel surface area that is in contact with the electrodes and the rest of the surface area that is not obstructed by any solid surface. The balance between these two surface areas determines the amount of heat lost to the electrodes from the kernel and the amount of heat released due to combustion, which determines the rate of kernel growth. During this stage an overly aggressive flow field may tear off the kernel from the electrodes and, hence, the power supply, thereby quenching the flame.

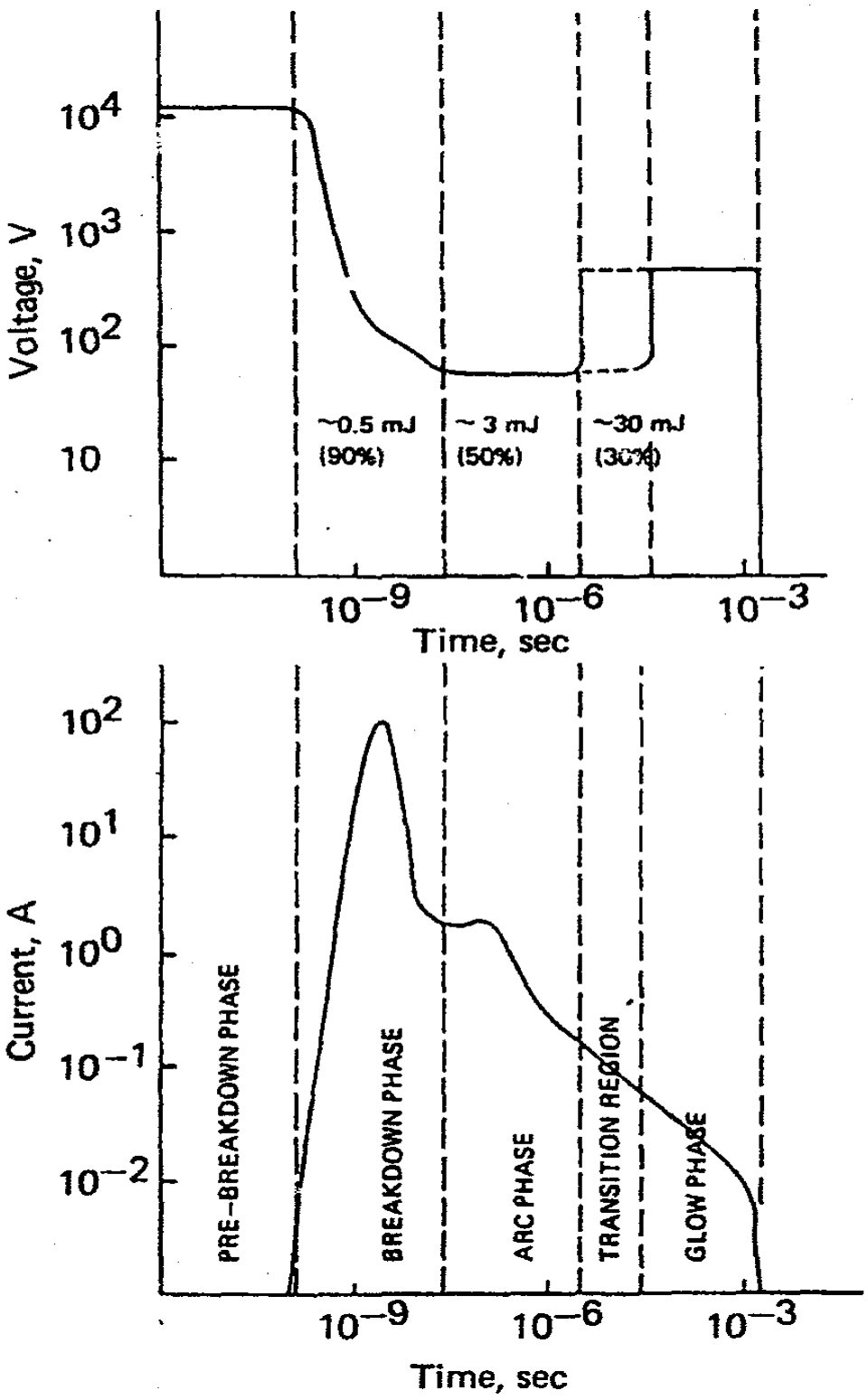

Figure 1: Current and voltage characteristics of the discharge from a typical coil ignition system [7].

When the kernel reaches a size such that it can be influenced simultaneously by the large eddies, it continues its growth into the turbulent flame propagation stage that is described in the next paragraph.

Turbulent flame propagation stage encompasses the period during which the main portion of the in-cylinder charge is burned. This is typically referred to as the 10-90% burn duration. Beyond this stage is the flame termination stage which occurs when the flame front reaches the cylinder walls and is quenched. At any instance, the burning rate is strongly dependent on the active flame front area. Previous observations have shown that the kernel growth is roughly spherical during the first few crank angles after the spark breakdown and can possibly have the greatest flame front area as it grows if it is located in an area central to the combustion chamber [10]. A higher flame front area translates to a higher burning rate; which, even if the kernel is subjected to higher convection due to the mean directed flow around the vicinity of the spark plug, does not deviate much from a spherical shape. Therefore, the spark plug location is an influencing factor in the turbulent flame propagation stage. The flame propagation is affected by the mixture laminar burning rate, which is a characteristic of the fuel air mixture and by the unburned charge entrainment into the flame front area which is generally controlled by the flow interactions with the combustion chamber and very specifically affected by the associated turbulent intensity. Therefore, the cyclic variability and associated lean combustion limits are strongly influenced by the interactive effects of spatial as well as cycle-to-cycle variations in equivalence ratio, charge dilution, temperature, mean flow and turbulence intensity. Those of these which most significantly affect cyclic variability are discussed in the next section.

Factors affecting cyclic variability of combustion

The factors affecting the cyclic variability of combustion can be broadly classified into the following categories;

1) Mixture composition
2) In-cylinder mixture motion
3) Spark and spark plug effects

Mixture composition:

The influence of the initial kernel development on the cyclic variability of combustion is directly influenced by the laminar burning velocity, which is a quality attribute of a fuel. In previous research experiments designed to measure the maximum laminar flame speed at different equivalence ratios for different fuels showed that the maximum value of laminar flame speed in the range of 40 m/sec to 55 m/sec occurred over a range of equivalence ratios from 1.0 to 1.45 for different fuels, as shown in figure 2 [2]. In another study, the flame development in the combustion chamber of a single cylinder engine was studied using propane and hydrogen fuels [12]. It was found that the laminar burning velocity of hydrogen was about 8 times higher than that of propane. This resulted in a higher burning rate and reduced time for the air-hydrogen mixture to reach a certain flame kernel size, the shape of the flame kernel remained close to spherical and centered at the spark gap. Furthermore and most significantly these parameters were observed to have low cycle-to-cycle variability relative to typical hydro-carbon fuels. These results are in agreement with the observation mentioned earlier that higher burning rates reduce the effect of in-cylinder mean motion during initial flame development stage.

Burning rates are also affected by the fuel mixture properties, higher heating value and equivalence ratio. Higher heating value affects the burning rates through higher adiabatic flame temperature which increases rates of chemical reaction and expansion of the burned gas. The equivalence ratio affects the combustion cyclic variability through the laminar flame speed. The laminar flame speed is the highest for equivalence ratios near stoichiometric to slightly enriched mixtures. The higher the laminar flame speed, the shorter is the ignition delay, thus faster burn rates are observed.

The amount of residuals remaining in the cylinder as a fraction of the fresh charge intake in a particular engine cycle is always finite because of the imperfect scavenging of the prior cycle. Results of a previous study show that increase of dilution of the fresh charge either with exhaust gas residuals or other gases caused increase in the cyclic variations in the pressure development [11]. In another research study, mixture samples were obtained from near the spark plug in successive cycles. Higher cyclic variability was observed for both, total unburned hydrocarbons (UHC) and carbon dioxide (CO_2), and concentrations increased as the extent of exhaust gas recirculation (EGR) increased [13]. One way to reduce charge dilution in the cylinder is by increasing the volumetric efficiency of the engine. Volumetric efficiency of an engine can be defined as the ratio of the volume of working substance admitted into the cylinder, measured at a specified temperature and pressure, to the full piston displacement volume. An increase of 5% volumetric efficiency leads to an increase of 13% in the mixture burning velocity [14]. The increase in volumetric efficiency not only effects better scavenging but also influences the thermodynamic properties of the mixture in terms of pressure, temperature and mixture specific heat.

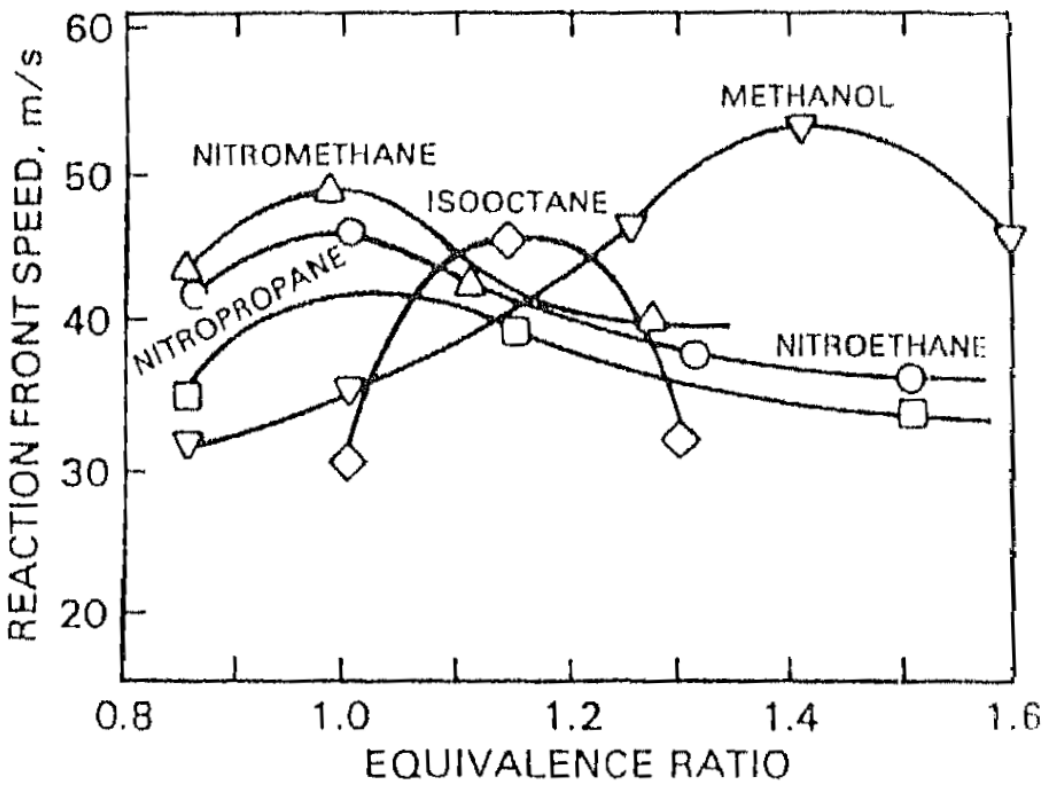

Figure 2: Reaction front speeds for different fuels [Young, 1981].

A lower burning rate in the initial stages of combustion was also observed when the compression ratio of an engine was reduced. This effect was attributed to increase in the residual fraction of the fresh charge with decrease in the compression ratio [15].

Although perfectly homogeneous air-fuel mixtures are typically assumed to exist within the combustion chambers of conventional SI engines, the process of fuel atomization and evaporation either by fuel injection or carburetion and subsequent mixing with combustion air is never perfect. Because of this it is possible at times that fuel droplets of non-negligible sizes remain in the cylinder up to ignition. Also imperfect mixing between mixture components including residuals and recirculated gases can lead

to spatial mixture inhomogeneity in the combustion chamber. Therefore, inhomogeneity in the air-fuel ratio (AFR) and the amount of diluents in the vicinity of the spark plug is not only present within a particular cycle, but the inhomogeneities can be different from cycle to cycle, causing cyclic variability in charge formation. One research study concluded that at lean conditions, a well-mixed propane-air mixture exhibited less cyclic variability than a carbureted indolene-air charge [16]. This was expected because propane is a gaseous fuel whereas indolene is a liquid fuel. In another study it was found that inhomogeneous mixtures containing fuel droplets can actually result in less cyclic variability in the cylinder pressure and reach lower lean misfire limit values than for well mixed gaseous mixtures. Lower mixture burning rate for the gaseous fuel was cited as the reason for the higher cyclic variability [17]. In-cylinder mixture inhomogeneity in the vicinity of the spark plug can be estimated by measuring mixture composition near the spark plug through gas analysis. In one study a gas sampling valve built-in to the spark plug was used to collect samples shortly after ignition. The concentrations of CO, CO_2, NO and UHC were measured through gas analysis from which the AFR of the sample was determined. Consecutive cycle pressure history diagrams were created along with mixture composition from the spark plug. The results showed that leaner air-fuel ratio near the spark gap resulted in longer heat release delay and lower IMEP in that cycle [18].

<u>In-cylinder mixture motion</u>:

The in-cylinder air/mixture motion of an IC engine is highly turbulent. Although we try to generalize the in-cylinder mixture motion by using parameters such as mean

velocity or bulk motion of flow, at the smallest level it is highly probabilistic in nature, which is a cause for cyclic variability. Turbulence is beneficial in that it accelerates combustion by increasing the flame front area and enhancing heat and mass transport between the burned and unburned mixture, effectively reducing cyclic variability of combustion. On the other hand turbulence can cause random variations in the equivalence ratio, degree of mixture dilution and in the mean velocity in the vicinity of the spark plug. These are important reasons for cyclic variability in the early kernel development stage [19, 20]. These phenomena are strongly affected by the combustion chamber shape, spark plug location and other design factors that vary from engine to engine.

Mean flow velocity near the spark plug is defined as the ensemble average of the velocity near the spark gap vicinity at the onset of the spark. During the sparking and flame initiation stage, the presence of a mean flow velocity in the vicinity of the spark gap lengthens the discharge channel and, therefore, provides a higher energy discharge into the plasma kernel during the breakdown phase. Later during the initial flame kernel development stage, the mean flow can effectively convect the flame kernel away from the electrodes thereby reducing the heat losses to the electrodes [21]. This may not be true if the ground electrode faces downstream of the mean air flow direction. In this situation, the flame kernel is convected towards the spark plug electrode by the mean air flow. This will lead to a larger surface area contact of the flame kernel with the spark plug electrode, causing increased energy losses from the flame kernel to the electrode through heat transfer. If the mean flow direction is such that it convects the flame kernel towards the combustion chamber walls, the flame kernel will experience heat losses to the cylinder walls. Lastly, if the flame kernel is convected towards the center of the combustion

chamber, then by increasing the flame front surface area higher rates of mass burn in the flame initiation stage can take place, which reduces ignition delay and increases flame kernel radius at a given crank angle [11]. The results of an investigation in which organized charge motion was introduced through a modified intake manifold showed a strong correlation between the flame expansion speed and the flame convection velocity. As mentioned earlier, the flame expansion speed is an indicator of the flame growth rate while the flame convection velocity describes its overall movement. Bianco et. al. explained that higher convection velocity caused larger flame stretching, which reduced heat losses to the electrodes by pushing the flame away from the spark gap, and higher turbulent fluctuations that increased the flame growth rate were caused by the higher bulk motion velocity [8].

Swirl, tumble and squish are the most common in-cylinder turbulence generating mean flow structures. It is also widely accepted that higher turbulence is beneficial to higher burning rate and lower cyclic variability of combustion. The energy release rate from combustion is dependent on the instantaneous mass burning velocity and the flame front area, both of which are influenced by turbulence. Turbulence increases the flame front area by wrinkling and corrugating the flamelets, which in turn increases the rate of entrainment of unburnt mass into the flame front, increasing burning rate. A flamelet regime is defined as an interface that separates the fresh unburnt reactants from the burned products, as shown in Figure 3. It is this interface that is a thin continuous region where chemical reactions occur. This concept of flamelet regimes is used in studies of premixed turbulent combustion. An important parameter under the flamelet assumption in turbulent combustion is flame stretch. Flame stretch controls the growth of the flame

surface area by flame surface production and flame quench, which occur simultaneously during turbulent combustion [22]. The idea of flame quench by flame overstretching is referred to at various sections in the discussion. Such an effect of turbulence on the flame kernel growth stage is beneficial. In the kernel growth stage the small size of the flame kernel can only be affected by eddies that are smaller than the flame kernel, thereby not creating too much stretching on the flame kernel. At this stage the large fluctuations can only convect the flame kernel as a whole. As the flame kernel radius increases, a larger spectrum of fluctuations starts influencing the flame kernel growth. While some of these fluctuations are beneficial to the kernel development, some eddies with higher velocities may locally quench the flame. The larger the turbulent intensity, the more the probability of such eddies to be present near the spark gap vicinity [23, 24, 25].

Turbulence generation not only results from the induction process of fresh charge into the cylinder and the subsequent breakdown during piston travel towards top center, it is also very dependent on the effects due to combustion. During the flame propagation process, the preflame gas experiences a large induced mean velocity in the direction of flame propagation due to the rapid expansion of the combustion products. The preflame gas is also associated with higher levels of turbulence due to the expanding combustion products. Thus the faster the burn rate, the higher is the turbulence in the preflame gas [26].

At this point it is worthwhile to carry forward the discussion on the overall effect of in-cylinder flow pattern on cyclic variability. As indicated above swirl, tumble and squish are the three main large-scale turbulence generating flow patterns in the engine cylinder. Swirl is the rotation of the charge about the cylinder axis. During tumble flow the charge

rotates about an axis perpendicular to the cylinder axis and squish forces the charge radially inward to the center of the combustion chamber at the end of the compression stroke.

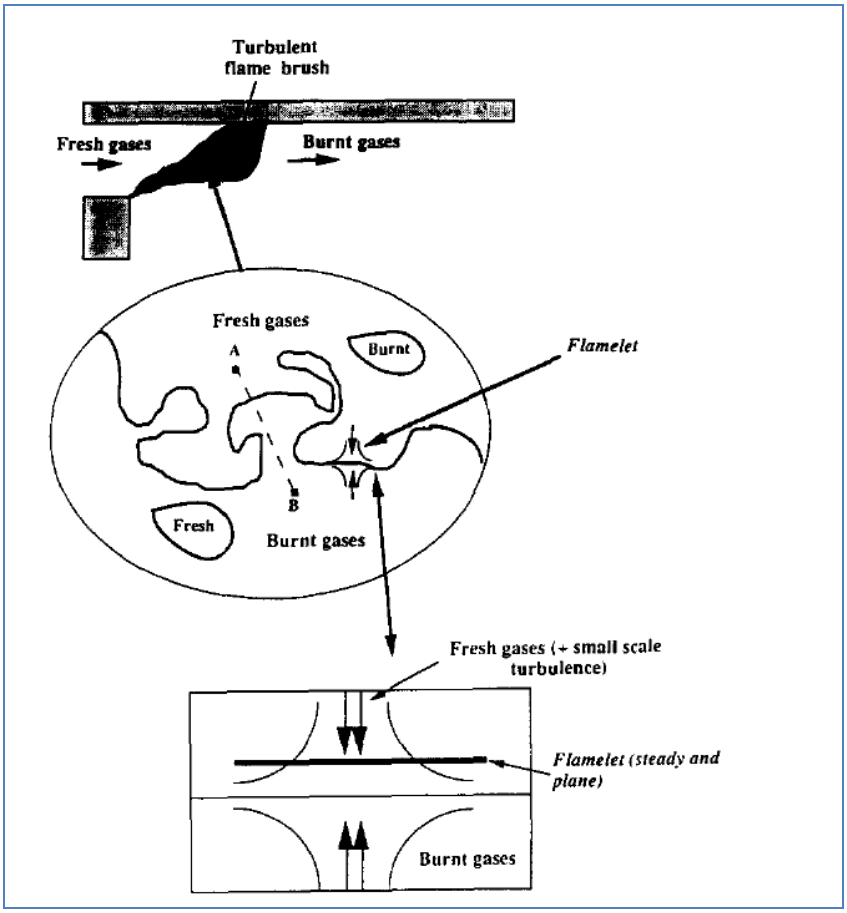

Figure 3: Principle of flamelet assumption [22].

As discussed earlier the initial flame kernel is convected by the mean velocity vector in the vicinity of the spark plug. If the spark plug is located at the center of the combustion chamber, then the breakdown of tumble into small scale turbulence will influence the turbulence intensity in the spark gap vicinity. Whereas, if the spark plug is located at the periphery of the combustion chamber then swirl is the dominant flame kernel convection

mechanism. Therefore, it can be seen that the mean in-cylinder flow can influence the initial flame kernel development stage based on the combustion chamber design. The degree of flame kernel convection during the flame initiation and development stage influences the flame kernel growth rate, which affects the burning rate and cyclic variability of the later stages of combustion. Therefore, the overall flow pattern is one of the mechanisms that influence the cyclic variability of combustion through early flame convection.

Another mechanism of flow pattern that affects combustion is the convection of the fully developed flame. Once the initial flame is established, characterized by 0-10% mixture burn, the final burn characterized by 10-90% burn is very dependent on the turbulent fluctuations and mean charge motion. Tumble and squish can only help to increase the burn rate near top center piston travel when the large scale motions break down to small eddies or turbulence fluctuations. Finally these fluctuations dissipate into heat and can no longer influence combustion. On the other hand, even after the piston reaches top center swirl can preserve its mean flow motion and help in turbulence production. Swirl has proved to decrease variability in pressure and combustion development and also to improve combustion parameters like burning rate, IMEP, P_{max}, etc. [11, 27, 28]. Swirl has also been found to be most beneficial in lean mixture combustion. The main attributes of swirl that affect combustion through overall in-cylinder flow pattern are increased flame front area, larger volume of charge swept past the spark plug during the spark event and lower cyclic variability in the velocity near the spark gap vicinity.

Spark and spark plug effects:

This section is focused on the discussion of the effects of the spark plug on the cyclic variability of combustion. The various factors related to the spark plug that affect cyclic variability are spark timing, spark discharge characteristics, spark gap, spark plug electrode shape and spark plug location. In a study of cyclic variability of IMEP with respect to ignition timing by Young [10], the least value of cyclic variability of IMEP was found to occur at MBT timing. The same study with different spark plug design, ignition system type and burning rate presented a similar trend with the minimum variability in IMEP occurring at MBT timing [29]. The effects of the different sparking phases on combustion cyclic variability were investigated in various research studies and are discussed in the next paragraph.

With regards to the initial flame kernel development stage it has been found that the breakdown phase of the sparking event is far better suited for ignition than the arc or glow discharge phases due to its high energy transfer efficiency [5]. From different studies it was concluded that the development of the initial flame kernel not only influenced the subsequent main combustion stage but is also an essential parameter in lean burn combustion. Lean operation in an IC engine increases the efficiency but is often limited by the onset of unacceptable cyclic variations in the overall combustion rate. This can in one part be attributed to the cyclic variations in the initial flame kernel growth rate. Lean burn conditions reduce the flame kernel growth rate in part due to lower energy density of the combustible mixture. The flame kernel growth rate can be increased by increasing the rate and amount of energy deposited by the ignition system. If the energy deposited in the plasma kernel is sufficient to raise and sustain the gas temperature as

well as the active radical concentration above a critical level to sustain the chemical reactions, then ignition will occur. Once ignition occurs the energy released by the chemical reactions will have to be accommodated by the flame kernel expansion. Therefore, the flame kernel growth rate is determined by both the expansion and mass burn rate. As indicated earlier, the initial flame kernel expansion depends on ignition energy density and the mass burn rate, which is influenced by the turbulence intensity. Turbulence intensity can increase the mass burn rate in stoichiometric or rich mixtures but in lean mixtures it can cause flame quenching due to flame overstretching. With the deposition of high energy density in the breakdown ignition phase, the flame kernel expansion is dominated by ignition energy rather than turbulence [25]. Another finding illustrates the higher effectiveness of an ultra short-high current ignition pulse over a long duration-low current discharge in successfully igniting a very lean highly turbulent mixture [30]. Due to the very high energy density and energy transfer efficiency of the ultra-short ignition pulses, very high pressure is developed in the plasma kernel, causing supersonic expansion which detaches the plasma kernel from the electrodes, thus minimizing heat losses to the electrodes. On the other hand, for a long duration discharge the plasma kernel latches onto the electrodes till the end of the discharge time, resulting in very high energy losses to the electrodes and minimal energy transfer to the flame kernel. Another phenomenon, called re-striking or multiple discharges, occurs across the electrodes at higher flow velocities. At higher flow velocities in the vicinity of the spark gap, the discharge length described as the distance traveled by the spark, increases. After the first strike a high ion density exists in the electrode channel. The flowing electrons have a tendency to find a shorter low impedance path than the discharge length

established by the first strike, thus creating a second strike of lesser discharge length. This may occur many times in a single discharge event, and is not beneficial to the flame initiation process because the total energy is distributed among the multiple strikes, decreasing their capability to ignite the lean-turbulent mixture [30]. Although longer spark duration has adverse effects on energy losses to the electrodes, it can in certain situations help in the initial flame development process. This was shown in a particular study where longer spark duration was applied along with a very high energy density breakdown phase. The high energy of the breakdown phase helped in creating a larger kernel volume, whereas the longer spark duration of lower energy helped to extend the non-self-sustaining flame growth period till the steady state flame growth velocity was reached [7, 14]. This property is particularly helpful in lean burn conditions as it reduces the ignition delay time.

The spark discharge characteristics are a function of the spark gap and spark plug electrode shape. With the increase in the spark gap, the breakdown potential of the intermediate mixture between the electrodes is increased. This ensures higher energy deposition during the breakdown phase of the sparking event. The result is a larger ratio between the flame kernel volume and wetted electrode surface area, in other words a larger flame kernel is established [6, 21]. The dominant effect of the spark plug electrode shape is on the energy losses to the electrodes from the flame kernel. With thicker electrodes the effective flame front area in contact with the electrodes surface area increases, leading to increased energy losses. Experiments using different spark plugs with different electrode thickness showed higher flame velocity associated with thinner electrodes [6, 21]. Thus, a combination of increased spark gap and thinner spark plug

electrodes can increase the lean limit operation of an engine and reduce cyclic variability of combustion.

The last spark plug related factor affecting combustion cyclic variability is the number and location of spark plugs per cylinder. By increasing the number of spark plugs the number of ignition sites can be increased and cyclic variability of combustion reduced by elimination of slow burning or partial burn cycles that occur with one spark plug. Cyclic variations in general can be reduced by reducing the flame travel distance or reducing the flame travel time by increasing the mass burning rate. This can be achieved by placing the spark plug centrally in the combustion chamber in an engine with no swirling mean mixture motion. With the presence of strong swirling motion faster burning rates can be obtained by placing multiple spark plugs at the periphery of the combustion chamber [11, 31, 32].

Dissertation Organization

The focus of this dissertation is the application of lean engine operation to reduce engine-out emissions. The majority of 4S-OHV small engines are designed with two valves per cylinder and a carbureted fuel supply system. The spark plug is generally placed at the periphery of the combustion chamber in this configuration. The disadvantages with this configuration are longer flame travel distances and larger cylinder wall surface area exposure to the developing flame front, which cause significant heat transfer losses. Nevertheless this is one of the most widely practiced combustion chamber designs for 4S-OHV small engines. A Honda GX series single cylinder engine with similar combustion chamber configuration is used in one part of the research to

explore the possibility of lean combustion without making any major combustion chamber modifications. The stress of this dissertation research, though, is on a novel engine configuration that utilizes direct gasoline fuel injection into the combustion chamber of a side valve (flat head) engine. Although direct gasoline injection has already been applied to OHV SI engines, its application on side valve engines has not yet been explored. Some of the advantages of a SV engine are low manufacturing costs, simplicity of design, and lower engine weight and height. There are some major disadvantages too, such as higher engine-out emissions and high surface to volume ratio of the combustion chamber that enhances heat transfer losses. For applications where operating costs as well as initial costs of equipment are important, the SV engine has a definite advantage. In some applications where the engine-out emissions and engine performance is more critical, the SV engine may lose the competition to the OHV engine. The direct-injection flat head (DIFH) engine design is an effort to address these disadvantages and to render the SV engine competitive with the OHV engine designs.

Chapter 2 is an experimental investigation of the application of lean burn strategy to achieve engine-out emissions reduction without the use of external catalytic converters. The major impediment to stable lean burn combustion is the onset of cyclic variability in combustion. A large number of engine parameters play an instrumental role, often complicated by parametric interactions, in the process of combustion. The combustion chamber design of every engine platform is unique and is influenced by varying engine parameters differently. The experimental investigation in the current study is based on an OHV Honda GX series engine platform. Without making major engine modifications, the major parameters investigated were related to spark plug

variations, load control and charge stratification. It was shown that significant engine-out emissions reduction can be obtained while still maintaining acceptable cyclic variability in combustion.

Chapter 3 is a description of the DIFH engine design for which a non-provisional patent has already been obtained. The description of the DIFH engine is based on the patent application itself.

Chapter 4 presents an experimental investigation into the dynamics of the DIFH engine combustion chamber. The DIFH engine was retrofitted on to an already available engine platform and, therefore, is not an optimized design. Using the current original equipment manufacturer (OEM) combustion chamber design, in-cylinder flow analysis was performed using particle image velocimetry (PIV). The results from the PIV measurements made available an insight to the air motion inside the combustion chamber, which later provided explanation to experimental observations and suggested recommendations for further combustion chamber design improvements. The results of the experiments showed that the current DIFH combustion chamber design is inadequate in addressing the issue of reduced engine-out emissions.

CHAPTER 2

LEAN BURN OPTIMIZATION STRATEGIES IN SPARK IGNITED SMALL ENGINES

Abstract

An experimental investigation into the application of lean burn strategy was carried out on a single cylinder OHV utility engine to reduce engine-out emissions and at the same time maintain acceptable cyclic variability in combustion. The parameters of interest to investigate cyclic variability in combustion were spark plug variations, load control and charge stratification. It was shown that EPA Phase III limits of 8.0 g/kW-hr for ($HC+NO_x$) can be achieved without the use of catalytic converter. It was also shown that a reduction of about 97% in CO emissions can be achieved by the application of lean strategy. A 6% reduction in fuel consumption was also observed.

Introduction

Small gasoline engines outsell car engines by 15 to 35 million units and, although each car engine on average operates 100 to 1000 times longer than each small gasoline engine, the latter pollute 100 to 1000 times more [1]. Modern cars use many times more expensive combustion and after treatment technologies than do small engines. Using such advanced technology for automobiles while operating small engines inefficiently with a

motive to cut costs basically contradicts the very idea of environmental protection. A major pollutant species emitted from small engines is carbon monoxide (CO). Carbon monoxide is a colorless, odorless gas that can cause sudden illness and death. The red blood cells in humans and animals have much higher affinity for CO than oxygen, because of which in environments containing high concentrations of CO, the oxygen content in the blood gets cut off by CO resulting in tissue damage and death [33]. Currently government agencies such as the Environmental Protection Agency (EPA) and the California Air Resource Board (CARB) are pushing towards more stringent emissions regulations for small engines but these are still about 100 times less stringent than automotive regulations.

Another group of pollutants emitted from engines are unburned hydrocarbons (UHC) and oxides of nitrogen ($NO + NO_2$), collectively known as NO_x. Nitrogen dioxide (NO_2) is a brown gas which is highly toxic and easily dissolves in water to form nitric acid. If inhaled, the gas dissolves in the moisture of the throat and lungs and can cause permanent damage [34]. The maximum concentration of NO_2 for short term exposure is about 5 parts per million (ppm). Typically NO_2 forms 2% of the total NO_x formation in a spark ignition (SI) engine [3], and the majority of the NO_x emissions consist of nitric oxide (NO). NO is also suspected to be a cardiovascular or blood toxicant, neurotoxicant, and respiratory toxicant [34]. Most NO is converted to NO_2 in the atmosphere over a period of minutes or a few hours after emission from an engine. UHCs produced by vehicular and non-road internal combustion (IC) engines, as well as other combustion and biological processes. Along with NO_2, UHCs are responsible for a major environmental nuisance known as photochemical smog. This phenomenon is most

prevalent in cities because of high levels of NO_x emissions from engines. The overall smog formation mechanism is shown in Figure 4 [35].

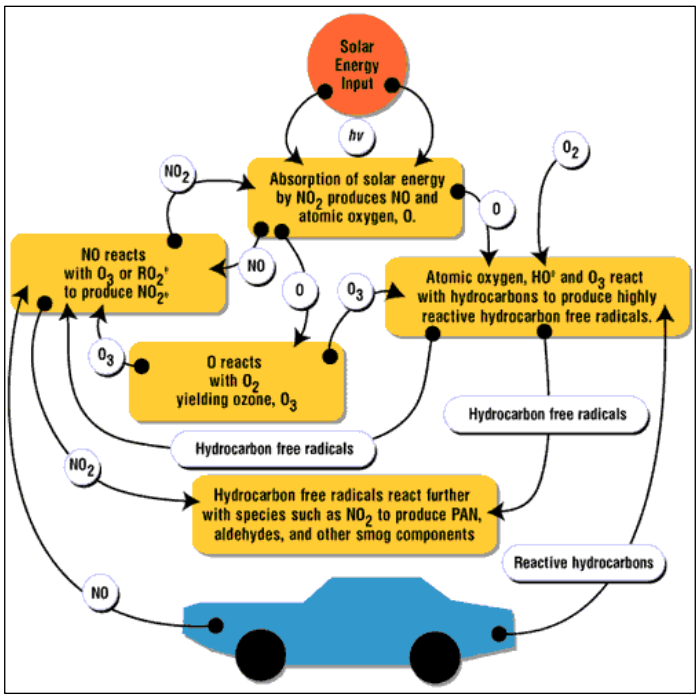

Figure 4: Smog formation mechanism [39].

As discussed earlier small engines make a major contribution to the formation of all the three types of pollutants mentioned above. The application of automotive technology to small engines in a simpler form could prove a viable solution for emissions reduction in small engines. Simply stated, “automotive technology” means the application of computer controlled electronic fuel injection (EFI) using an engine management system (EMS) and exhaust gas catalysis.

Almost all small SI engines are air cooled. Therefore, to prevent overheating during engine operation, rich engine operation is practiced as a cheap fix solution to the temperature control problem. The excess fuel in the air-fuel mixture absorbs the latent heat of vaporization from the heat available inside the engine combustion chamber

thereby cooling off the cylinder head. The penalty paid in this process is excessive engine-out emissions of UHC and CO. Engine-out CO is directly proportional to equivalence ratio (Φ), where Φ is defined as the ratio of the stoichiometric air-to-fuel ratio to the actual air-to-fuel ratio. Thus, CO formation can be reduced by running the engine lean (at lower Φ). UHC also decreases with decreasing Φ but upon further decrease of Φ, the combustion quality deteriorates, thereby increasing UHC emissions. NO_x formation is dependent on the combustion temperature as well as the concentration of oxygen available in the combustion chamber. The combustion temperature is highest when the engine is operated just lean of stoichiometric (~ 14.9 AFR), and also with the availability of excess oxygen contributes to higher NO_x formation [3]. Although lower combustion temperatures can be obtained by burning leaner mixtures, which can be a solution for reduced NO_x formation, this may lead to higher COV of IMEP. COV of IMEP is defined as the coefficient of variation of indicated mean effective pressure. It is considered one of the main criteria for determining cyclic variability of engine operation. Cyclic variability is the benchmark for determining whether a particular combustion strategy is better for maximizing key engine parameters like efficiency and emissions.

In a bid to reduce fuel consumption and engine-out emissions from small air cooled engines, lean burn technology has already been investigated by small motorcycle engine manufacturers [36, 37, 38, 39, 40]. Some of these technologies include use of oxygenated or emulsified fuels, air-assisted fuel injection for better atomization of the fuel droplets, and use of catalytic material in the combustion chamber to accelerate combustion. Although some technologies may appear overwhelmingly expensive for small, low cost utility engines, they do indicate the feasibility of lean operation of small

engines. The application of leaner AFRs and a suitable catalytic converter have already been shown to reduce the CO, ($HC+NO_x$) emissions significantly [41]. Engine-out emissions are a strong function of fuel supply control, and the best way to achieve accurate fuel quantity metering is by fuel injection. Motorcycle engines have already applied fuel injection over carburetion and now this route is slowly gaining acceptance with small utility engines.

A literature review of the effect of lean operation on cyclic variability of combustion has pointed out some key parameters of interest [11]. These parameters are classified as mixture composition, in-cylinder mixture motion and spark plug related parameters previously described in the background section. The orientation of the valves and the spark plug of the Honda GX engine are shown in Figures 5a and 5b. It can be seen from Figure 5a that the valves are inclined to the cylinder axis and the spark plug is located at the periphery of the combustion chamber, more clearly shown in Figure 5b. The effects of the placement of the valves in the combustion chamber on in-cylinder air flow were not studied on a flow bench as part of this research. The combustion chamber shape is one of the most important parameters that affect the combustion process but, in simple small SI engines this parameter may get secondary importance as compared to simplicity in engine design for cost reduction. Established knowledge of flame propagation in SI engines also tends to disagree with the placement of the spark plug in the combustion chamber as in shown in Figure 5a and 5b.

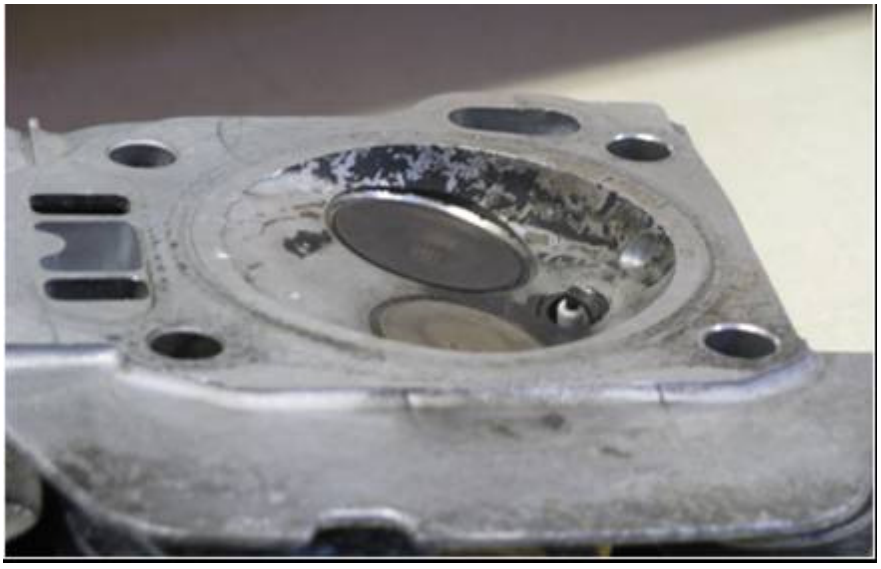

Figure 5a: Honda GX series cylinder head with inclined intake and exhaust valves.

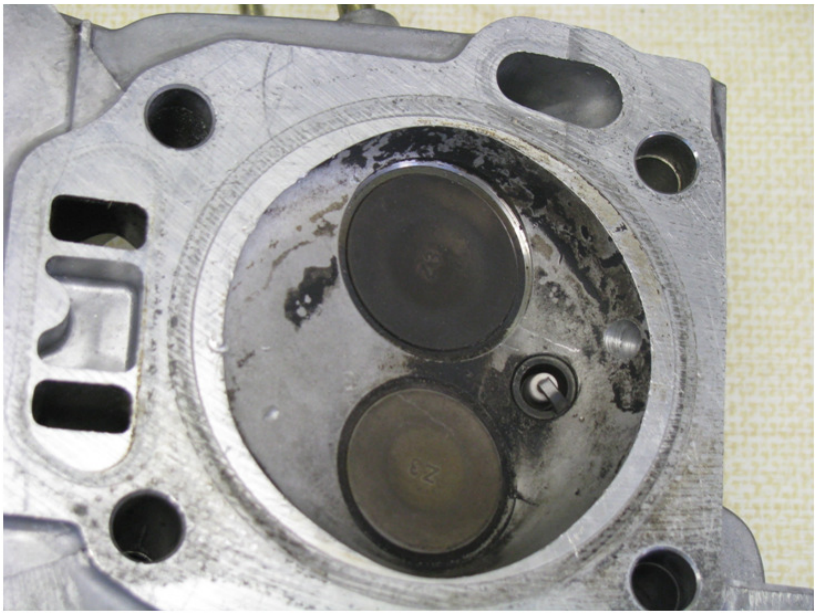

Figure 5b: Top view of cylinder head showing spark at the periphery of combustion chamber.

With the initial flame developing at the spark plug electrode, a large flame front area is wetted by the combustion chamber walls contributing to extensive heat transfer losses. Conventionally small engines are operated at about 10-15% rich of stoichiometric (just enough oxygen present to fully oxidize the hydrocarbon fuel to H_2O and CO_2) across the operating range of the engine. The fuel rich mixture helps to sustain the stabilized flame although with a penalty of thermal efficiency loss. As the fuel-air mixture is made leaner; the laminar burning velocity of the mixture decreases reducing the burning rate, and the probability of flame quenching due to flame over stretching increases because flame convection by mean mixture motion gains predominance over mixture burning rate.

The most detrimental limitation of the experimental combustion chamber appears to be the non-symmetrical location of the spark plug, which increases the flame travel distance and time. With leaner air-fuel mixture the burning velocity is reduced, which increases flame travel time, so MBT occurs at more advanced timings to produce the same amount of work as with faster burning cycles [42]. And with non-symmetrical spark plug location the flame travel distance increases, which may quench the flame before it can engulf the whole combustion chamber. This can lead to increased CO and HC emissions and poor thermal efficiency.

The ignition system and the fuel supply system are important parameters that can help reduce the cyclic variability in combustion during lean engine operation. The spark plug and the high voltage generator can be collectively termed as the ignition system, but in this study only the high voltage generator is referred to as the ignition system. The sparking system used in this study is based on transistorized coil ignition. Transistorized coil ignition (TCI) systems and capacitive discharge ignition (CDI) systems provide

higher energy sparks and derive their energy from a battery. In TCI systems, the current from the battery flows through the primary windings of the coil and, when interrupted by the electronics of the coil driver, produces a high voltage in the secondary windings. In CDI ignition systems a capacitor is used to store the ignition energy rather than an induction coil. A detailed description of the TCI and CDI ignition systems can be found in [3]. Apart from the ignition system, spark plugs with thinner electrodes very effectively change the spark characteristics. The effect of spark plugs on the cyclic variability of combustion and lean operation has already been discussed in the background section. In this study, the TCI ignition system and a choice of conventional thick electrode spark plug and an ultra thin electrode spark plug has been made to investigate their effect on the lean limit and combustion variability in combustion. The spark energy dissipated by the two different spark plugs at different electrode gaps is one part of the study and is presented in the experimental procedure section below.

The other parameter of interest is related to the fuel supply and mixing mechanism. In conventional premixed SI combustion systems the engine load is controlled through the amount of fuel-air mixture admitted into the combustion chamber. This is accomplished by the use of a throttle plate in the carburetor to manipulate the inlet restriction. Once the main jet size which controls the amount of fuel drawn into the intake air stream is fixed, no more fuel-air mixture control can be exercised in a carburetor system. This limitation is alleviated by the application of port fuel injection (PFI). Not only can the desired AFR be achieved by this system, but charge stratification can also be achieved to a certain extent. The idea of charge stratification is relevant because, with very lean mixtures it is advantageous to have pockets of fuel rich regions that can be

ignited easily while still having an overall lean AFR throughout the combustion chamber. As mentioned earlier, the engine load in a premixed SI engine is controlled through a throttle that controls the mass flow rate of charge into the combustion chamber. It should be noted that the flow characteristics of the charge through the intake valve during the intake stroke forms the initial conditions to the subsequent development of turbulence in the combustion chamber [43]. When the engine with fixed AFR is operated at lower loads, the amount of combustible mixture in the combustion chamber is lower due to reduced volumetric efficiency. This sets up weaker tumble and swirl motions in the combustion chamber that can adversely affect the combustion rate. Another way of load control can be achieved by admitting leaner AFR mixtures into the combustion chamber at higher volumetric efficiencies. This is accomplished by the application of port fuel injection where all the fuel can be injected during small crank angle duration over the intake stroke. This will keep the overall AFR to the desired value but create a pocket of rich air-fuel mixture that is carried around by the bulk charge motion within the combustion chamber. This feature allows maintaining a higher air flow rate during the intake stroke, increasing the volumetric efficiency and lowering the engine pumping work.

Motivation for Research

Engine out emission from small engines can be reduced by upgrading the fuel delivery system and control flexibility over key engine performance parameters like spark timing and air-fuel ratio. While operating the engine lean it is also important to ensure stable engine operation. Therefore, the two main objectives of the research are;

- Application of lean burn strategy to reduce engine-out emissions.
- Investigation of factors affecting cyclic variability in combustion..

Experimental Procedure

The experimental setup consists of an air-cooled single-cylinder Honda GX series engine coupled to an AC dynamometer through a Himmelstein MCRT 48000V torque transducer. The engine has been subsequently retrofitted with an EMS and a PFI system. The EMS has the capability to interface with an external PC for developmental work. By being able to communicate with the EMS in real time, it is possible to adjust key operating parameters including AFR and spark advance (SA). There are a host of other tuning parameters that can be adjusted in real time that are not discussed here because a simple open loop control strategy is pursued in this effort. In open loop operation, no use of a feedback control system is made. During closed loop operation a narrow range oxygen sensor (switching sensor) is used to detect the stoichiometric exhaust gas composition and used as a feedback mechanism for correcting the amount of fuel injected during the intake stroke. The carburetor was modified to accommodate the fuel injector, essentially making it a throttle body, as shown in Figure 6.

The fuel supply pressure to the fuel injector is regulated through a pressure regulator to 2.5 bar as recommended by the manufacturer. A universal exhaust gas oxygen (UEGO) sensor is mounted on the exhaust manifold to measure the actual AFR. The configuration of the modified engine is shown in Table 1. The exhaust manifold is also instrumented with a sampling tube for emissions analysis. A 5-gas emissions bench capable of measuring CO, CO_2, O_2, UHC, and NO_x is used. The engine speed and torque

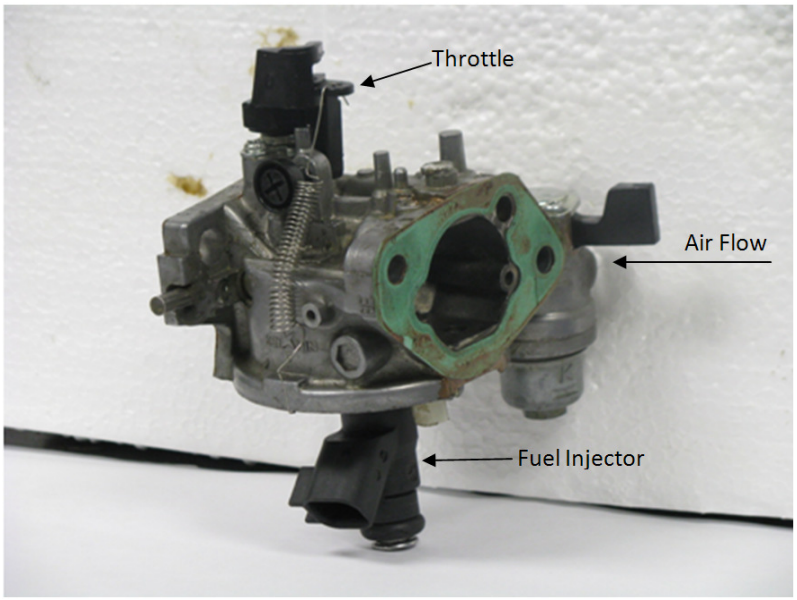

Figure 6: Throttle body with fuel injection system.

are measured by the torque transducer mounted in line between the engine and the AC dynamometer. The AC dynamometer consists of an inverter duty AC motor controlled by a 4-Quadrant controller manufactured by ABB. The 4-Quadrant controller can turn the motor in either direction and motor the engine as well as absorb power. While in power absorbing mode it sends the power generated by the AC motor back into the grid. The fuel consumption is measured gravimetrically using a high precision SAW series electronic fuel scale manufactured by ARLYN scales. The data from all the associated instrumentation is acquired and logged in a National Instruments (NI) based data acquisition system. A graphical user interface (GUI) was designed to interface the system hardware with the data acquisition system and monitor the important engine parameters real time.

Table 1: Summary of modified test engine.

Engine Configuration	Stock Engine	Modified Engine
Type	Air cooled, single cylinder, 4 stroke cycle	Air cooled, single cylinder, 4 stroke cycle
Engine capacity	389 cc	389 cc
Fuel System	Carburetor	EFI
Ignition System	Fixed timing magneto coil. 25° SA.	Variable programmable spark advance TCI ignition system.
EMS	Not applicable	Yes
Feedback Control Mechanism	Not Applicable	Open loop control.

Figure 7 shows a schematic of the experimental setup. The engine was first run in the stock condition, i.e., with unmodified ignition system and carburetor. The EPA B-cycle as shown in Table 2 was followed for selecting the load points. The engine-out emissions were also measured to establish baseline values. Subsequently the engine was modified with engine management, fuel injection system and spark ignition system. Within the scope of study, spark plug related parameters, fuel injection system and air-fuel ratio strategies were identified as subjects of investigation to study cyclic variability in combustion and reduce emissions. The design of experiment (DOE) is shown in Table 3 below. The initial set of experiments were completed using the low flow injector as a fixed factor while varying the spark plug and air fuel ratio levels over the entire engine operating range.

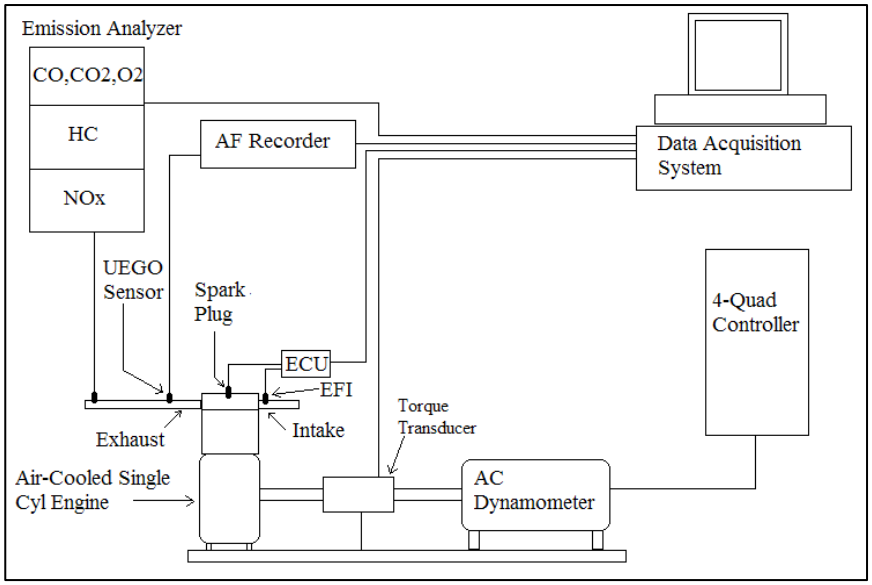

Figure 7: Schematic of experimental setup.

Table 2: EPA/CARB 6-mode SORE test cycle.

	MODE 1	**MODE 2**	**MODE 3**	**MODE 4**	**MODE 5**	**MODE 6**
Speed (% rated)	100	100	100	100	100	idle
Load (%)	100	75	50	25	10	0
Weight Factor (%)	9	20	29	30	7	5

Table 3: Design of Experiment

Factors	Level	Engine operating mode
Spark plug	Electrode thickness: - OEM (2.5 mm) - Thin (0.4 mm) Electrode gap: - 0.5 mm - 0.75 mm - 1.0 mm	1,2,3,4,5,6
Injector type	High Flow Low Flow (OEM)	
Air fuel ratio	14.9, 15.5, 16, 16.5, leanest AFR	

Results and Discussion

Ignition system analysis:

This study consists of investigating the effects of spark plug electrode thickness and gap on the spark discharge characteristics. The TCI ignition system, which consists of a coil with an in-built driver is an OEM part supplied by the EMS manufacturer. For the TCI ignition system, an 'ON TIME' is specified on a dwell table as a function of battery voltage and engine speed as shown in Table 4. The ON TIME (ms) determines the strength of the magnetic field that is developed in the secondary windings. When the current flowing through the primary coil is switched off by the transistor of the TCI system, the magnetic field created in the secondary collapses to generate a very high voltage flowing through the secondary coils, inducing a spark to jump across the spark plug electrode gap. There are a number of different types of spark plugs available with varying electrode geometries such as J-type, circular electrodes, surface gap type, etc. Normally J-type spark plugs are used in automotive applications with different electrode thicknesses. Two commercially available J-type spark plugs are used for the experiments, as shown in Figure 8. The specifications of the spark plug are given in Table 5.

Table 4: Dwell table interpolated for all break points

VBatt / *RPM*	6	6.8	7.6	8.4	9.2	10	10.8	11.6
0	21.05	19.61	15.60	11.75	8.88	7.34	6.38	5.64
800	21.05	19.61	15.60	11.75	8.88	7.34	6.38	5.64
1600	18.31	15.55	13.13	10.89	8.87	7.34	6.38	5.64
2400	14.54	12.50	10.94	9.66	8.49	7.34	6.38	5.64
3200	12.39	10.73	9.45	8.45	7.64	6.94	6.27	5.62
4000	11.02	9.58	8.46	7.59	6.89	6.31	5.84	5.40
4800	10.02	8.74	7.74	6.95	6.32	5.80	5.38	5.02
5600	9.25	8.08	7.18	6.46	5.88	5.40	5.01	4.67
6400	8.65	7.57	6.73	6.07	5.53	5.08	4.72	4.41
7200	8.15	7.14	6.35	5.72	5.22	4.80	4.46	4.17
8000	7.73	6.78	6.04	5.45	4.97	4.57	4.25	3.97
8800	7.38	6.49	5.80	5.25	4.79	4.41	4.11	3.84
9600	7.11	6.27	5.63	5.13	4.67	4.31	4.02	3.75
10400	6.92	6.12	5.53	5.06	4.60	4.26	3.98	3.71
11200	6.81	6.04	5.50	5.02	4.56	4.24	3.97	3.70
12000	6.81	6.03	5.50	5.02	4.55	4.24	3.97	3.70
12750	6.81	6.03	5.50	5.02	4.55	4.24	3.97	3.70

Table 5: Spark plug specifications.

Spark plug type	NGK	DENSO
Electrode thickness (mm)	2.5	0.4
Center electrode resistance (ohms)	5K	5K
Capacitance (pF)	13.5	12.5

Figure 8: J-type spark plugs with thick and thin electrodes.

The performance of the ignition system can be evaluated by measuring the spark energy. The total spark energy can be obtained by summing the ionization energy and the arc energy. The ionization energy is given by Equation 3 below;

$$E_{ion} = \frac{1}{2} C V_b^2 \tag{3}$$

where C is the capacitance of the spark plug and V_b is the breakdown voltage. The spark energy can be measured by integrating the product of the current and the voltage generated at the spark plug. It is given by Equation 4 below;

$$E_{sp} = \int_{t_{start}}^{t_{end}} I_{sp}(t) \times V_{sp}(t) dt \tag{4}$$

where E_{sp} is the calculated spark energy, I_{sp} is the measured current in the secondary and V_{sp} is the generated voltage in the secondary. The discharge current was measured by a LEM RR3035 current probe. The voltage was measured by a Tektronix P6015A high voltage probe. The voltage can be measured at the top of the spark plug center electrode or at the spark gap. There is a voltage drop from the voltage measured at the spark gap to that at the top of the center electrode. It is impossible to measure the voltage at the spark gap in a running engine; therefore, the voltage was measured at the top of the spark plug center electrode. Both the current waveform and the voltage waveform were displayed and recorded on a Tektronix DPO 4033 digital phosphor oscilloscope. The spark plugs were indexed such that the orientation of the ground electrode with respect to the mean mixture flow direction can be established. All tests were carried out with the cross flow configuration of the spark plug because it has been established by previous researchers that significant sparking energy losses to the electrodes is experienced due to flame convection for upstream or downstream electrode orientations [21,44]. It should also be mentioned that the exact orientation of the spark plug electrode gap was not optimized but the same orientation was used for all DOE points.

During the following discussion the baseline engine configuration is referred to as 'OEM' and the lean strategy is referred to as 'Lean'. With reference to the spark plug, the thick electrode spark plug is referred to as 'OEM', whereas the thin electrode spark plug is referred to as 'Thin'. Figures 9-18 provide data on the effect of the spark plug parameters on cyclic variability in combustion.

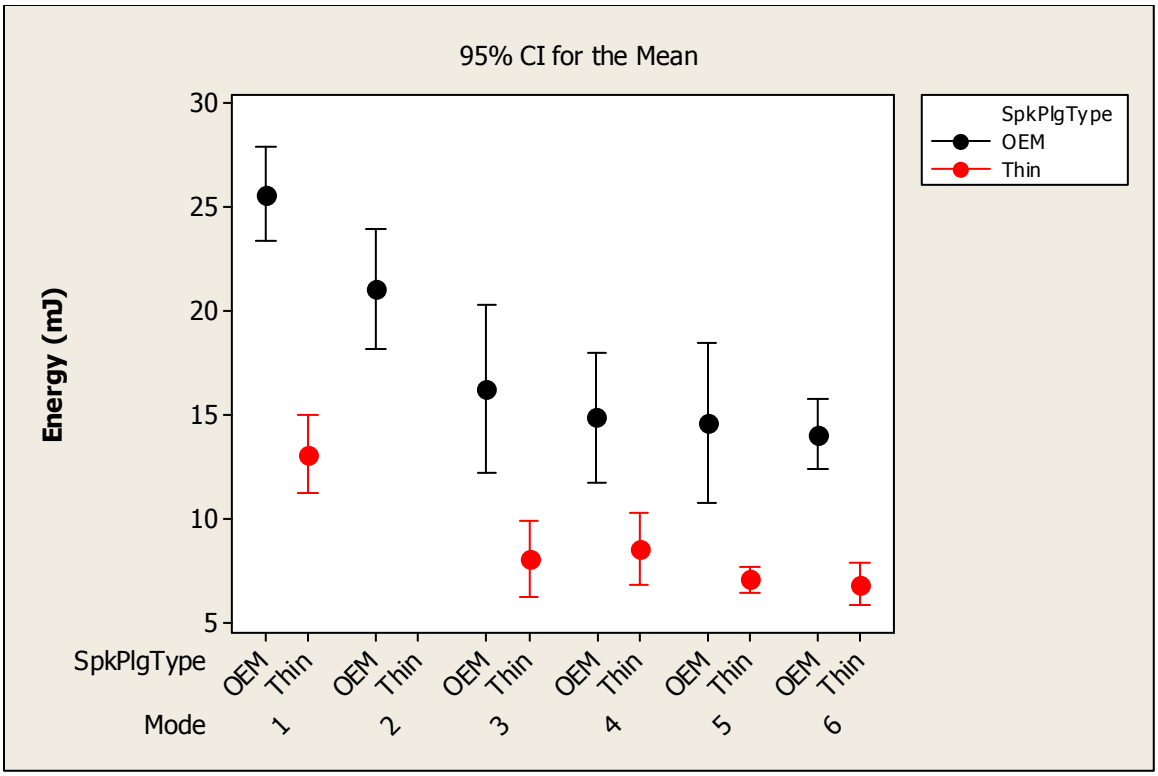

Figure 9: Interval plot of ignition energy vs. engine mode and spark plug type; 0.75 mm spark gap

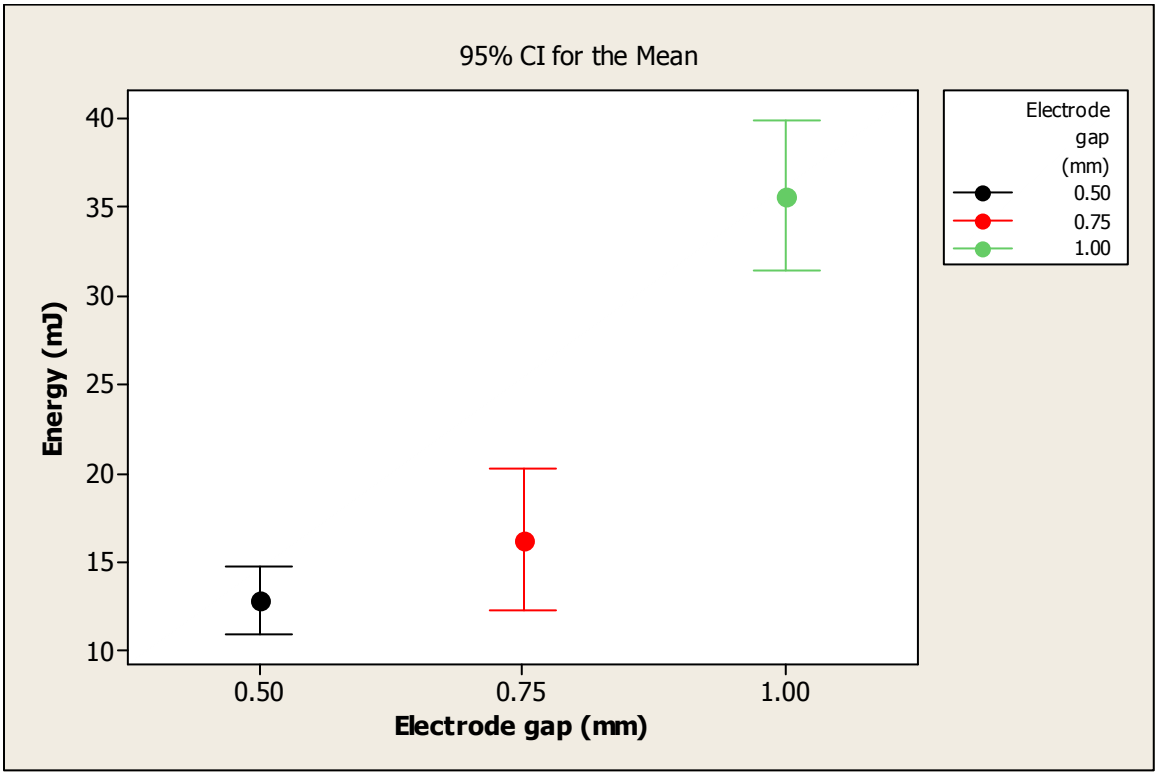

Figure 10: Interval plot of ignition energy vs. electrode gap; engine mode 3, OEM spark plug.

From Figure 9 it can be seen that the OEM spark plug requires a higher minimum ignition energy for initiating combustion as compared to the 'Thin' spark plug. It is also noted that the ignition energy decreases as the engine operating mode (load) decreases. The spark gap for the above study was held constant at 0.75 mm. This observation is further verified in Figure 11, where the breakdown voltage is plotted against spark plug type and engine mode. As a potential difference is applied across a spark gap, electrons are emitted from the cathode. Electrons being much lighter move faster than positive ions and under high pressure (> 1 atm) carry most of the current. As the voltage across the spark gap further increases, electron multiplication takes place by collision with gas atoms. With further increase of the potential difference across the spark gap positive ions collide with the cathode to emit secondary electrons, ultimately leading to breakdown. The breakdown voltage is related to the gas pressure and the electrode gap. Only a small fraction of the delivered energy is transferred to the breakdown phase, the majority of which is distributed to the arc and glow discharge phases. The critical parameters that influence the distribution of the total energy between the three different phases are the gas pressure, mixture composition, electrode gap, electrode material, electrode shape and size, and flow around the electrodes. Based on this understanding it can be explained that at higher gas pressures (higher engine loads), higher breakdown voltage is required as seen from Figure 11. In Figure 10, the minimum ignition energy is plotted as a function of electrode gap for the OEM spark plug. It shows that as the electrode gap is increased, the minimum ignition energy requirements also increase.

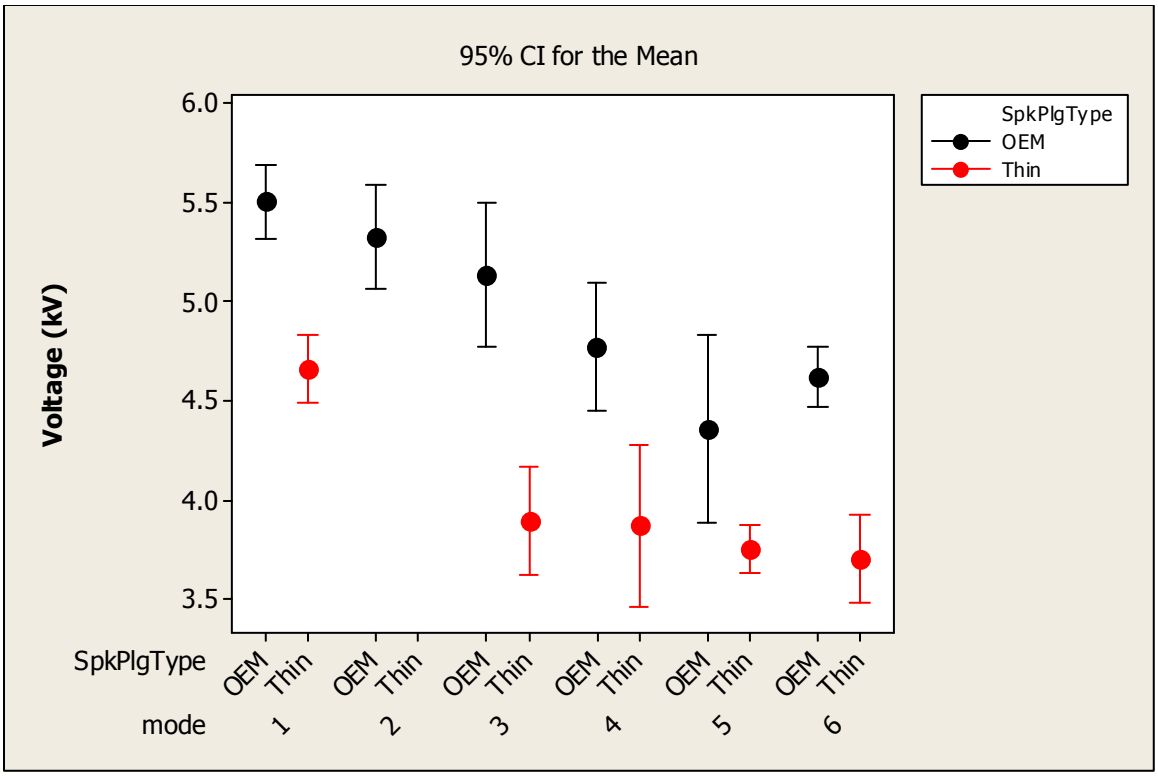

Figure 11: Interval plot of breakdown voltage vs. spark plug type and engine mode; 0.75 mm electrode gap.

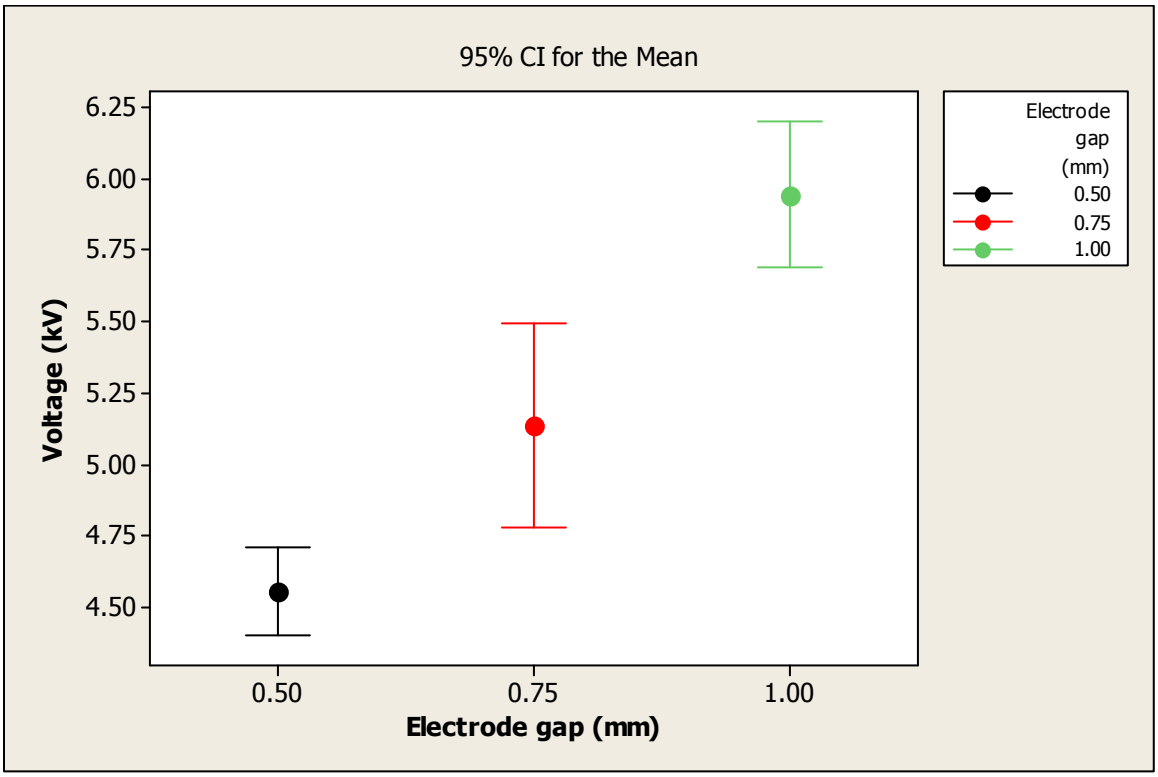

Figure 12: Interval plot of breakdown voltage vs. electrode gap; OEM spark plug.

This can again be explained with the help of Paschen's law, which states that the breakdown voltage is proportional to the product of the gas pressure and electrode gap [45]. This is also verified by the increasing breakdown voltage with electrode gap distance as shown in Figure 12. The OEM spark plug has a much thicker center electrode (2.5 mm) as compared to the 'Thin' electrode (0.4 mm). This would promote a larger surface area over which the current conducting path is established, promoting higher heat transfer losses to the electrodes. As the arc phase is very dependent on a cathode hot spot to sustain the current flow, higher minimum ignition energy is required to offset energy loss due to heat transfer to the electrodes. Flame initiation defined as 0-10% burn duration is shown in Figures 13 and 14 for spark plug type and electrode gap, respectively. With decreasing load as the charge density decreases, the 0-10% burn duration increases. The mean flame initiation time is lower for the 'Thin' electrode than for the OEM electrode. At higher charge density the 'Thin' electrode showed lower variability in the 0-10% burn duration than the OEM electrode. Larger electrode gaps also help in reducing the 0-10% burn duration. This lends support to the observation that even though the minimum ignition energy is higher for the OEM spark plug, a smaller fraction of the total energy is deposited into the breakdown phase as compared to the 'Thin' electrode. A major portion of the total energy is deposited into the arc and glow discharge phases for the OEM spark plug that can help in extending the spark duration, a strong factor that helps to extend the non-self-sustaining flame growth period during flame propagation, especially in lean mixtures. The 10-90% burn duration characterizing the flame propagation period is shown in Figures 15 and 16 for spark plug type and electrode gap, respectively. From Figures 15 and 16 it can be seen that the 10-90% burn

duration is strongly dependent on the mixture composition. Even though the flame initiation is shorter at modes 2 and 3, the flame propagation period is the longest due to very lean operating conditions. Figure 15 also indicates that the mean burn duration for the main combustion period is reduced for the OEM spark plug at each mode. This can be attributed to the extended spark duration characteristics of thicker electrode spark plugs. A larger electrode gap tends to extend the main combustion duration at each mode for the OEM spark plug. Table 6 shows the engine operating conditions for the spark parameter study, where the units of spark angle (SA) are crank angle degrees (CAD).

Table 6: Engine operating conditions.

Mode	AFR	SA (CAD)	Power (hp)
1	14.6	25	10.0
2	17.6	32	7.8
3	17.6	32	5.0
4	15.2	32	2.9
5	14.7	32	1.1
6	14.9	30	Idle

Figures 17 and 18 show the coefficient of variation (COV) of torque measured at the crankshaft of the engine. Until mode 4, the COV torque is under 10% but increases greatly at modes 5 and 6. This trend is consistent with both spark plug type and electrode gap.

Load control:

The next parameter of interest that influences cyclic variability in combustion is volumetric efficiency. Although treated separately, volumetric efficiency has a strong effect on the spark plug related parameters discussed above and also on charge stratification, which will be discussed as a separate parameter later. Increasing volumetric efficiency decreases the pumping losses due to reduced throttling and also increases the intake pressure as a larger mass of air is inducted. Running the engine at higher volumetric efficiencies allows higher relative air-fuel ratios that increase the ratio of specific heats due to the thermodynamic effects, increasing efficiency through higher expansion work. One other premise adopted in the lean strategy is engine derating. The OEM engine was rated at 11 hp at full load, 3600rpm. In the lean strategy the engine was derated to 10 hp. This was done because at higher loads the cylinder head temperature would exceed the limits (~250°C), forcing to decrease the air-fuel ratio for cylinder head cooling. The cylinder head temperature map is shown in Figure 19 for baseline and lean strategy. The operating conditions of the lean strategy engine were as per Table 6. By reducing the rated load it automatically reduces the other mode points which makes it more feasible to run at higher relative air-fuel ratios. Figure 20 shows the substantial increase in volumetric efficiency achieved at modes 2 and 3 while running at higher relative air-fuel ratios.

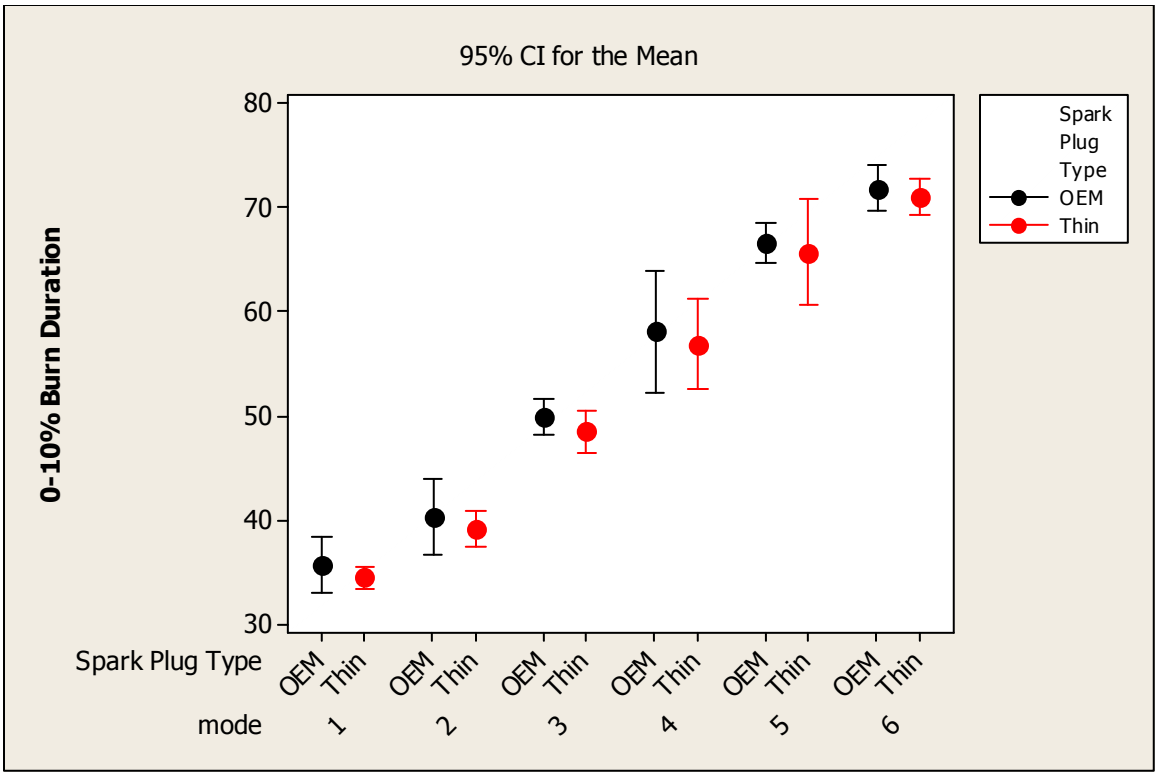

Figure 13: Interval plot of 0-10% burn duration vs. spark plug type and engine mode.

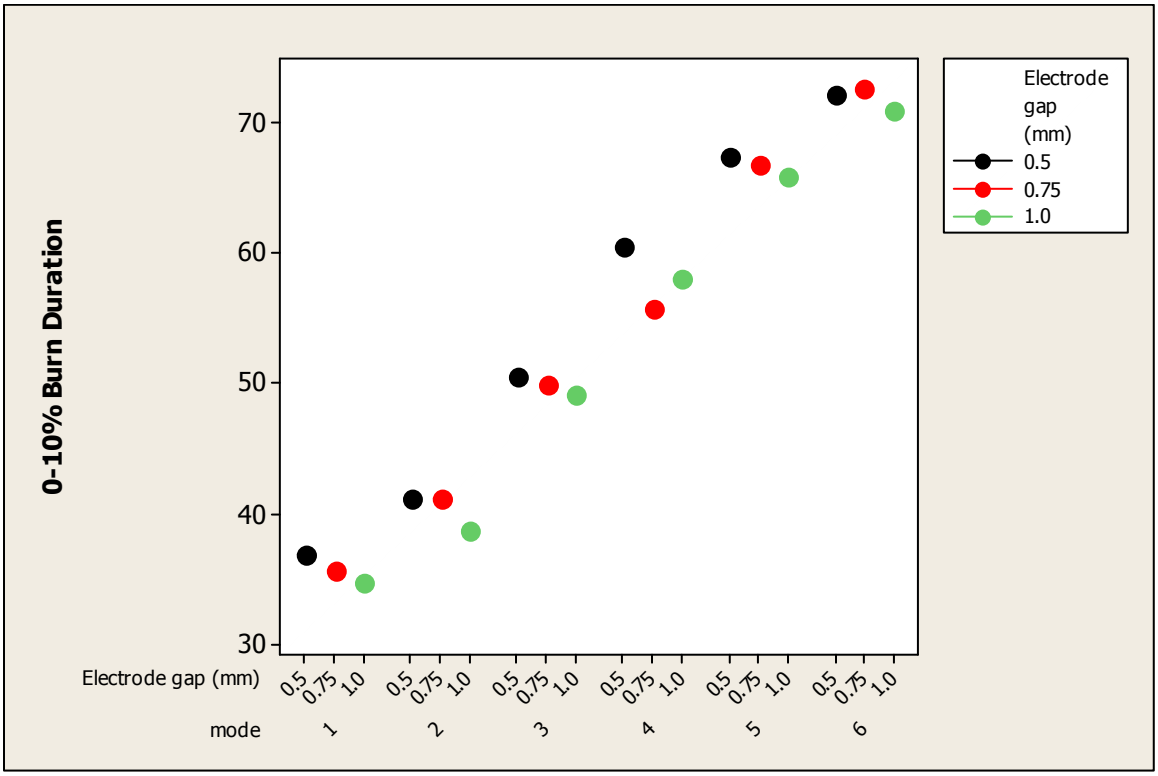

Figure 14: Interval plot of 0-10% burn duration vs. electrode gap and engine mode; OEM spark plug.

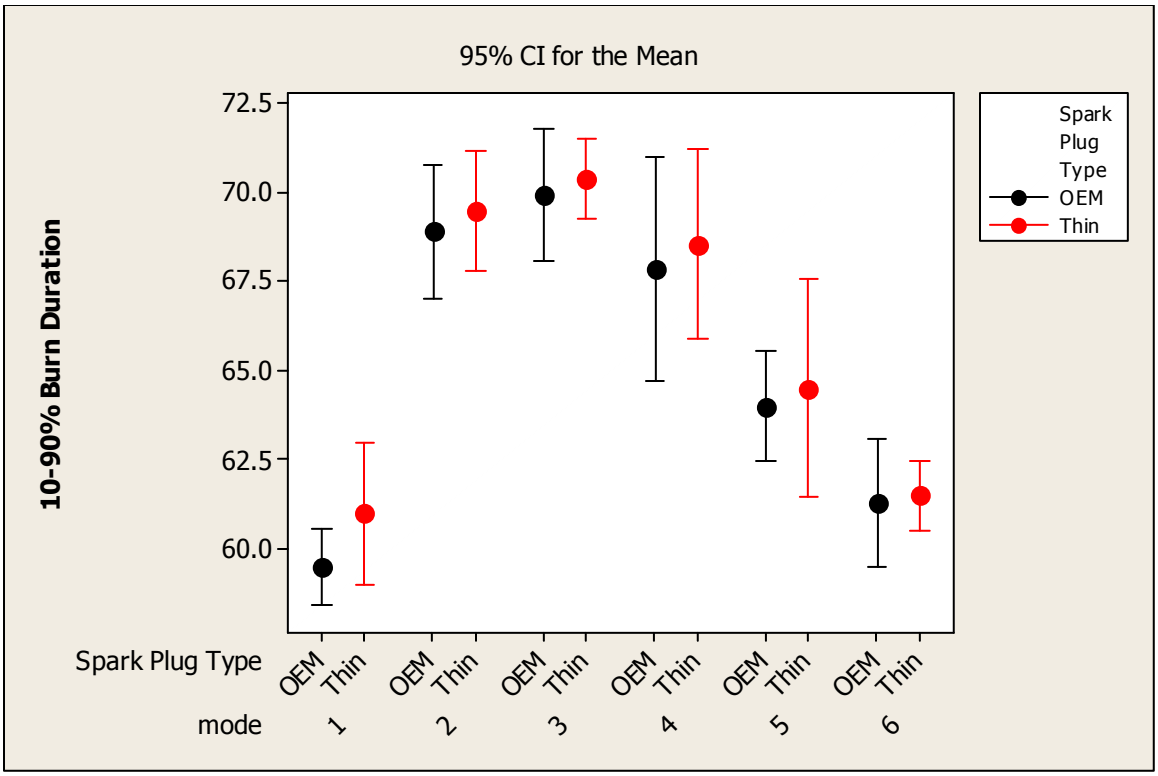

Figure 15: Interval plot of 10-90% burn duration vs. spark plug type and engine mode.

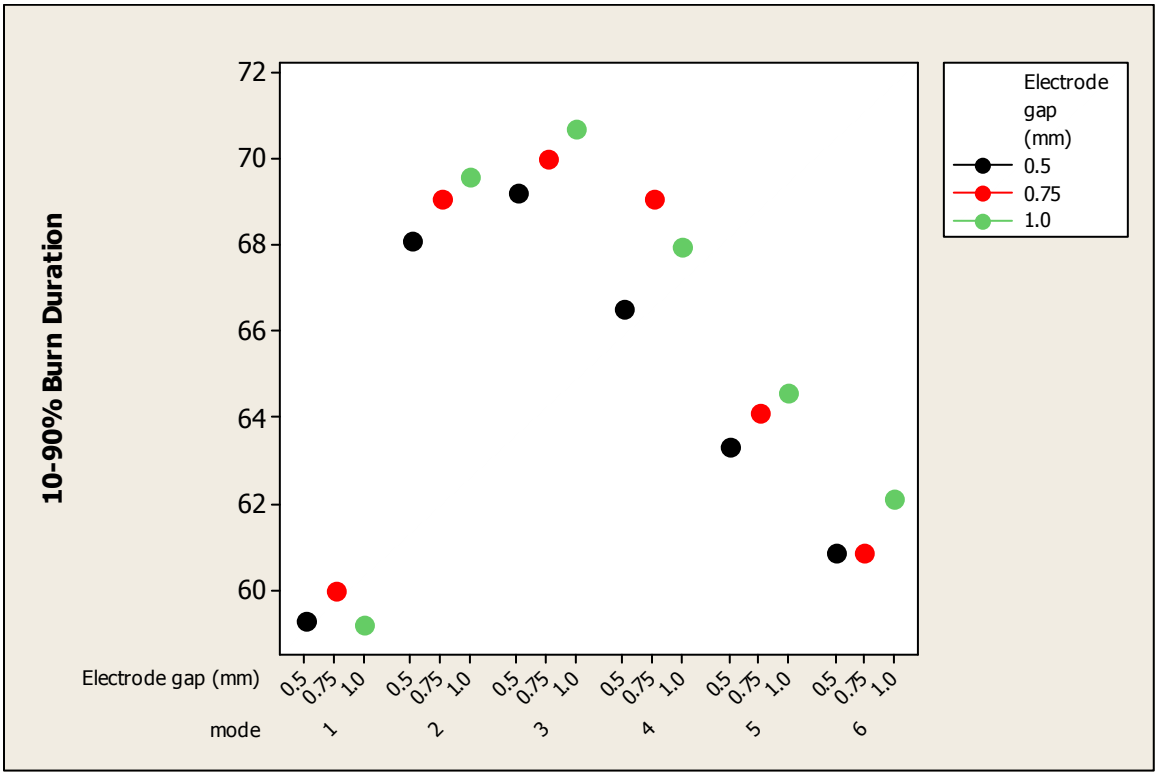

Figure 16: Interval plot of 10-90% burn duration vs. electrode gap and engine mode; OEM spark plug.

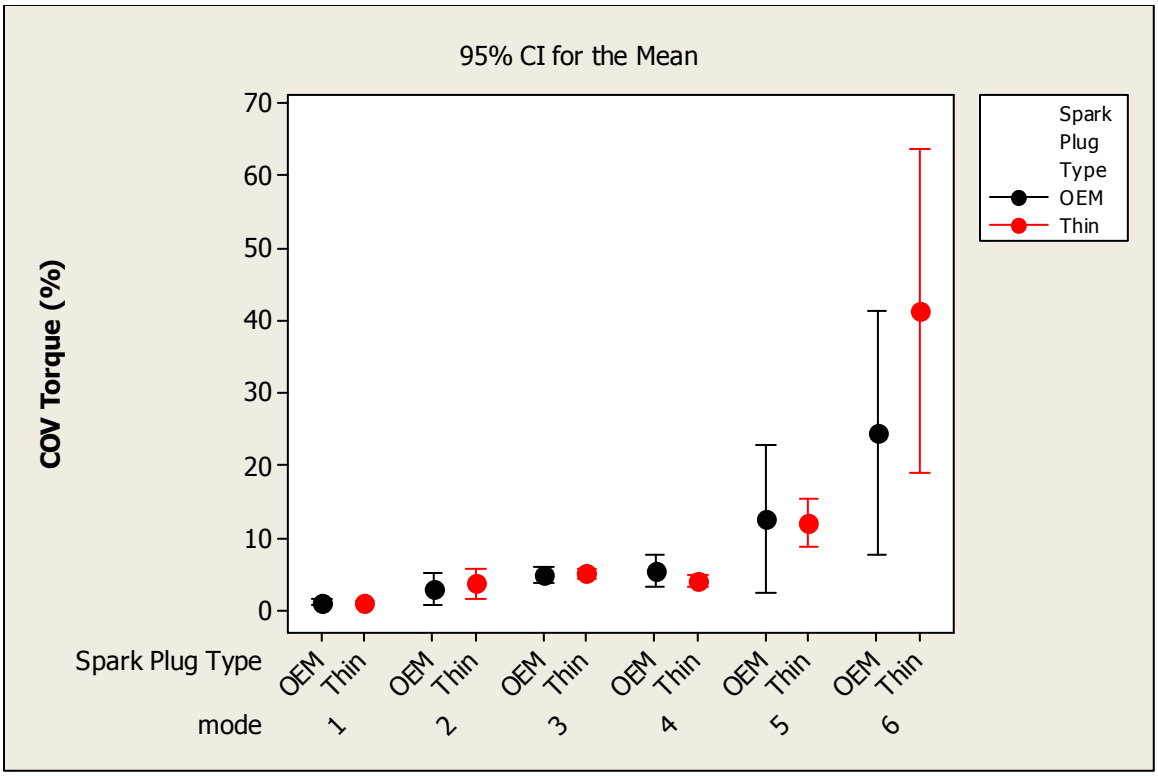

Figure 17: Interval plot of cov torque (%) vs. spark plug type and engine mode.

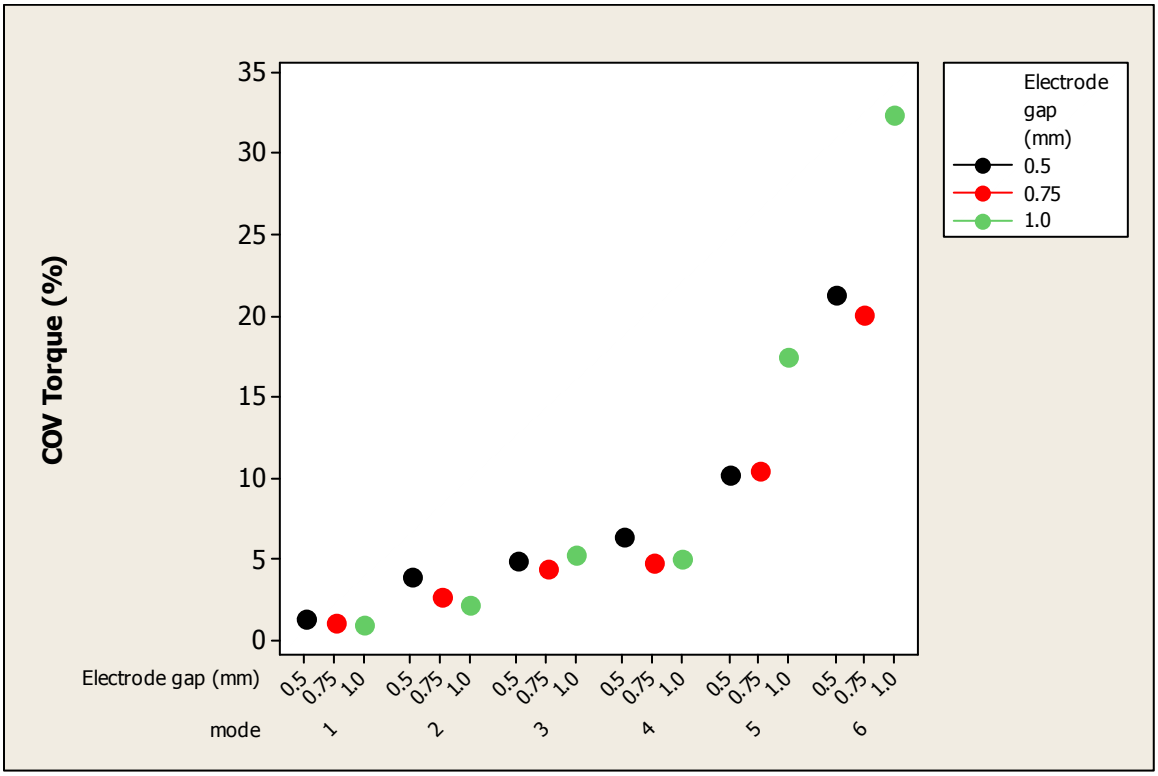

Figure 18: Interval plot of cov torque (%) vs. electrode gap and engine mode; OEM spark plug.

Charge stratification:

The last parameter investigated in this study was the effect of charge stratification on cyclic variability in combustion. This was achieved by using a fuel injector with higher fuel flow, as shown in Figure 21. It was hypothesized that if a higher quantity of fuel is injected over a small crank angle duration, it would prevent better mixing of the air and fuel, causing inhomogenity in the air-fuel charge. In other words promote charge stratification. Therefore, even though the overall air-fuel ratio in the combustion chamber is lean, a stratified pocket can be created that has a rich air-fuel ratio. Depending on the mean air motion of the charge in the combustion chamber, a successful ignition of the stratified charge can help create a stable flame front. As seen in Figure 22, the flame initiation stage (0-10% burn) shows no improvement due to a high flow fuel injector, but there is a significant reduction in the flame propagation duration (10-90% burn). This suggests that the flame initiation stage is strongly dependent on the sparking characteristics but the main combustion duration is more influenced by the mixture composition, in this case a fuel rich stratified charge in created in the combustion chamber due to the high flow injector.

Emissions optimization:

The following discussion is focussed on the effects of the above discussed factors, i.e., spark plug related, load control and charge stratification, on the engine-out ($HC+NO_x$) and CO emissions. Figure 23 shows the comparison between the OEM and the 'Thin' spark plugs for ($HC+NO_x$) emissions. The mean engine-out ($HC+NO_x$)

emissions for the OEM spark plug is about 12 % lower than the 'Thin' spark plug. Figure 24 shows the comparison between the OEM and the 'Thin' spark plugs for CO emissions. The mean engine-out CO emissions for the OEM spark plug is about 6 % higher than the 'Thin' spark plug. The OEM spark plug shows higher variability in Torque as a function of electrode gap, than the 'Thin' spark plug, as shown in Figure 25. Within each spark plug type, 0.75 mm spark gap shows the least variability in Torque. A similar comparative study was carried out with the OEM injector and the high flow injector. Both cases were run with the same spark plug and spark gap. From Figures 26-28 it is evident that the high flow injector has lower engine-out emissions both in terms of ($HC+NO_x$) and CO. The variability in torque is also less as compared to the OEM fuel injector. Figure 29 is the comparison between the baseline engine configuration and the lean strategy in terms of COV in torque. This comparison is an indicator whether the lean strategy can be accepted as a feasible approach for operating the engine. It can be seen that across all engine operating modes the lean strategy is comparable to the baseline engine configuration.

From the experimental findings and the discussion above it is evident that lean engine operation can be a feasible solution to reduce engine-out emissions. Based on the response of the combustion chamber of the test engine in the present study, an optimization study was conducted for minimizing ($HC+NO_x$) and CO separately. The findings are presented in Table 7 below. It is observed that it is possible to achieve very close values for ($HC+NO_x$) as per the EPA phase III guidelines of 8.0 g/kW-hr for class II small non-road engines.

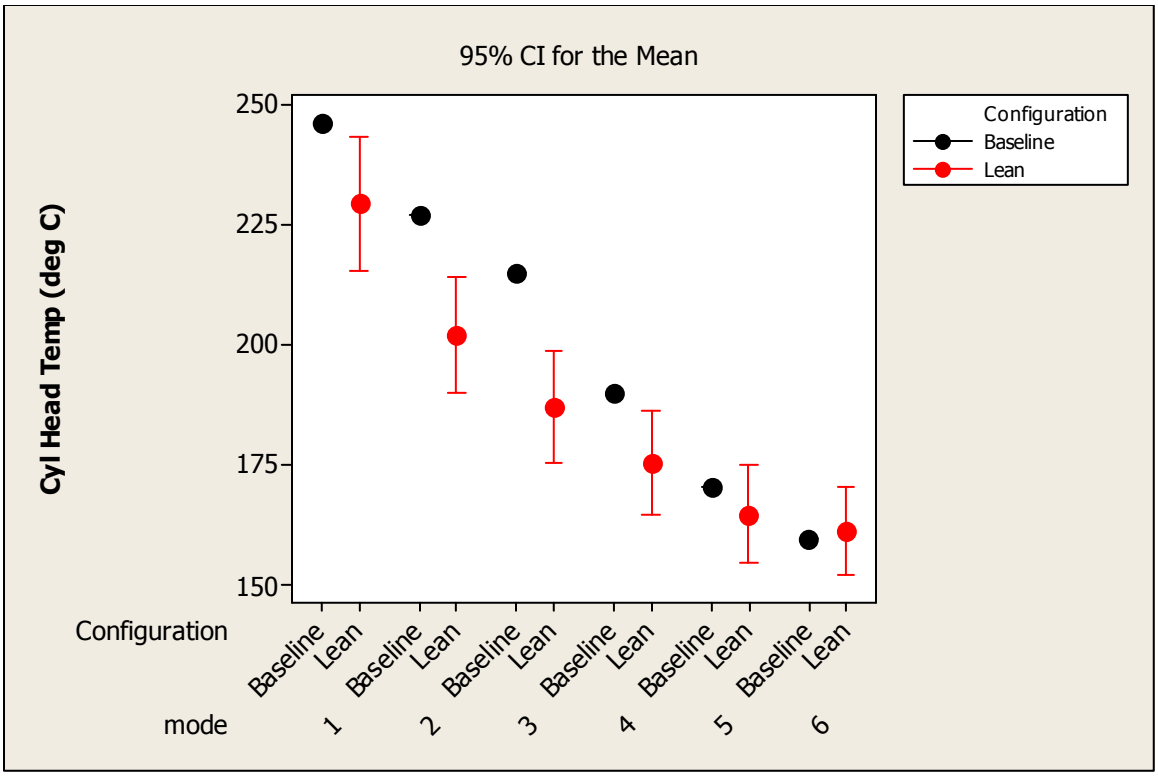

Figure19: Interval plot of cylinder head temp (deg C) vs. engine mode.

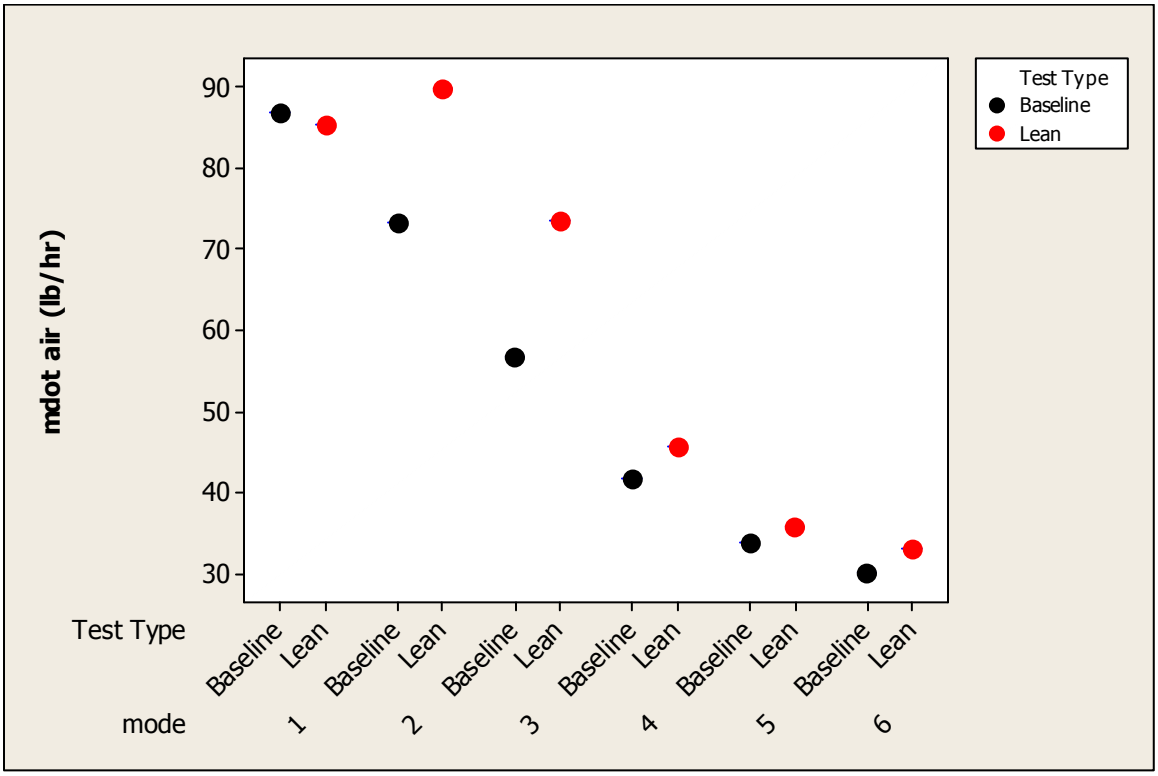

Figure20: Interval plot of air mass flow rate (lb/hr) vs. engine mode.

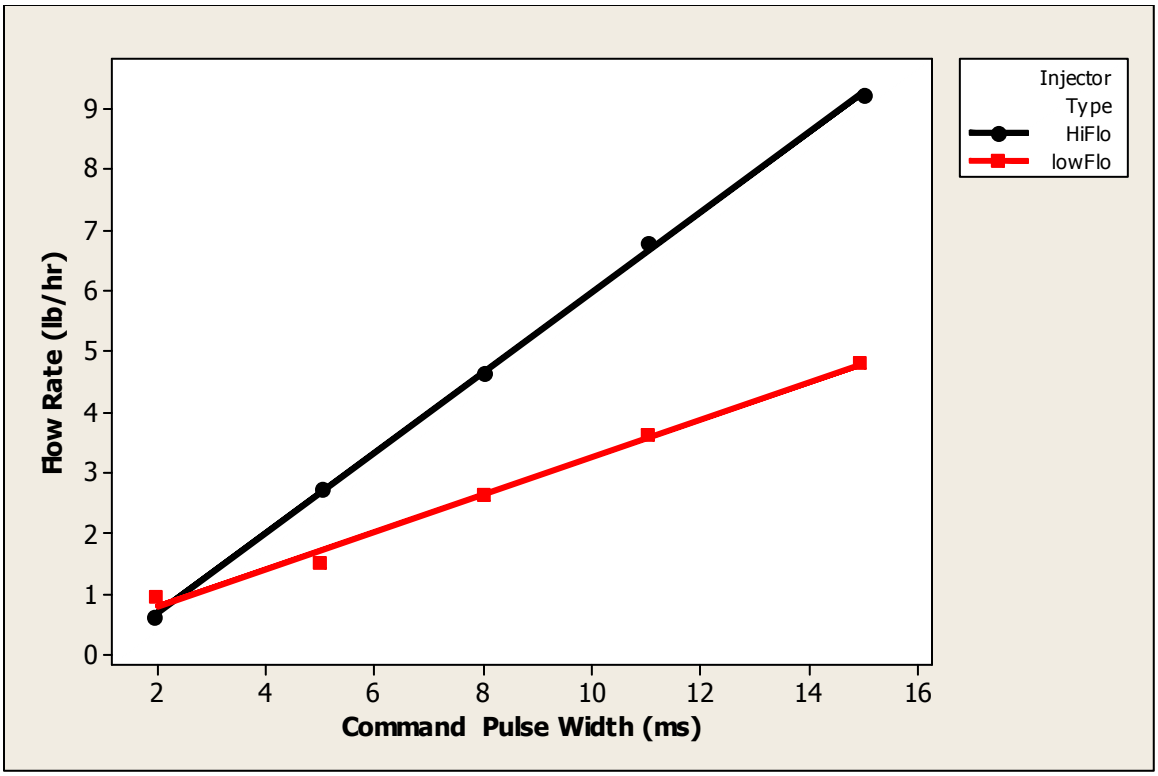

Figure21: Plot of injector fuel flow rate (lb/hr); OEM (low flow) vs. high flow.

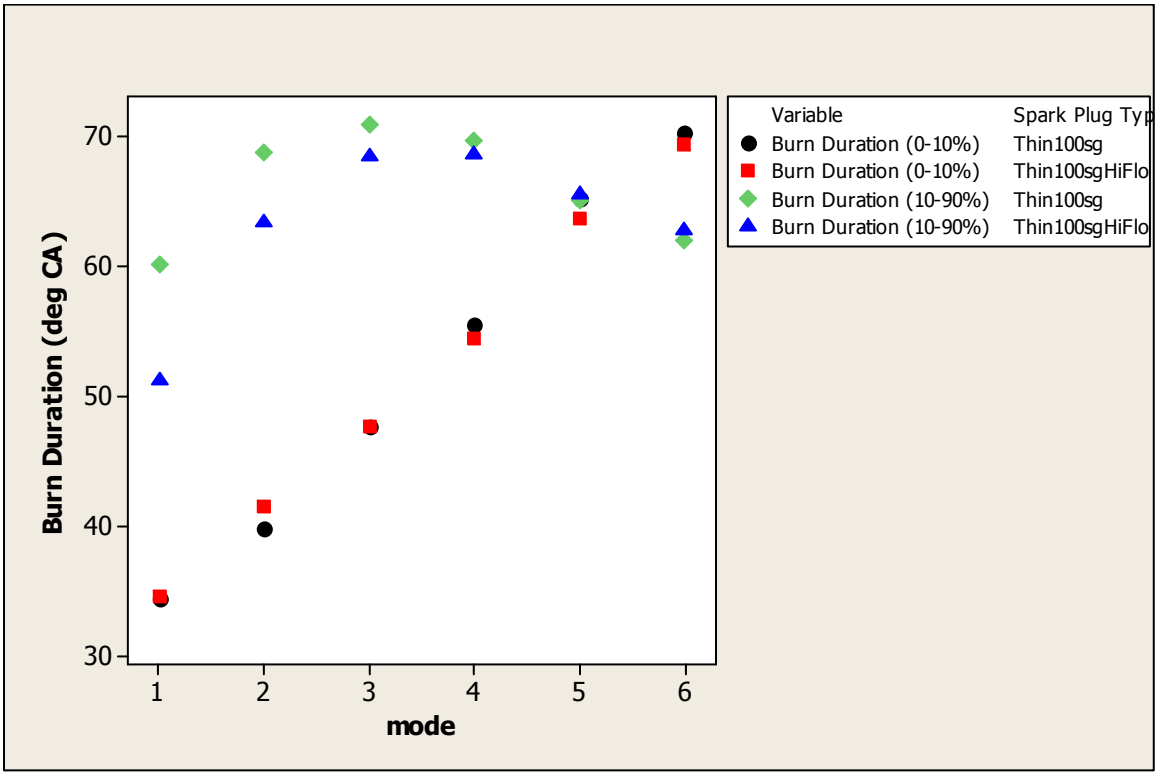

Figure22: Plot of burn duration; OEM vs. high flow injector.

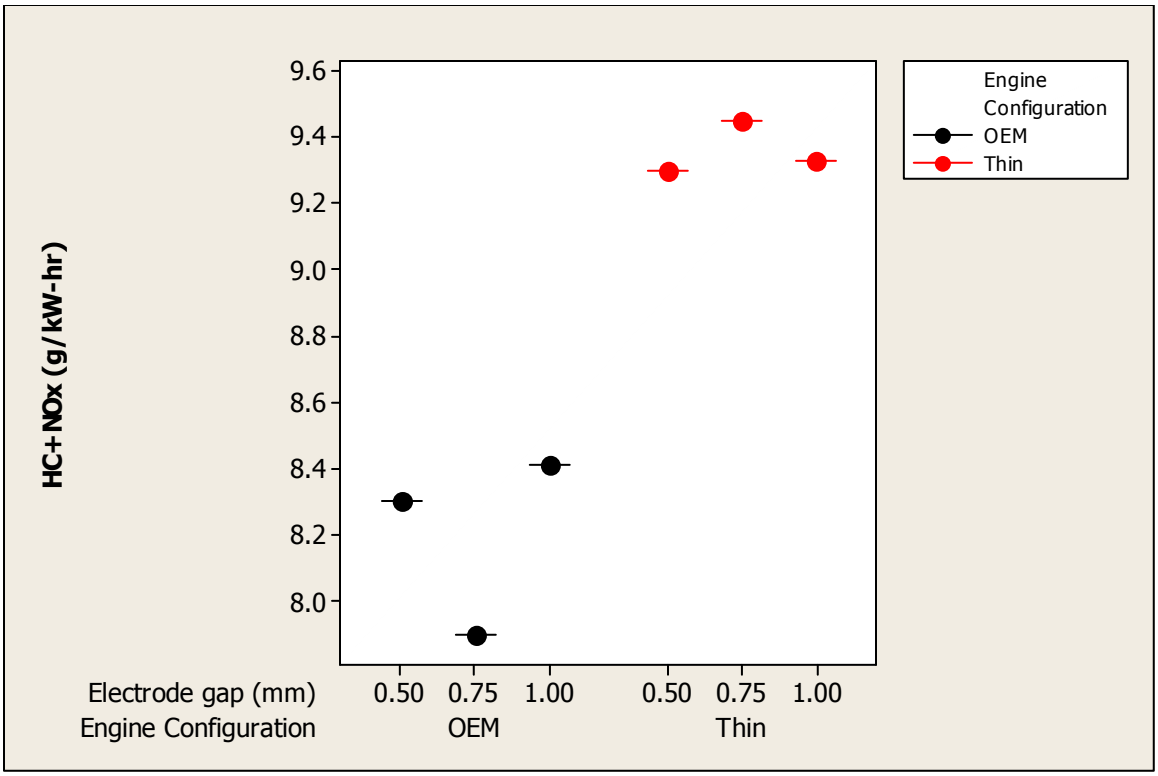

Figure 23: Interval plot of ($HC+NO_x$) (g/kW) vs. spark plug type, electrode gap.

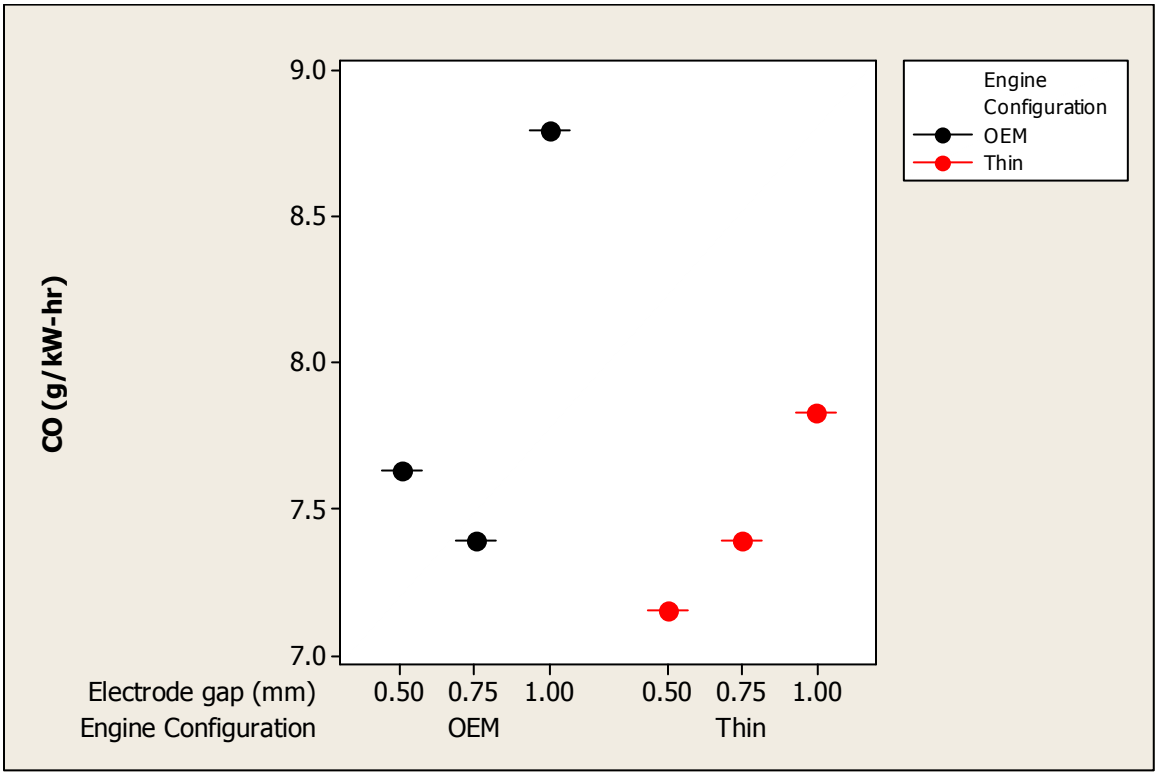

Figure 24: Interval plot of CO (g/kW) vs. spark plug type, electrode gap.

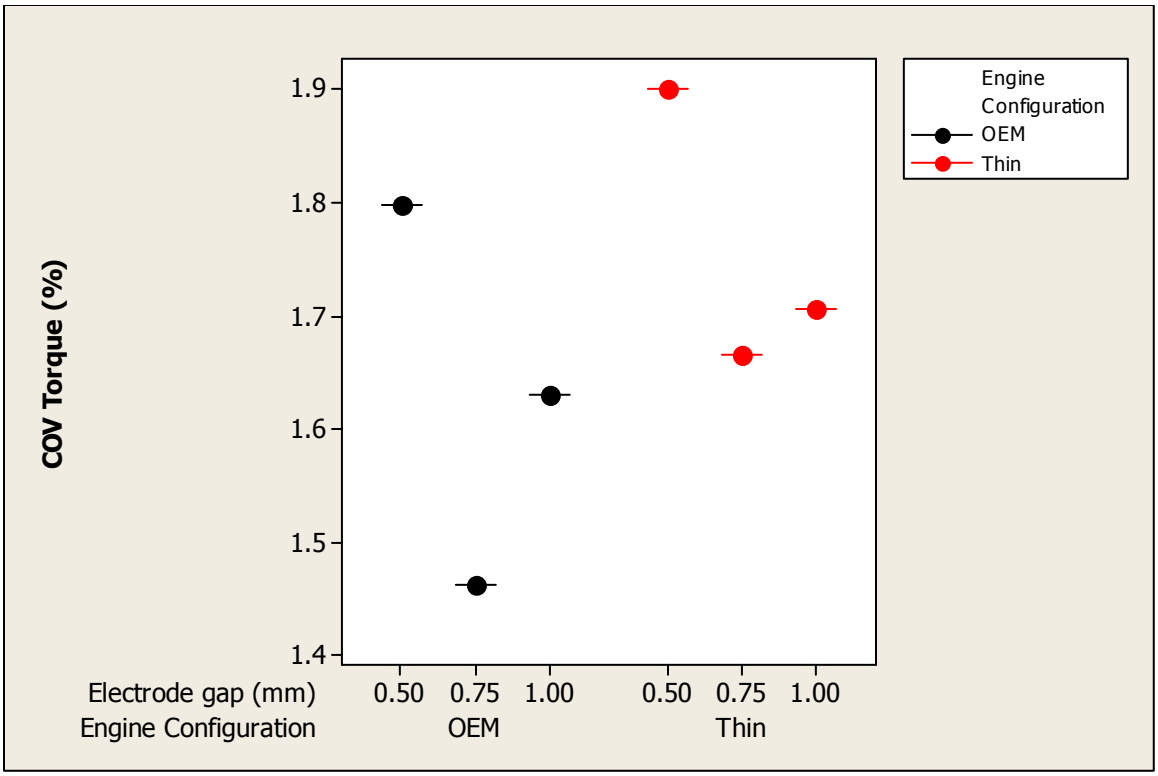

Figure 25: Interval plot of cov torque (%) vs. spark plug type, electrode gap .

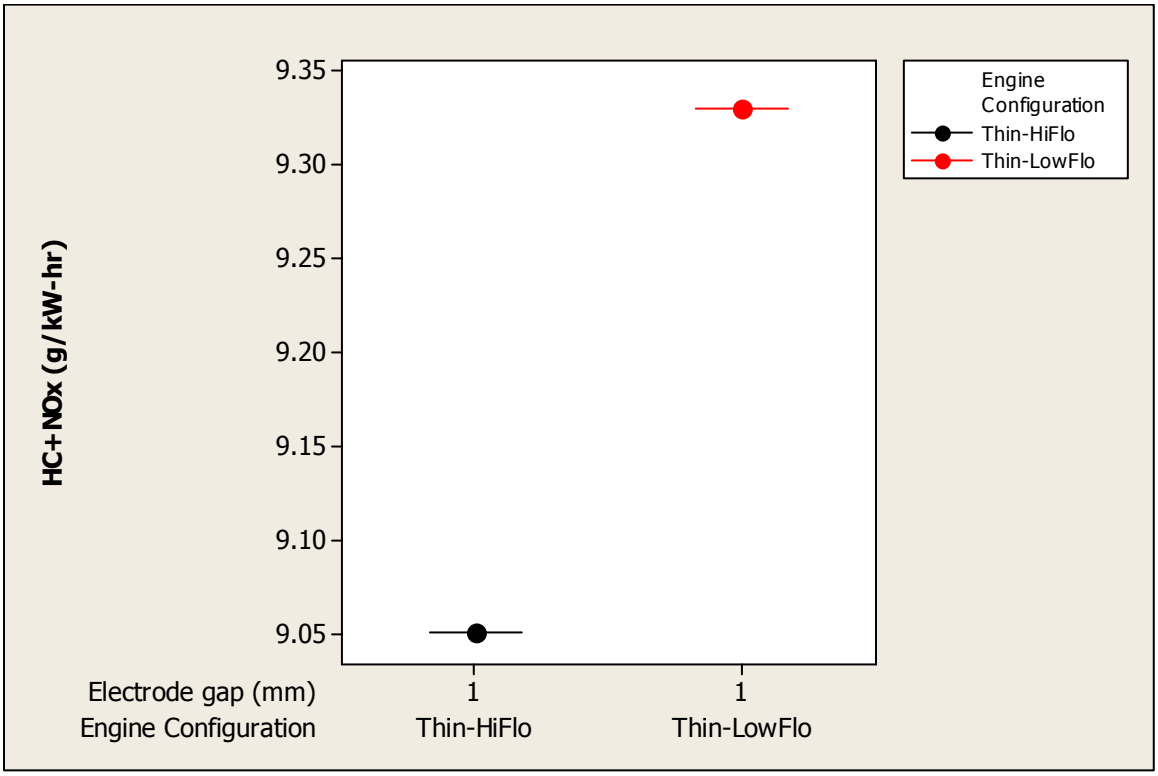

Figure 26: Interval plot of ($HC+NO_x$) (g/kW) vs. injector type, electrode gap.

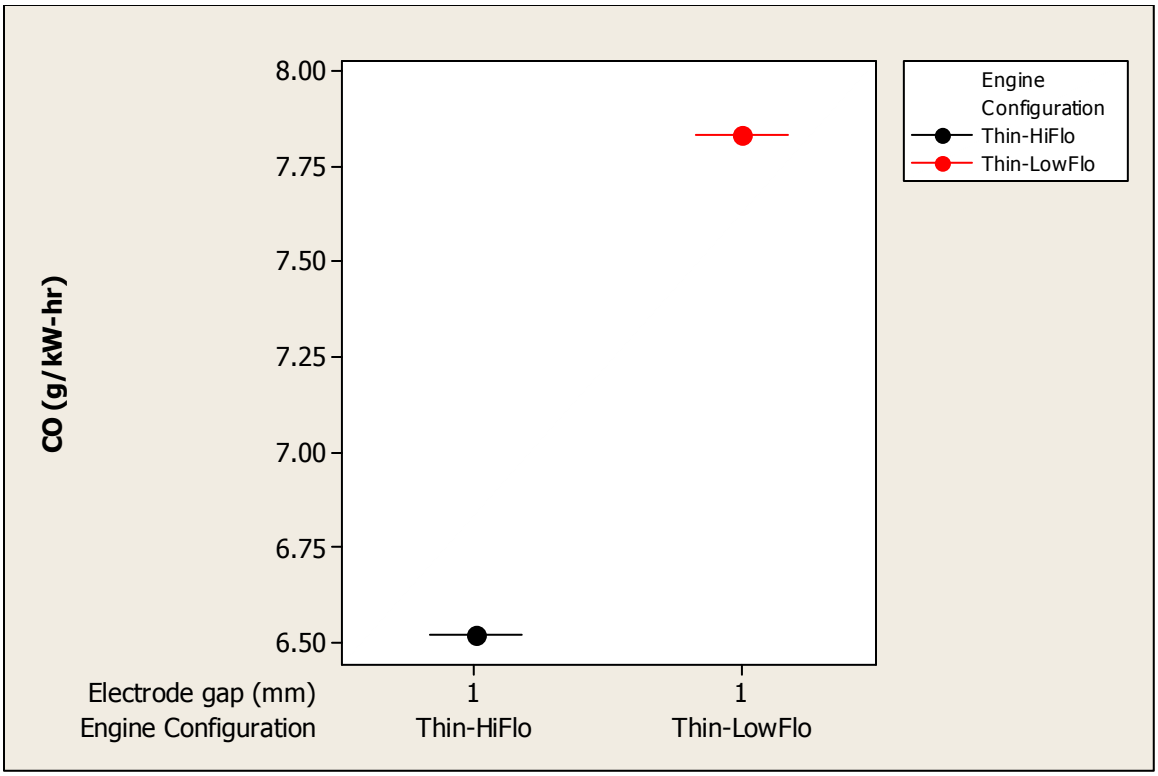

Figure 27: Interval plot of CO (g/kW) vs. injector type, electrode gap.

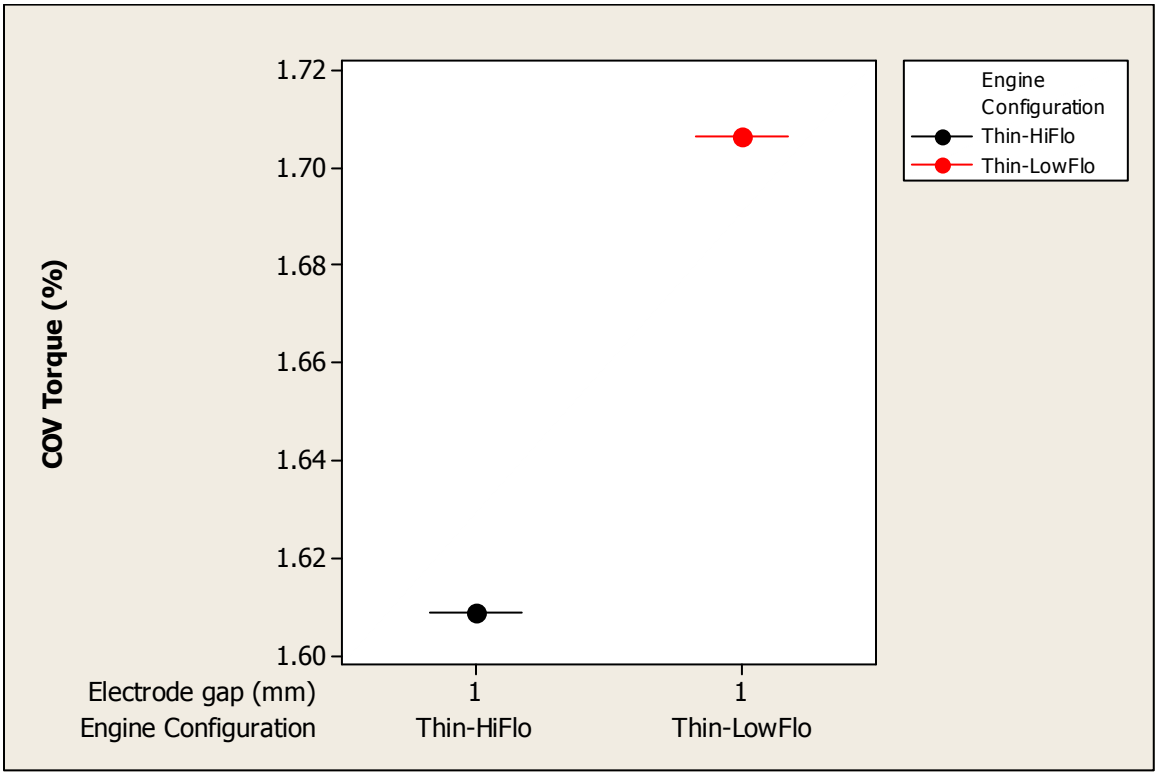

Figure 28: Interval plot of cov torque (%) vs. injector type, electrode gap .

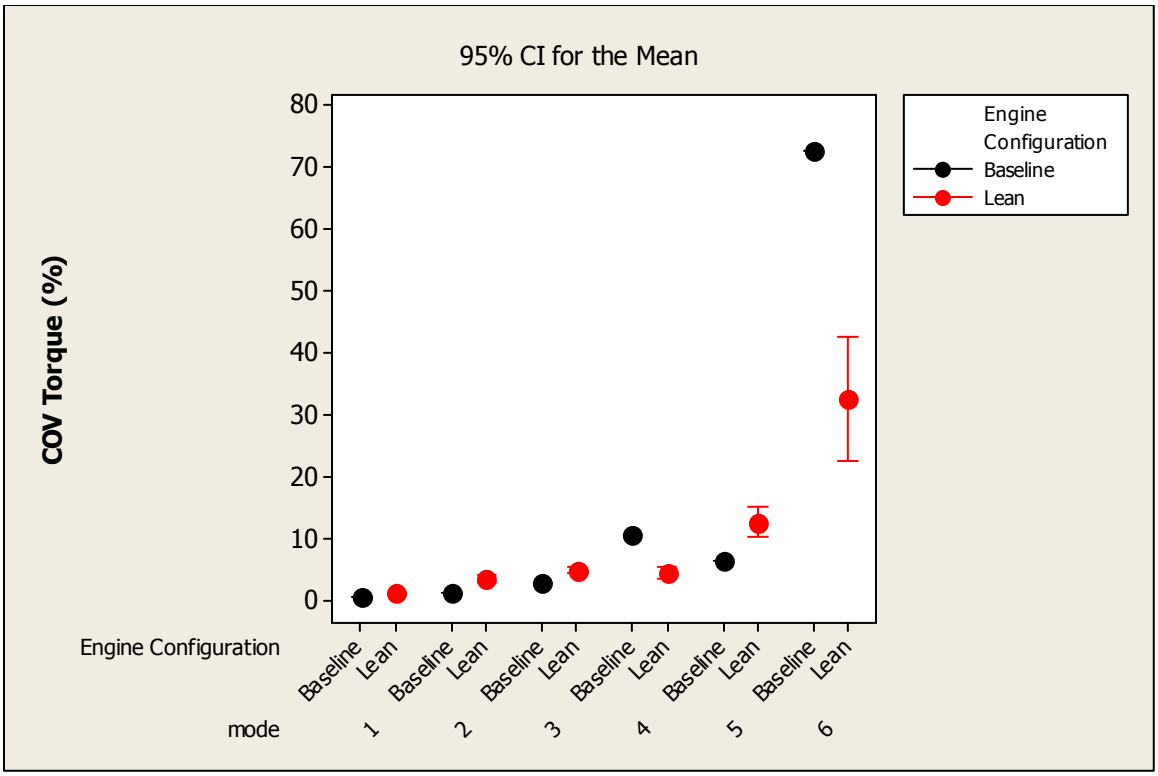

Figure 29: Interval plot of cov torque (%) vs. engine configuration, engine mode.

This suggests that there is enough room for engine optimization without the use of expensive catalytic converters to reduce engine-out emissions, although catalytic converters can help in further reducing the engine-out emissions to lower levels.

Table 7: Strategies to optimize ($HC+NO_x$) and CO emissions

Engine Configuration	Mode	SA	AFR	Engine Power (kW)	Weighting Factor	$HC+NO_x$ (g/kW-hr)	CO (g/kW-hr)	Fuel Consumption (lb/hr)
Baseline	1	25	13.4	8.26	0.09	12.8	218.6	1.060
	2	25	13.8	6.27	0.20			
	3	25	14.2	4.04	0.29			
	4	25	12.8	2.15	0.30			
	5	25	12.2	0.86	0.07			
	6	25	11.8	0.05	0.05			
Lean Strategy- HC+NOx optimization	1	25	14.6	7.47	0.09	8.0	6.9	1.002
	2	32	17.6	5.85	0.20			
	3	32	17.6	3.72	0.29			
	4	32	15.2	2.21	0.30			
	5	28	16.0	0.78	0.07			
	6	30	15.7	0.10	0.05			
Lean Strategy- CO optimization	1	25	14.6	7.50	0.09	10.2	6.0	1.012
	2	20	16	5.68	0.20			
	3	32	17.6	3.72	0.29			
	4	32	15.2	2.21	0.30			
	5	28	16	0.78	0.07			
	6	30	16.5	0.22	0.05			

Conclusions

The main findings of this experimental study can be summarized as below;

- Minimum ignition energy requirements depend on the spark plug type. Although only one type of ignition system (TCI) was used in the current study, it was evident that the OEM spark plug had higher minimum energy requirements as compared to the 'Thin' electrode spark plug.
- The COV of torque varied significantly as a function of spark plug electrode diameter. The OEM spark plug had a higher variation in COV of torque as a function of electrode gap than the 'Thin' electrode spark plug. Both types of spark

plug showed lower COV of torque at 0.75 mm electrode gap as compared to 0.5 mm and 1.0 mm electrode gap.

- The minimum ignition energy is a function of the gas pressure as verified by the decreasing ignition energy requirements with decreasing engine load for both spark plug types.
- The 0-10% burn duration increases with decreasing load, increasing the COV of torque suggesting that initiating a stable flame gets harder with decreasing charge density.
- Although the burn duration for complete combustion increases with increasing AFR, it is still possible to achieve an acceptable COV of torque at higher engine loads by increasing the volumetric efficiency of the engine.
- Charge stratification can be achieved by injecting fuel over shorter crank angle duration with the help of high flow fuel injectors. Although no effect was noticed on the 0-10% burn duration, a significant reduction in the 10-90% burn duration was observed, indicating a faster burn cycle. This also translated in the reduction of COV of torque.
- An engine derate strategy was applied in which mode 1 (highest load) was reduced by about 9.5%. By doing this the engine could be operated at higher AFR as compared to baseline engine configuration at mode 1. With this approach not only the cylinder head temperature could be controlled within limits while running at higher AFR, but also engine-out CO emissions was reduced by 85% at mode 1.

- An engine operation optimization study showed that EPA phase III limits of 8.0 g/kW-hr for ($HC+NO_x$) for class II small non-road engines can be achieved without the use of catalytic converters to reduce engine-out emissions. It was also shown that a reduction of about 97% in engine-out CO can be achieved with the application of lean strategy and an overall fuel economy gain of about 6% can be obtained.

CHAPTER 3

THE DIRECT INJECTION FLAT HEAD (DIFH) ENGINE – A NOVEL APPROACH TO LEAN COMBUSTION.

Abstract

Flat head engines lost their commercial popularity because of their inferior emission and engine performance as compared to OHV engines when operated in the premixed combustion mode. A novel approach to lean combustion in a flat head engine is proposed by directly injecting gasoline fuel into the combustion chamber. The main advantage of the direct injection flat head (DIFH) engine over the conventional GDI engine is its simplicity in design, low cost and, greater flexibility in placement of key engine performance hardware in the cylinder head.

Introduction

Major automotive manufacturers have directed their attention toward gasoline direct injection (GDI) engines in a bid to improve fuel efficiency and reduce exhaust emissions. Conventionally, GDI technology has only been applied to OHV engines. One of the major disadvantages of an OHV GDI engine is that the cylinder head is overcrowded with various components leaving little room for spark plug/fuel injector placement optimization. At part load conditions during GDI engine operation, the fuel is

injected late during the compression stroke. Due to the high fuel pressure the fuel droplets possess significant momentum; some of the droplets with high momentum impinge onto the cylinder wall and form a fuel film on the cylinder wall. This is called fuel wall wetting. Fuel wall wetting pose a challenge in UHC emissions as well as lubricating oil dilution. The fuel film on the cylinder wall mixes with the lubricating oil film on the cylinder wall causing dilution of the lubricating oil with gasoline. In the direct injection flat head (DIFH) engine concept the injected fuel is not directed towards the cylinder. Thus fuel wall wetting can be reduced significantly [46].

Inability to operate at higher compression ratios and poor engine-out emissions were two important reasons for abandoning flat head engines many years ago. The major design factor that affected both is the long combustion chamber design. High compression ratio compounded with poor fuel quality in years past lead to end gas auto ignition and engine knocking. Flame quenching at the far end of the combustion chamber away from the spark plug was responsible for high (UHC) emissions. Modern advancement in fuel quality and computer control of engine operation, along with improvements already made in GDI technology, creates new potential for the flat head engine. Intense turbulence created in the combustion chamber of a flat head engine due to squish is presumed to be an advantage in the stratified charge combustion process. The squish effect is significantly higher in the DIFH engine design than in OHV GDI engines. This is clearly evident from the schematic diagram of the DIFH engine shown in Figure 30 (Also shown as FIG. 1, as published in the patent application. Similarly, Figures 31 and 32 refer to FIG.2 and FIG.3 as published in the patent application), which shows a minimal gap between part of the cylinder head and piston at top dead center whereas in

conventional OHV GDI engines there is always a clearance volume over the piston, defined by the compression ratio of the engine. The advantages offered by this concept are: (1) greater freedom in spark plug/fuel injector placement for engine performance and emissions optimization, (2) unlike in OHV GDI engines, there is minimal piston and cylinder wall wetting caused by the impinging fuel spray, the former contributing to undesirable engine-out emissions particularly at part load conditions and the latter causing lubricant oil contamination, (3) a compact and light engine results because there is no valve train mechanism on the cylinder head, which requires less intricate casting/machining operations and yields lower manufacturing costs.

The following document is a copy of the PCT application for the DIFH engine design. The author of this dissertation is also the primary inventor of the DIFH engine design. The DIFH engine research forms the major bulk of this dissertation and the experimental study of the DIFH combustion system is described in chapter 4.

CROSS-REFERENCE TO RELATED APPLICATIONS

[0001] This application claims benefit of U.S. Provisional Application No. 60/889,678, filed February 13, 2007, which is hereby incorporated herein by reference in its entirety.

FIELD OF THE INVENTION

[0002] The present invention relates to an internal combustion engine. More specifically, the invention relates to a direct injection flathead engine.

BACKGROUND OF THE INVENTION

[0003] The term flathead engine refers to an internal combustion engine with valves placed in the cylinder block beside the piston, instead of in the cylinder head, as in an overhead valve engine. The design was common on early engine designs, but has since fallen from use.

[0004] Generally the flathead uses a small chamber on one side of the cylinder to carry the valves. This has a number of advantages, primarily making the cylinder head much simpler. It also means a valve can be operated by pushing directly up on it, as opposed to needing some sort of mechanical arrangement to push it down or to drive overhead cams, as on a "valve-in-head" engine. It may also lead to slightly easier cooling, as valve and pushrods are out of the way of the cylinder, making a cooling jacket simpler to construct.

[0005] The advantage of the flathead engine lies in its simplicity of design. There are

fewer moving parts as compared to conventional over-head valve ("OHV") engines. This not only makes it very simple and relatively inexpensive to manufacture, but also reduces maintenance costs. The flathead engine was discontinued despite these advantages, mainly because of poor emissions characteristics. In conventional stoichiometric flathead spark ignited engines, the fuel is premixed with air outside the engine. This air-fuel mixture is then inducted into the engine and combusted inside the combustion chamber. The flathead engine typically has a long combustion chamber, in which the spark plug is located at one end. The flame initiated at the spark plug sometimes gets quenched at the cold walls before it can reach the other end of the combustion chamber. This leads to unburned hydrocarbon ("UHC") emissions.

[0006] The direct injection spark ignited engines were developed in the early 1900s' and were known as the Hesselman engines. In the early days the technology for high pressure gasoline injection was not developed enough to handle the low lubricity of gasoline. With major advancement in the area of high pressure fuel injection, direct injection gasoline engine technology is being revisited. A large number of automotive manufacturers have already come out with direct injection gasoline engine powered production vehicles, all of them based on OHV engine design. The basic idea behind the direct injection gasoline engine is charge stratification. Instead of premixing the fuel and air outside the engine as in conventional stoichiometric spark ignited gasoline engines, gasoline is directly injected into the combustion chamber. The gasoline spray is aimed at a cavity on top of the piston which deflects the fuel spray towards the spark plug, thus forming a localized cloud of rich air-fuel mixture around the spark plug. This is known as charge stratification. This stratified charge is easily ignited by the spark plug. Thus, although the air-fuel ratio is

rich near the spark plug, the overall air-fuel ratio is lean. The deflection of the fuel spray from the top of the piston crown causes a thin film of fuel to form on the piston surface. This is called wall wetting and due to the cooler piston temperature it is difficult to vaporize this fuel film in time to take part in combustion. This is one major source of UHC emissions.

[0007] What is needed is an engine with the benefits of the flathead engine, that does not have the negative emissions characteristics nor problems with efficiency.

SUMMARY OF THE INVENTION

[0008] The present invention relates to a direct injection flathead engine. In one aspect of the invention, the flathead engine comprises an internal combustion cylinder block comprising at least one fuel injector positioned substantially transverse to the cylinder axis A_c. The engine also comprises at least one exhaust valve positioned substantially near the at least one fuel injector, where the exhaust valve is on the same side of the piston as the fuel injector.

[0009] In one aspect, a fuel injector is positioned substantially transverse to the cylinder axis Ac, whereby a substantial portion of the fuel may be sprayed on top of the hot exhaust valve and deflected towards the spark plug, thus forming a stratified charge around the spark plug. This helps to minimize the formation of fuel film and largely helps in fuel vaporization and better combustion, thereby reducing UHC emissions. This tends to alleviate the emissions problem experienced in OHV direct injection gasoline engines and still enjoy the advantage of better engine performance at higher fuel economy.

[0010] These and other objects of the present invention will be clear when taken in view of the detailed specification and disclosure in conjunction with the appended figures.

DETAILED DESCRIPTION OF THE DRAWINGS

[0011] The accompanying drawings, which are incorporated in and constitute a part of this specification, illustrate certain aspects of the instant invention and together with the description, serve to explain, without limitation, the principles of the invention. Like reference characters used therein indicate like parts throughout the several drawings.

[0012] Fig. 1 is a cross-sectional view of the invention for direct fuel injection flathead engine, showing one aspect of the piston, fuel injector and spark plug arrangement;

[0013] Fig. 2 is the top plan view of the cylinder block of the flathead engine of Fig. 1;

[00141 Fig. 3 is the bottom plan view of the cylinder head of the flathead engine of Fig. 1

DETAILED DESRIPTION OF THE INVENTION

[0015] The present invention may be understood more readily by reference to the following detailed description of the invention and the Examples included therein and to the Figures and their previous and following description.

[0016] Before the present systems, articles, devices, and/or methods are disclosed and described, it is to be understood that this invention is not limited to specific systems, specific devices, or to particular methodology, as such may, of course, vary. It is also to be understood that the terminology used herein is for the purpose of describing particular embodiments only and is not intended to be limiting.

[0017] The following description of the invention is provided as an enabling teaching of the invention in its best, currently known embodiment. To this end, those skilled in the relevant art will recognize and appreciate that many changes can be made to the various aspects of the invention described herein, while still obtaining the beneficial results of the present invention. It will also be apparent that some of the desired benefits of the present invention can be obtained by selecting some of the features of the present invention without utilizing other features. Accordingly, those who work in the art will recognize that many modifications and adaptations to the present invention are possible and can even be desirable in certain circumstances and are a part of the present invention. Thus, the following description is provided as illustrative of the principles of the present invention and not in limitation thereof.

[0018] As used in the specification and the appended claims, the singular forms "a," "an" and "the" include plural referents unless the context clearly dictates otherwise. Thus, for example, reference to "a fuel injector" includes two or more such fuel injectors, and the like.

[0019] Ranges can be expressed herein as from "about" one particular value, and/or to "about" another particular value. When such a range is expressed, another embodiment includes from the one particular value and/or to the other particular value. Similarly, when values are expressed as approximations, by use of the antecedent "about," it will be understood that the particular value forms another embodiment. It will be further understood that the endpoints of each of the ranges are significant both in relation to the other endpoint, and independently of the other endpoint. It is also understood that there are a number of values disclosed herein, and that each value is also herein disclosed as

"about" that particular value in addition to the value itself. For example, if the value "10" is disclosed, then "about 10" is also disclosed. It is also understood that when a value is disclosed that "less than or equal to" the value, "greater than or equal to the value" and possible ranges between values are also disclosed, as appropriately understood by the skilled artisan. For example, if the value "10" is disclosed the "less than or equal to 10"as well as "greater than or equal to 10" is also disclosed. It is also understood that throughout the application, data is provided in a number of different formats and that this data represents endpoints and starting points, and ranges for any combination of the data points. For example, if a particular data point "10" and a particular data point 15 are disclosed, it is understood that greater than, greater than or equal to, less than, less than or equal to, and equal to 10 and 15 are considered disclosed as well as between 10 and 15. It is also understood that each unit between two particular units are also disclosed. For example, if 10 and 15 are disclosed, then 11, 12, 13, and 14 are also disclosed.

[0020] "Optional" or "optionally" means that the subsequently described event or circumstance may or may not occur, and that the description includes instances where said event or circumstance occurs and instances where it does not.

[0021] The present invention relates to a direct injection flathead engine. In one aspect of the invention, the flathead engine comprises an internal combustion cylinder block 100 that has at least one cylinder 200 defining an interior cavity 210. The cylinder block 100 also defines an exhaust port 300 and an intake port 400 adjacent to the cylinder 200 on a first side of the cylinder block. The exhaust port 300 has an exhaust valve 310 disposed therein, and the intake port 400 has an intake valve 410 disposed therein.

[0022] In one aspect, the direct fuel injection flathead engine also comprises a cylinder head 500 substantially coveting the cylinder block. In another aspect, the engine comprises a combustion chamber 600 that is defined by portions of the cylinder head 500, the cylinder block 100, and the top faces 312, 412 of the exhaust and intake valves. In this aspect, the distal end 610 of the combustion chamber 600 is in fluid communication with a portion of the interior cavity 210 of the cylinder.

[0023] In another aspect, the engine also comprises an ignition device 700 at least partially disposed therein the cylinder head and in communication with a portion of the combustion chamber. As one skilled in the art can appreciate, the ignition device 700 may be, for example and not meant to be limiting, a conventional spark plug, or similar spark producing device.

[0024] In yet another aspect, the engine comprises at least one fuel injector 800 positioned in a fuel injector plane P_f substantially transverse to the cylinder axis A_c. The at least one fuel injector 800 is configured to inject fuel into the combustion chamber substantially toward the ignition device. By "toward," it is meant that the fuel injector injects fuel in the general direction of the ignition device such that at least a portion of the fuel comes in close proximity to the spark.

[0025] In one aspect of the invention, the exhaust valve is configured to move between a closed position and an open position, where, in the closed position, at least a portion of the top face of the exhaust valve 310 protrudes into the combustion chamber 600. The same may be true for the intake valve 410. In another aspect, the fuel injector plane P_f bisects the combustion chamber into an upper portion and a lower portion. In this aspect, the ignition device 700 is positioned in the upper portion 620 of the combustion chamber

600 and the exhaust valve is positioned in the lower portion 630 of the combustion chamber. In use, a substantial portion of the fuel may be sprayed from the fuel injector 800 on top of the hot exhaust valve 310 and deflected towards the ignition device 700, thus forming a stratified charge around the ignition device. This helps to minimize the formation of fuel film and largely helps in fuel vaporization and better combustion, thereby reducing UHC emissions. This also tends to alleviate the emissions problem experienced in OHV direct injection gasoline engines and still enjoys the advantage of better engine performance at higher fuel economy.

[0026] One aspect of the cross sectional arrangement of flathead engine is shown in Fig. 1. In this aspect, the fuel would be injected into the combustion chamber 600 as the piston 220 moves towards top dead center ("TDC"). The ignition device 700, which may be positioned substantially over the exhaust valve 310, as described herein above, fires after the fuel is injected into the combustion chamber.

[0027] In one aspect, the cylinder block 100 and the cylinder head 500 can be air cooled. In another aspect, the cylinder head can be liquid cooled. As one skilled in the art will appreciate any conventional cooling system will be used as appropriate and usually depends on the size and application of the engine.

[0028] In another aspect, a conical spray pattern single hole fuel injector 800 may be used. In this aspect, high pressure fuel is delivered to the injector inlet 8 through a high pressure fuel pump, driven directly by the engine. In yet another aspect, a slit nozzle injector may be used in lieu of the conical spray injector. The nozzle plane may be substantially parallel to the cylinder axis. In still another aspect, an air-assisted fuel injector may be used. The injection of air along with fuel increases the volumetric

efficiency of the engine and increases the turbulence inside the combustion chamber, which results in more complete combustion.

[0029] In still another aspect, the fuel injector 800 may be placed over the exhaust valve and directed towards the intake valve. The fuel injector may also be placed over the intake valve and directed towards the exhaust valve. In this aspect, the ignition device 700 may be located over the exhaust valve 310 or the intake valve. As one skilled in the art can appreciate, more than one ignition device may be present. For example, and not meant to be limiting, there may be a ignition device 700 positioned over the exhaust valve and one over the intake valve.

[0030] Although several embodiments of the invention have been disclosed in the foregoing specification, it is understood by those skilled in the art that many modifications and other embodiments of the invention will come to mind to which the invention pertains, having the benefit of the teaching presented in the foregoing description and associated drawings. It is thus understood that the invention is not limited to the specific embodiments disclosed herein above, and that many modifications and other embodiments are intended to be included within the scope of the appended claims.

[0031] Moreover, although specific terms are employed herein, as well as in the claims which follow, they are used only in a generic and descriptive sense, and not for the purposes of limiting the described invention, nor the claims which follow.

What is claimed is:

1. A direct fuel injected flathead engine comprising: a cylinder block comprising at least one cylinder defining an interior cavity and having a longitudinal cylinder axis, wherein the cylinder block defines an exhaust port and an intake port adjacent to the at least one

cylinder and on a first side of the cylinder block; an intake valve having a top face and being disposed therein the intake port; an exhaust valve having a top face and being disposed therein the exhaust port; a cylinder head substantially covering the cylinder block; a combustion chamber defined by portions of the cylinder head, the cylinder block, the top face of the intake valve, and the top face of the exhaust valve, the combustion chamber having a proximal end and an opposed distal end, wherein the distal end of the combustion chamber is in fluid communication with a portion of the interior cavity of the cylinder; an ignition device at least partially disposed therein the cylinder head and in communication with a portion of the combustion chamber; and a fuel injector positioned in a fuel injector plane substantially transverse to the cylinder axis, wherein the fuel injector is configured to inject fuel into the combustion chamber substantially toward the ignition device.

2. The direct fuel injected flathead engine of claim 1, wherein the exhaust valve is configured to move between a closed position and an open position, and wherein, in the closed position, at least a portion of the top face of the exhaust valve protrudes into the combustion chamber.

3. The direct fuel injected flathead engine of claim 2, wherein the fuel injector plane bisects the combustion chamber into an upper portion and a lower portion; and wherein the ignition device is positioned in the upper portion of the combustion chamber and the exhaust valve is positioned in the lower portion of the combustion chamber.

4. The direct injected flathead engine of claim 3, wherein, in use, at least a portion of the fuel from the fuel injector deflects off of a portion of the top face of the exhaust valve and is directed upward and toward the ignition device.

5. The direct fuel injected flathead engine of claim 1, wherein the intake valve is configured to move between a closed position and an open position, and wherein, in the closed position, at least a portion of the top face of the intake valve protrudes into the combustion chamber.

6. The direct fuel injected flathead engine of claim 5, wherein the fuel injector plane bisects the combustion chamber into an upper portion and a lower portion; and wherein the ignition device is positioned in the upper portion of the combustion chamber and the intake valve is positioned in the lower portion of the combustion chamber.

7. The direct injected flathead engine of claim 6, wherein, in use, at least a portion of the fuel from the fuel injector deflects off of a portion of the top face of the intake valve and is directed upward and toward the ignition device.

8. The direct injection flathead engine of claim 1, wherein the ignition device is a spark plug.

9. The direct injection flathead engine of claim 1, wherein the fuel injector is a conical spray injector.

10. The direct injection flathead engine of claim 1, wherein the fuel injector is a slit nozzle injector defining a slit for egress of fuel.

11. The direct injection flathead engine of claim 10, wherein the slit is substantially parallel to the cylinder axis.

12. The direct injection flathead engine of claim 1, wherein the fuel injector is an air assisted fuel injector.

13. A direct fuel injected flathead engine comprising: a cylinder block comprising at least one cylinder defining an interior cavity and having a longitudinal cylinder axis, wherein

the cylinder block defines an exhaust port and an intake port adjacent to the at least one cylinder and on a first side of the cylinder block; an intake valve having a top face and being disposed therein the intake port; an exhaust valve having a top face and being disposed therein the exhaust port; a cylinder head substantially coveting the cylinder block; a combustion chamber positioned on the first side of the cylinder axis defined by at least portions of the cylinder head, the cylinder block, the top face of the intake valve, and the top face of the exhaust valve, the combustion chamber having a proximal end and an opposed distal end that is in fluid communication with a portion of the interior cavity of the cylinder; a plurality of ignition devices at least partially disposed therein the cylinder head and in communication with a portion of the combustion chamber; and a fuel injector positioned in a fuel injector plane substantially transverse to the cylinder axis the fuel injector configured to inject fuel into the combustion chamber substantially toward the plurality of ignition devices.

14. The direct fuel injected flathead engine of claim 13, wherein the exhaust valve is configured to move between a closed position and an open position, and wherein, in the closed position, at least a portion of the top face of the exhaust valve protrudes into to the combustion chamber.

15. The direct fuel injected flathead engine of claim 14, wherein the fuel injector plane bisects the combustion chamber into an upper portion and a lower portion; and wherein the ignition device is positioned in the upper portion of the combustion chamber and the exhaust valve is positioned in the lower portion of the combustion chamber.

16. The direct injected flathead engine of claim 15, wherein, in use, the fuel from the fuel injector deflects off of a portion of the top face of the exhaust valve and is directed upward and toward the pair of ignition devices.

17. The direct fuel injected flathead engine of claim 13, wherein the intake valve is configured to move between a closed position and an open position, and wherein, in the closed position, at least a portion of the intake valve protrudes into to the combustion chamber.

18. The direct fuel injected flathead engine of claim 17, wherein the fuel injector plane bisects the combustion chamber into an upper portion and a lower portion; and wherein the ignition device is positioned in the upper portion of the combustion chamber and the intake valve is positioned in the lower portion of the combustion chamber.

19. The direct injected flathead engine of claim 18, wherein, in use, the fuel from the fuel injector deflects off of a portion of the top face of the intake valve and is directed upward and toward the plurality of ignition devices.

20. The direct injection flathead engine of claim 13, wherein each ignition device of the plurality of ignition devices is a spark plug.

21. The direct injection flathead engine of claim 13, wherein the fuel injector is a conical spray injector.

22. The direct injection flathead engine of claim 13, wherein the fuel injector is a slit nozzleinjector defining a slit for egress of fuel.

23. The direct injection flathead engine of claim 22, wherein the slit is substantially parallel to the cylinder axis.

24. The direct injection flathead engine of claim 13, wherein the fuel injector is an air assisted fuel injector.

25. The direct injection flathead engine of claim 13, wherein the plurality of ignition devices comprises a pair of ignition devices.

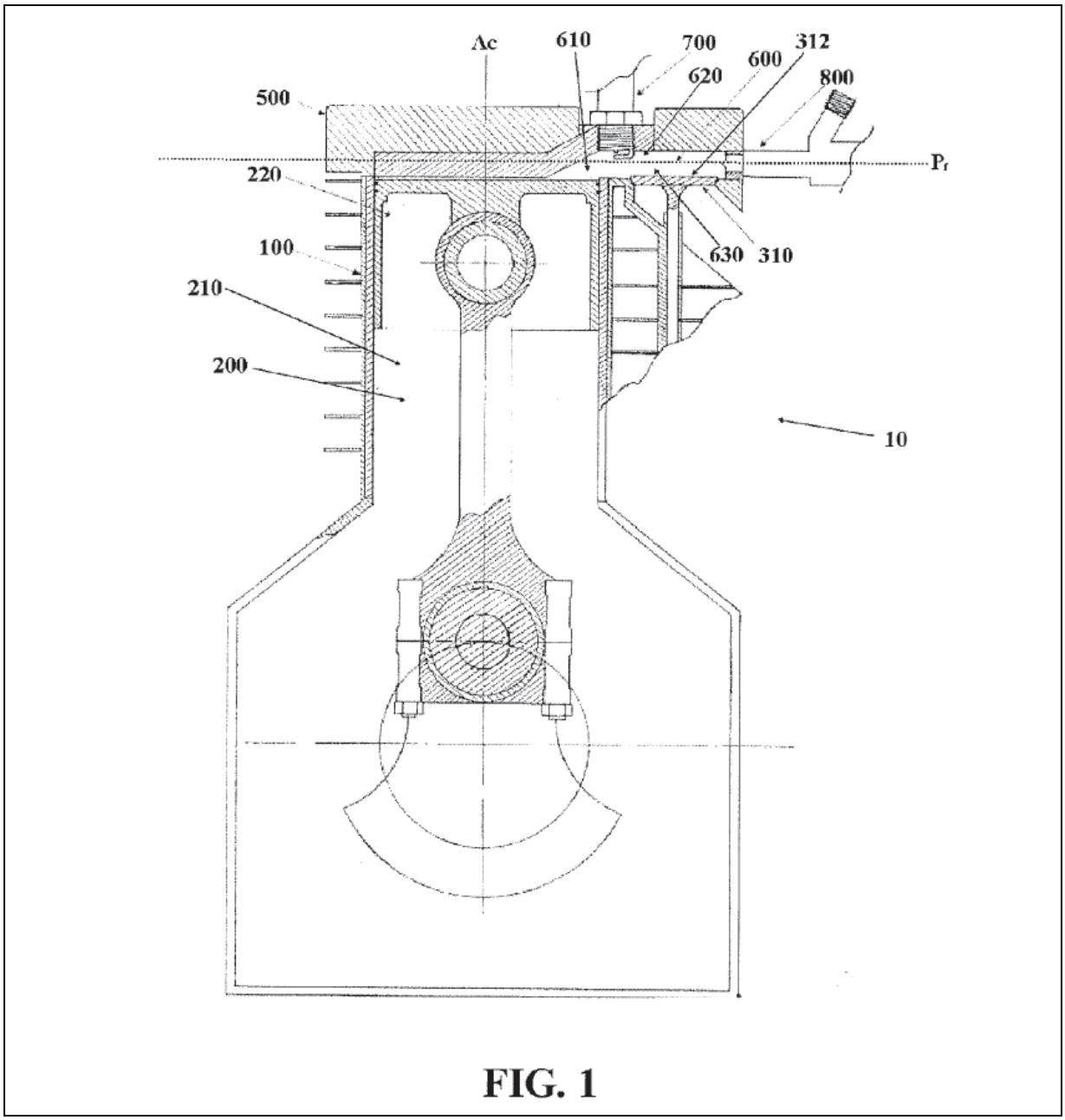

FIG. 1

Figure 30: Cross sectional view of DIFH engine.

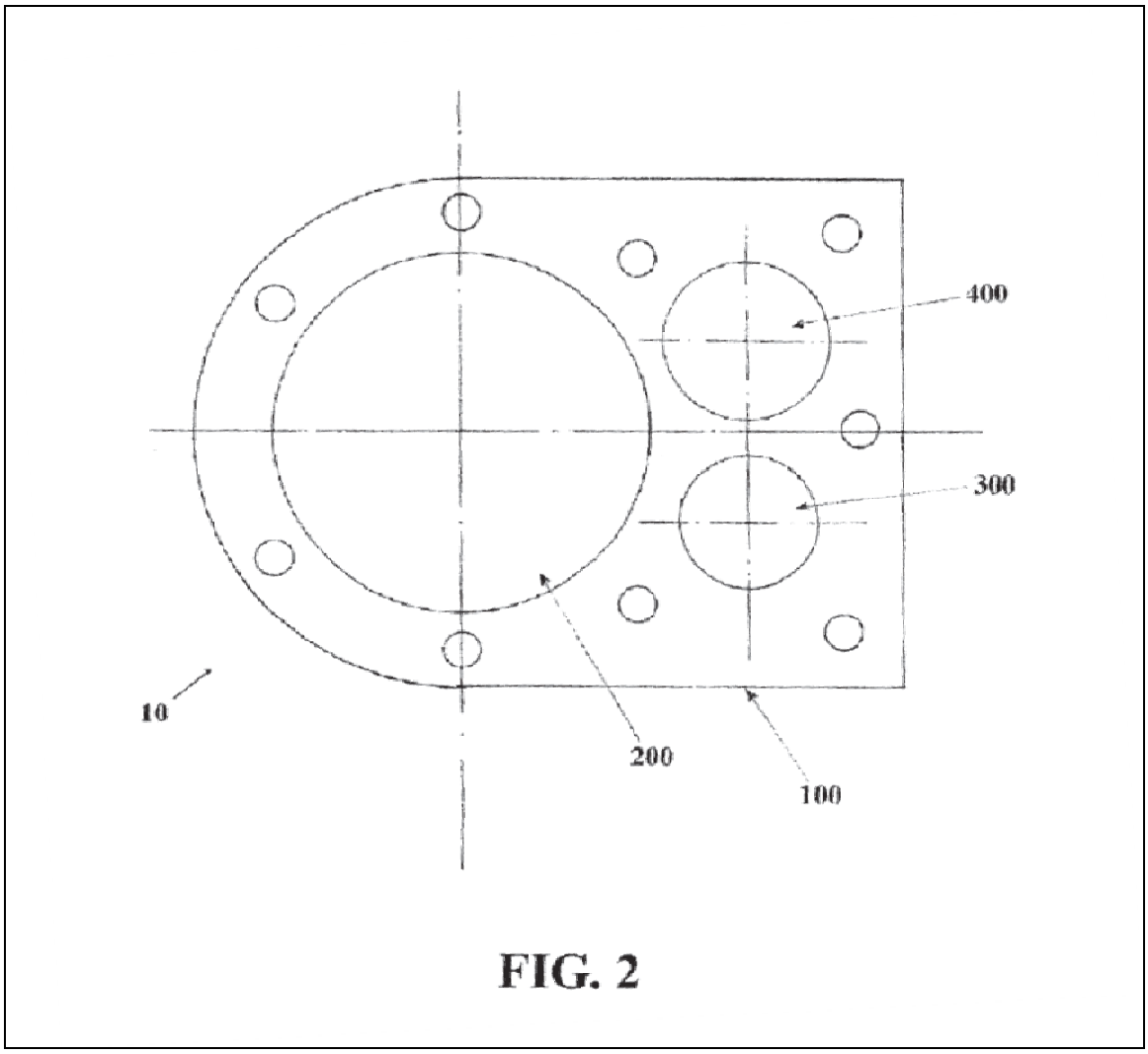

FIG. 2

Figure 31: Plan view of DIFH cylinder block.

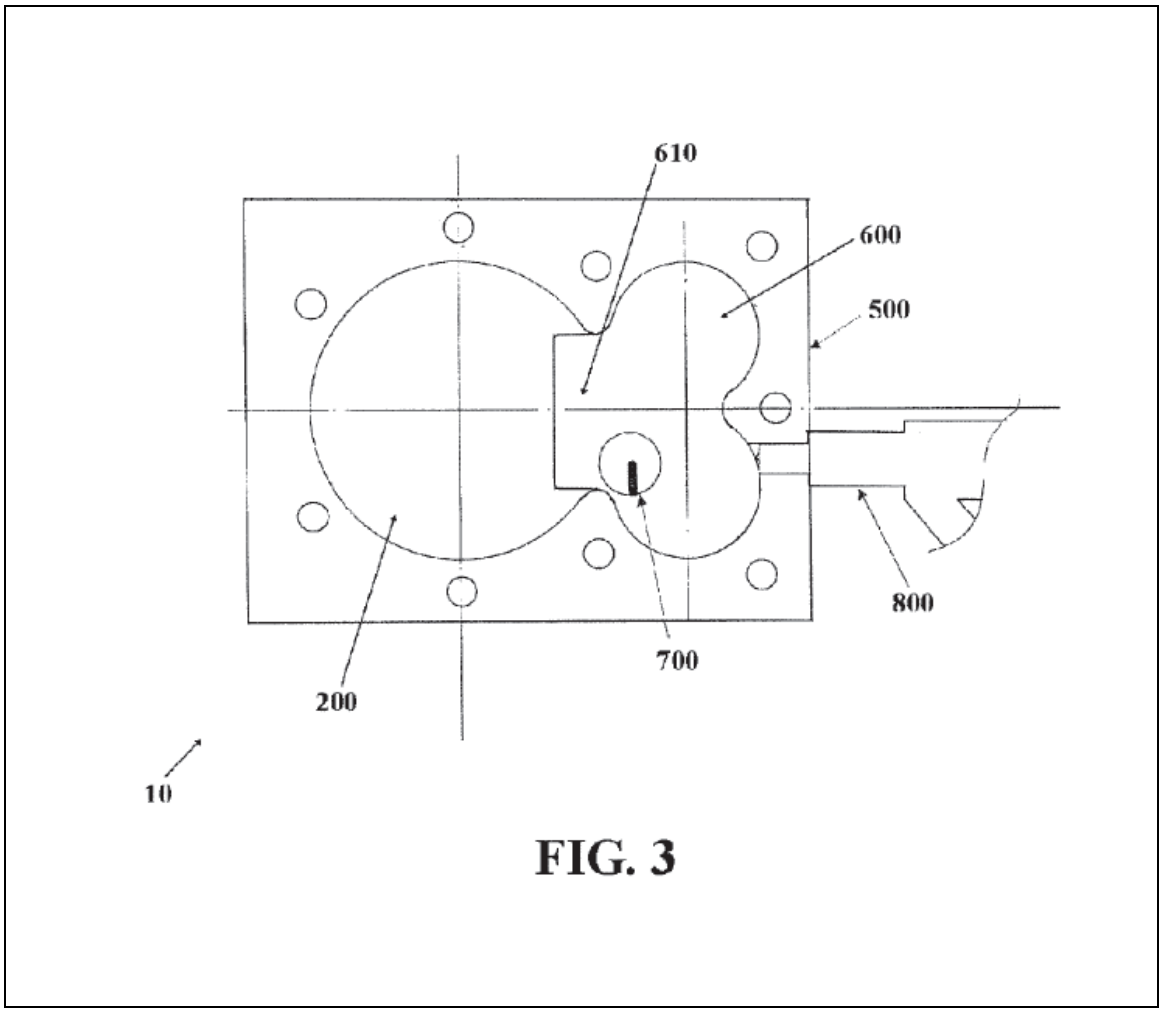

FIG. 3

Figure 32: Plan view of DIFH cylinder head.

CHAPTER 4

EXPERIMENTAL INVESTIGATION OF THE DIRECT INJECTION FLAT HEAD (DIFH) COMBUSTION SYSTEM AND QUANTIFICATION OF IN-CYLINDER FLOW USING TWO DIMENSIONAL PARTICLE IMAGE VELOCIMETRY

Abstract

Investigation of the in-cylinder air motion was carried out using PIV techniques revealing squish as the dominant turbulence generating mechanism in the combustion chamber of the DIFH engine. Although the DIFH engine produced about 8 times more UHC emissions as compared to the conventional spark ignited OHV engines, it produced about 5 times less CO emissions as compared to the OHV engine and showed a 16% improvement in brake specific fuel consumption. The current combustion chamber has a dual chamber design exhibiting both, premixed and stratified combustion mechanisms causing complex undesirable interactions between key engine performance parameters. A new combustion chamber design is proposed to reduce the key engine parametric interactions.

Introduction

In-cylinder gas flow has a profound influence on engine performance, and turbulence plays the most important part in this. During the beginning of the 20th century,

pioneering work by Ricardo established the influence of turbulence on combustion and heat transfer in engines. The main disadvantage suffered by the flat-head, side-valve engine in the earlier days could be attributed to a poor combustion chamber design and the low octane rating of gasoline, which initiated knocking at low compression ratios [47]. Although higher octane gasoline later allowed higher compression ratios to be employed in the side-valve engines, the side-valve engines still could not compete with the OHV engines with respect to power output and fuel economy. Poor mixing was one reason for this problem because the effect of turbulence was not well understood at that time until the turbulent head was developed, which introduced squish into the combustion chamber [47]. Squish is a phenomenon where the trapped air is squeezed out from the space between a portion of the piston crown and the bottom surface of the cylinder head. This forces the air out from the squish cavity at a very high velocity. This is another type of in-cylinder air motion like swirl and tumble, discussed previously in the background presented in Chapter 1.

Turbulence is very dependent on the initial conditions of its production, i.e., the inlet manifold conditions. Turbulence is created by converting the mean flow energy into large scale circular air motion, which in turn breaks down into smaller scales until the smallest scale is reached, and the turbulence is then dissipated by the viscous forces into heat. These small scale eddies can be classified as homogeneous (uniform) and isotropic (no preferred direction), characteristic of turbulent flow [43]. These highly turbulent eddies are approximately 10^4 times more effective in the transport of any fluid property, for example momentum and fuel vapor, as compared to molecular transport. This very significantly reduces the mixing times as well as burn times [43]. The contribution of

squish to turbulence occurs towards the end of the compression stroke when the piston nears top dead center (TDC). Squish is presumed to be the most important turbulence generating mechanism in a flat-head engine unlike swirl and tumble, which are the dominant turbulence generators in a conventional OHV GDI engine.

Considering the problems associated with the OHV GDI engine, the direct-injection, flat-head (DIFH) engine combustion chamber seems worth investigating. Figure 33 shows a cross-sectional schematic of a DIFH engine [48]. Figure 34 shows a schematic diagram of a DIFH engine cylinder head. As shown in Fig. 34, the fuel injector can be placed at any of the locations labeled A, B, and C, and the spark plug can be placed at locations D, E or at both. From the discussion in Chapter 1 the importance of a well-mixed charge for an efficient combustion process to occur is well established. This will directly influence the combustion stability, engine power output, and engine-out emissions. Therefore, it is very essential to have turbulence production in the combustion chamber during the concluding stages of the compression process.

In side-valve engines, the air after entering through the inlet valve has to perform two 90° maneuvers before entering the cylinder volume. This reduces the velocity of the incoming air substantially and also the energy of the large scale eddies. As the piston moves towards TDC, the turbulence strength is further debilitated due to turbulent energy dissipation. But in the DIFH engine over 90 percent of the piston surface is covered under the squish area. When the piston nears TDC, the squish forces the air into the main combustion chamber, setting up highly turbulent vortices.

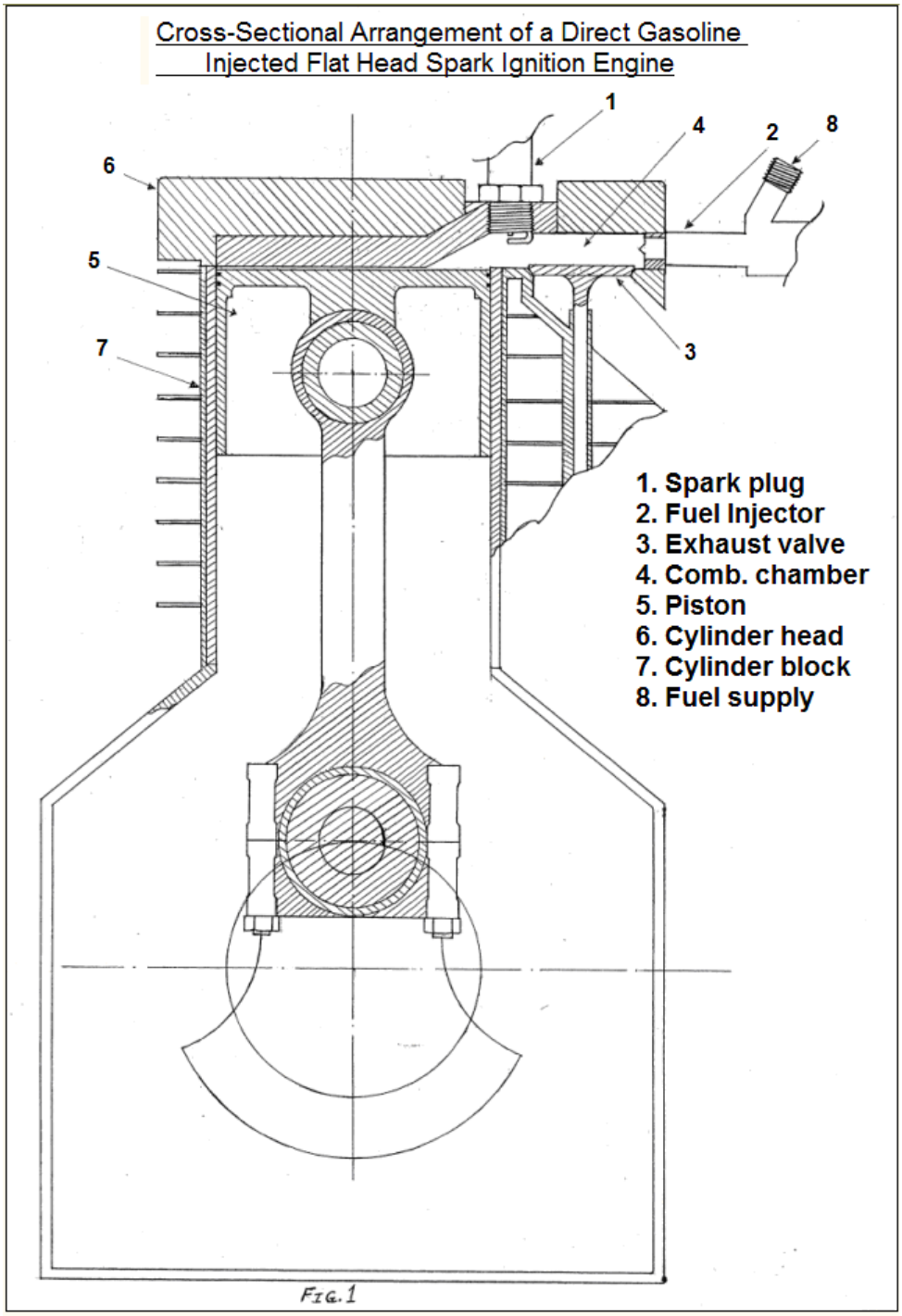

Figure 33: Cross-section of the DIFH engine.

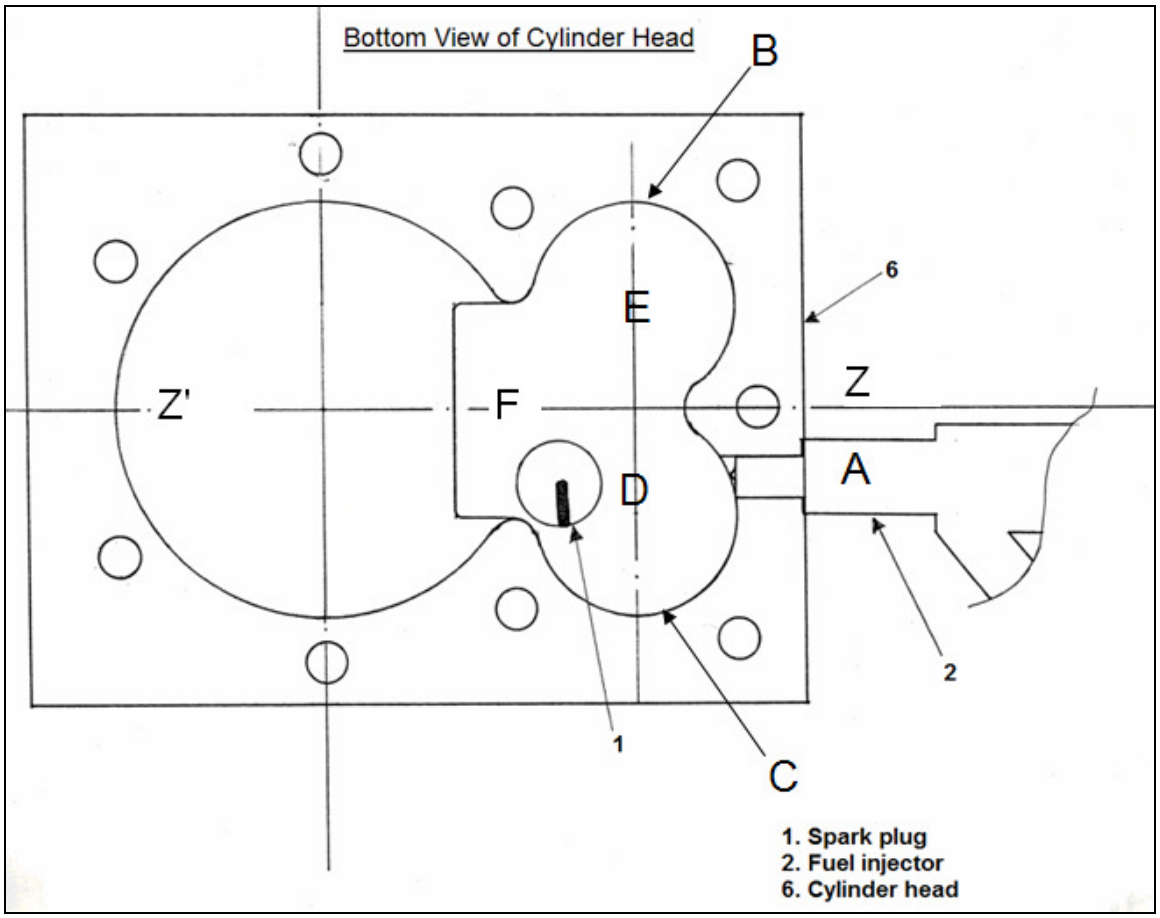

Figure 34: Schematic diagram of the DIFH cylinder head.

With the dual section design of the combustion chamber, the incoming air flow is presumed to be divided and directed into the two sections setting up the swirl type air motion. So the air flow structure will be predominantly swirl, associated with isotropic and uniform small scale eddies. Swirl is known to survive even into the combustion and expansion stroke of the engine process, which is desirable because it will accelerate the burn rate by mixing during combustion.

The DIFH combustion chamber is unsymmetrical and therefore, the in-cylinder air motion cannot be generalized with that of conventional OHV engines. In an OHV engine, the combustion chamber is formed by the cylinder walls and cylinder head on

three sides, and the moving piston surface forms the fourth boundary. Therefore, once the air/mixture enters the cylinder through the inlet valves, it predominantly follows the boundaries set up by this symmetrical volume and establishes a bulk motion, either swirl or tumble. On the contrary, in a DIFH engine there is a very narrow continuum joining the main combustion chamber to the cylinder volume. Considering the time scales (ms) of the compression and combustion events, the air once squished into the main combustion chamber from the cylinder volume sees a practically closed combustion chamber with all sides as fixed boundaries. This is analogous to the pre-chamber of an indirect injection diesel engine. It is already pointed out in Chapter 1 that the changing volume during combustion has a strong effect on the combustion parameters. Therefore, the DIFH combustion chamber and the OHV GDI combustion chamber may be operating under two slightly different combustion environments. The first step to investigate this is by studying the in-cylinder air motion inside a DIFH combustion chamber during the compression stroke. Thus the air motion set up during this event is of particular interest and the focus of this investigation.

Measurements of the in-cylinder flow can be obtained either by point measuring techniques or whole field measuring techniques. Time averaged single-point measurement techniques such as Laser Doppler Velocimetry (LDV) and Hot Wire Anemometry (HWA) provide useful information on in-cylinder flows. HWA may sometimes not be a tool of preference since it is an intrusive process and may affect the fluid dynamics of the actual flow. It also is incapable of predicting the flow direction. However, LDV is non-intrusive and can provide accurate estimates of the fluid velocity and turbulent intensity at a point. The actual fluid motion is highly transient and unsteady

so time averaged data and turbulence estimates by single-point measurement techniques are likely inadequate to completely describe the in-cylinder flow. Therefore, whole field measurement techniques need to be employed to visualize the overall in-cylinder flow process [49, 50].

Particle Image Velocimetry (PIV), Particle Tracking Velocimetry (PTV) and steak photography are some of the methods commonly used by researchers as whole field measurement techniques [50, 51]. In both, PTV and streak photography, individual particles are identified and matched between two consecutive exposures of known time lag in order to obtain particle displacement and velocity. A low seeding density is required to prevent streak crossover and help in particle matching. Because of low seeding density, sparse and randomly distributed velocity vector data are obtained. As a result, significant interpolation or ensemble averaging of many data sets is required to obtain a populated data set. PIV, however, does not require individual particle tracking. In PIV, two laser pulses of very short time interval (~10 μs) are used to record the position of the seed (tracer) particles and statistical correlation is used to determine the mean displacement of the particles in a small region of interest called the interrogation window. Since individual particle imaging is not required, a high particle density can be used, yielding velocity vector data on a closely spaced rectangular grid. In this experimentation PIV was chosen to study the in-cylinder flow process.

Certain parametric fine tuning is required to obtain a good image during PIV analysis. Parameters to be optimized include:

1. Selection of tracer particles.
2. Illumination

3. Time interval between two illuminating pulses.

Selection of tracer particles:

Two important considerations need to be made while selecting the tracer particles. The particles should be able to faithfully follow the flow path and they should have good light scattering properties. The response of the tracer particles to the flow velocity fluctuations depends on the size, shape and density of the particles as well as the density of the fluid. The flow-tracking behavior of the particle is dependent on the density ratio ρ_p/ρ_f and the Stokes number given by Equation 5:

$$N_s = \sqrt{\frac{\nu}{\omega d_p^{\,2}}} \tag{5}$$

where, d_p is the diameter of the particle, ρ_p is the density of the particle, ρ_f is the density of the fluid, ν is the kinematic viscosity of the fluid, and ω is the angular frequency of flow fluctuations. The Stokes number is the ratio of the viscous drag to the particle's inertia. The Stokes number decreases with the increase in angular frequency of the flow fluctuations, decreasing the amplitude ratio, which is defined as the ratio of the flow amplitude to the fluid amplitude. Thus the flow-tracking ability of a particle is a function of its mass [51]. While the scattering efficiency of a particle is directly related to the particle diameter according to Mie's theory, as given in Equation 6:

$$q = \frac{\pi d_p}{\lambda} \tag{6}$$

where, q is a normalized particle diameter that is characteristic of the Mie scattering efficiency and λ is the wavelength [49]. Thus for ideal flow behavior the particles should be as small as possible while they should be large enough for higher scattering efficiency.

As it is difficult to satisfy both criteria, the best tracer materials used in similar studies were found to be hollow plastic micro-spheres. A flow tracking response study done previously showed that about 30-40 μm diameter micro-balloons exhibited the best flow behavior with air as the fluid medium [50]. Plastic micro-spheres with a mean diameter of 40 μm manufactured by Expancel were used in this study as seeding particles.

Illumination:

Pulsed laser is generally used as a light source in PIV experiments. With the use of appropriate image optics, a sheet of light is created to illuminate the plane of interest in the flow field. A uniform spatial distribution of the light intensity on the plane of interest as well as an optimum sheet thickness is essential for proper measurements. A neodymium-doped yittrium aluminum garnet (Nd-YAG) laser was used as the light source in the experiments. The laser is a New Wave Research Gemini 15 hz. The laser contains two Nd-YAG heads that produce 1064 nm wavelength (infra-red), which, is then frequency doubled by a second harmonic generator to produce 532 nm visible light (green). The beam of light produced by the laser exits with a diameter of 5.5 mm which is then converted into a laser sheet using cylindrical lenses.

Time between two illuminating pulses:

One of the methods used for image capture is double frame/double exposure. The exposures are created by the illuminating laser pulses. The camera frames are also taken synchronously with the illuminating pulses. The time between the two pulses should be long enough that a valid estimation of the displacement of the particles can be made and short enough to avoid particles with strong out-of-plane velocity components leaving the

light sheet between two successive illuminations. The duration of each pulse should also be short enough that the motion of the particles is frozen during the pulse exposure in order to avoid any possible blurring due to 'particle streaks.'

The velocity information of the particles can be extracted from the images acquired by statistical correlation techniques. In order to obtain the vector fields; the image is divided into small interrogation windows wherein spatial correlation functions are applied to a particle ensemble belonging to these regions. Two types of correlation functions are generally used; auto-correlation and cross-correlation. In auto-correlation, two images from the first and second exposures are taken on the same frame at times Δt apart. The complete image is subdivided into interrogation windows and each window is evaluated by auto-correlation analysis. In auto-correlation the particles correlate with themselves creating a self-correlation peak, which is the highest peak in the correlation. This self-correlation peak corresponds to a (0,0) location. Further, the auto-correlation function creates two identical correlation peaks rotationally symmetrical about the self-correlation peak representing the positive and negative mean particle image displacements in the interrogation zone as shown in Figure 35. As a result image shifting or other compensatory measures must be employed to resolve the directional ambiguity of the particles [49, 50, 51, 52, 53]. In cross-correlation the scattered light from the first and second exposure of the particles is recorded in two different images. The single peak in Figure 36 represents the component of the cross-correlation function that corresponds to the correlation of images of particles obtained from the first exposure with the identical particles obtained from the second exposure.

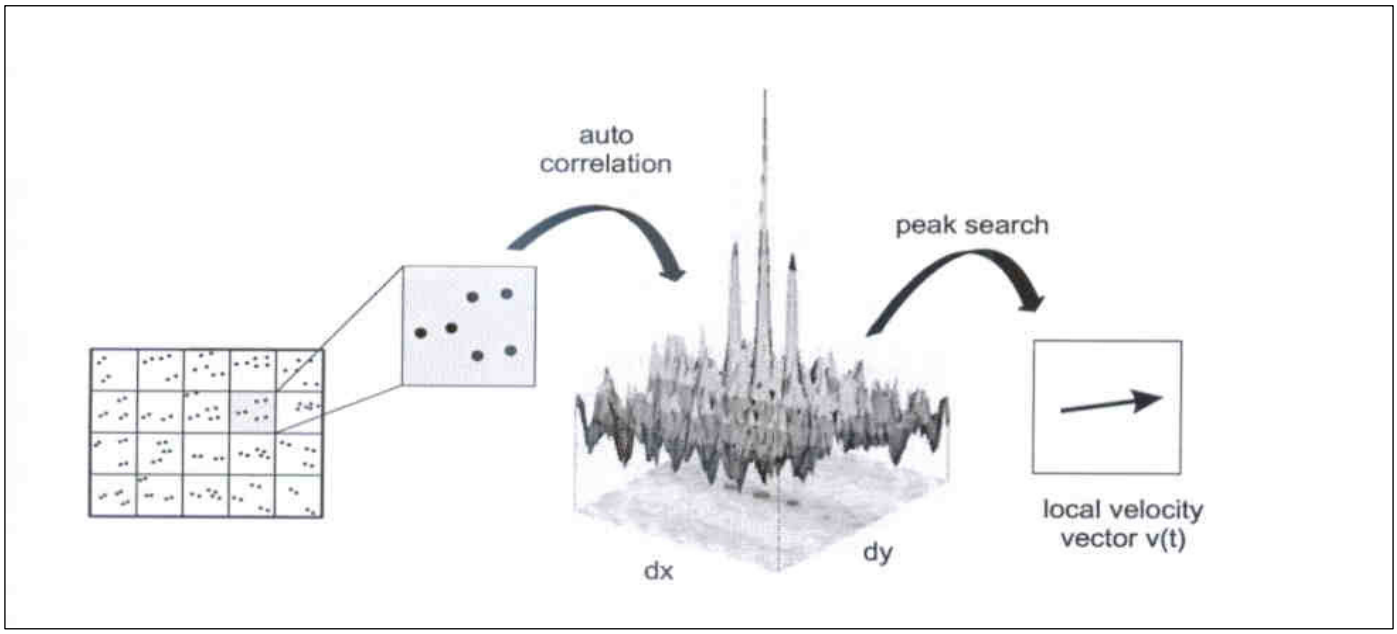

Figure 35: Evaluation of PIV recordings using auto-correlation [54].

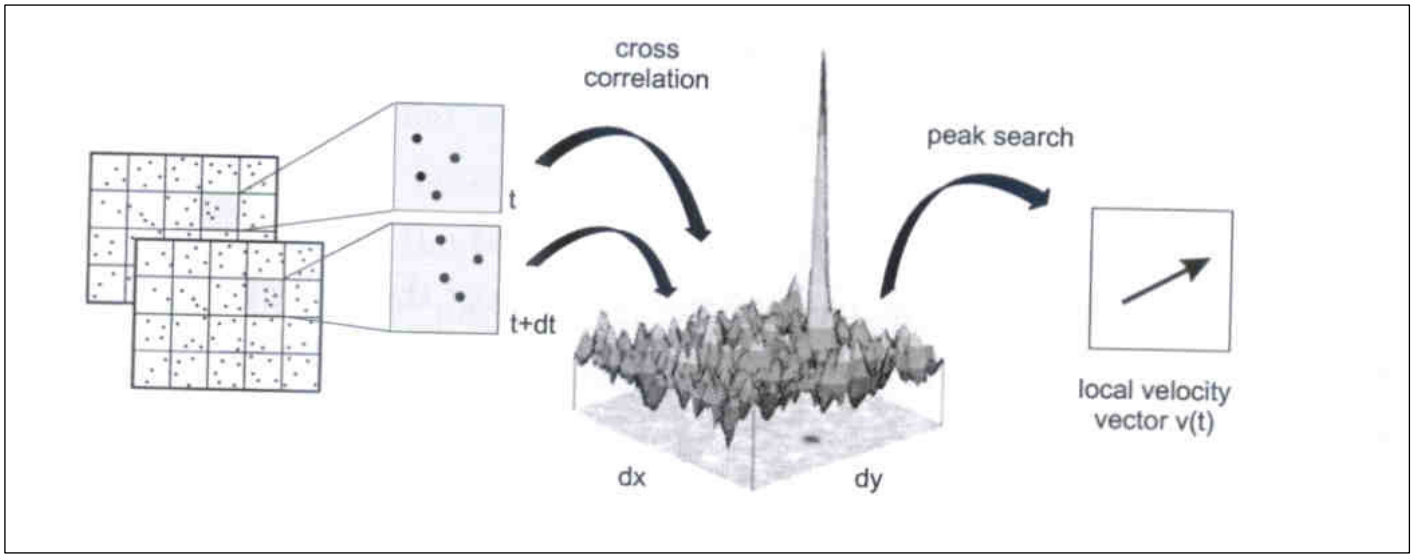

Figure 36: Evaluation of PIV recordings using cross-correlation [54].

There is no self-correlation peak, thereby eliminating any directional ambiguity as in auto-correlation. The elimination of the self-correlation peak also increases the dynamic range of the displacements that can be measured, since smaller particle image displacements can be detected.

Motivation for Research

Squish is presumed to be the principal source of turbulence generation inside the DIFH combustion chamber. But, it cannot be visualized how the final flow structure evolves within the two valve pockets of the combustion chamber. PIV is one of the tools that can be used to study the air flow structure as it flows into the valve pockets of the combustion chamber from the cylinder volume. There are a number of unknown interactions that can occur between the key engine parameters which cause variations in the combustion phenomena and, are strongly dependent on the in-cylinder air motion. Therefore, the principal motivations for this research are:

- To study the evolution of mean flow within the cylinder during intake and compression strokes.
- To investigate the effects of engine parameters such as fuel injector location, spark plug location, number of spark plugs, fuel injection pressure, fuel injection timing and spark ignition timing on engine performance and engine-out emissions.

Experimental Procedure

In-Cylinder Airflow Measurements:

The first part of the experimental procedure describes the experimental setup used to perform the PIV studies on the in-cylinder air motion. The DIFH cylinder head is unique in the sense that it does not contain any valve mechanisms. This allows replacing the metal cylinder head with an optically transparent cylinder head to provide a clear view of the moving piston and the valves from the top (plan) view. The DIFH engine is modified from a single-cylinder, four-stroke Briggs & Stratton flat-head engine. The optical cylinder head was machined from poly methyl methacrylate (PMMA) and subsequently polished to obtain optical transparency. A Kistler 6121 piezoelectric cylinder pressure transducer was mounted flush with the combustion chamber to record the cylinder pressure data. The engine was coupled to an AC motor used to motor the engine at a desired engine speed for the in-cylinder flow analysis. A rotary encoder was mounted on the crank shaft to measure the crank shaft angular position; this information is required by the combustion analysis system to phase the cylinder pressure trace with respect to the crank angle as well as provide the trigger (TTL) signal to fire the laser. A seeding system was devised that consists of a cylinder of very large volume compared to the engine cylinder volume (~87:1) connected to the intake port of the experimental engine. When the engine is motored, intake air mixed with the seeding particles already present in the large cylinder is drawn into the engine and then expelled out through the exhaust valve. The optical cylinder head, the laser/camera arrangement and a snapshot of the PIV as well as combustion analysis system are shown in Figures 37, 38 and 39, respectively.

A laser sheet is created at a section parallel to the surface of the cylinder block, midway between the top and bottom surfaces of the combustion chamber as shown in Figure 40. The distance of the laser sheet was fixed at 0.2 inches from the cylinder head deck, which is about midway between the top and bottom surfaces of the combustion chamber. At this plane of interest, PIV measurements of the in-cylinder flow were performed at an engine speed of 3600 rpm, with data collected over 250 cycles. With top dead center (TDC) indexed as 0° CA (crank angle), PIV measurements for the complete intake and compression stroke from 0-360° CA was made at increments of 45° CA. The engine was operated at wide open throttle as would be the case in a direct injection engine. The PIV data acquisition and analysis were accomplished using the LaVision GmbH PIV system. Figure 41 shows the valve timing diagram for the stock Briggs & Stratton engine platform used for conversion to the DIFH engine. Valve timing is a key engine performance parameter that defines the boundary conditions of the in-cylinder turbulence generating mechanisms. In the current system, the intake valve opens 25° before top dead center (BTDC) during the exhaust stroke and closes 70° after bottom dead center (ABDC) during the compression stroke. Similarly, the exhaust valve opens 115° after top dead center (ATDC) during the expansion stroke and closes 15° ATDC during the intake stroke.

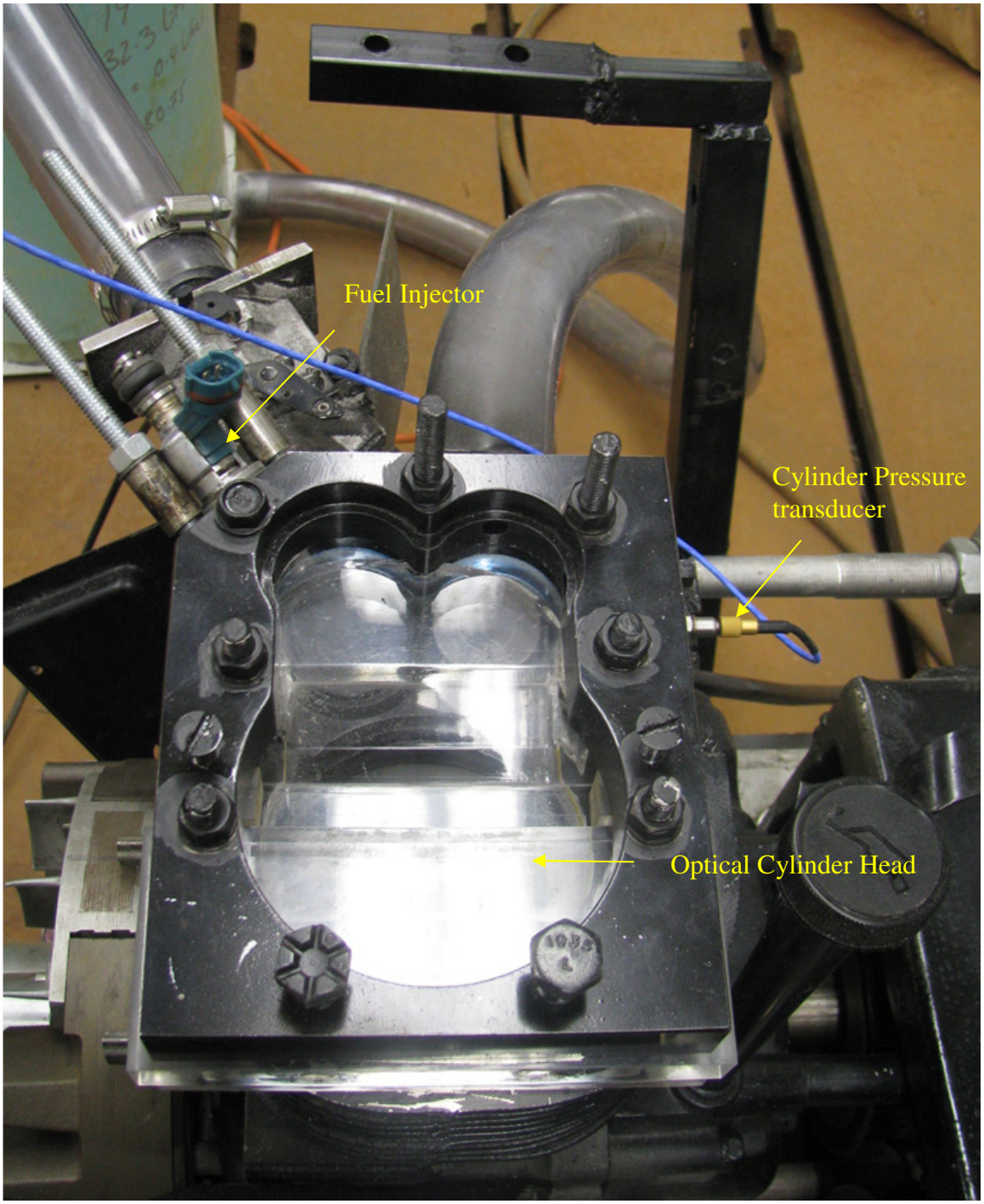

Figure 37: Top view of the optical cylinder head.

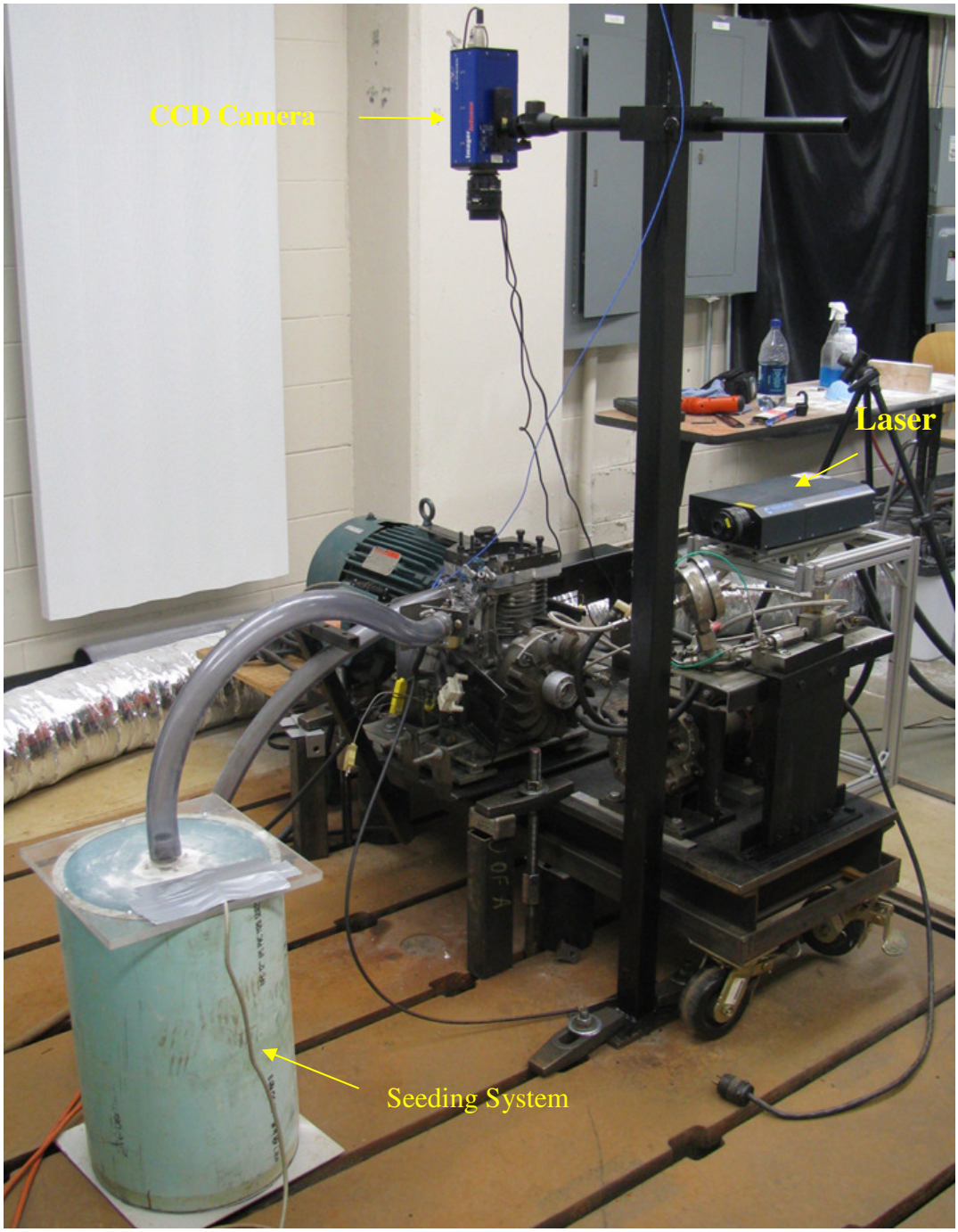

Figure 38: Experimental setup showing the engine, laser/camera system and, seeding system.

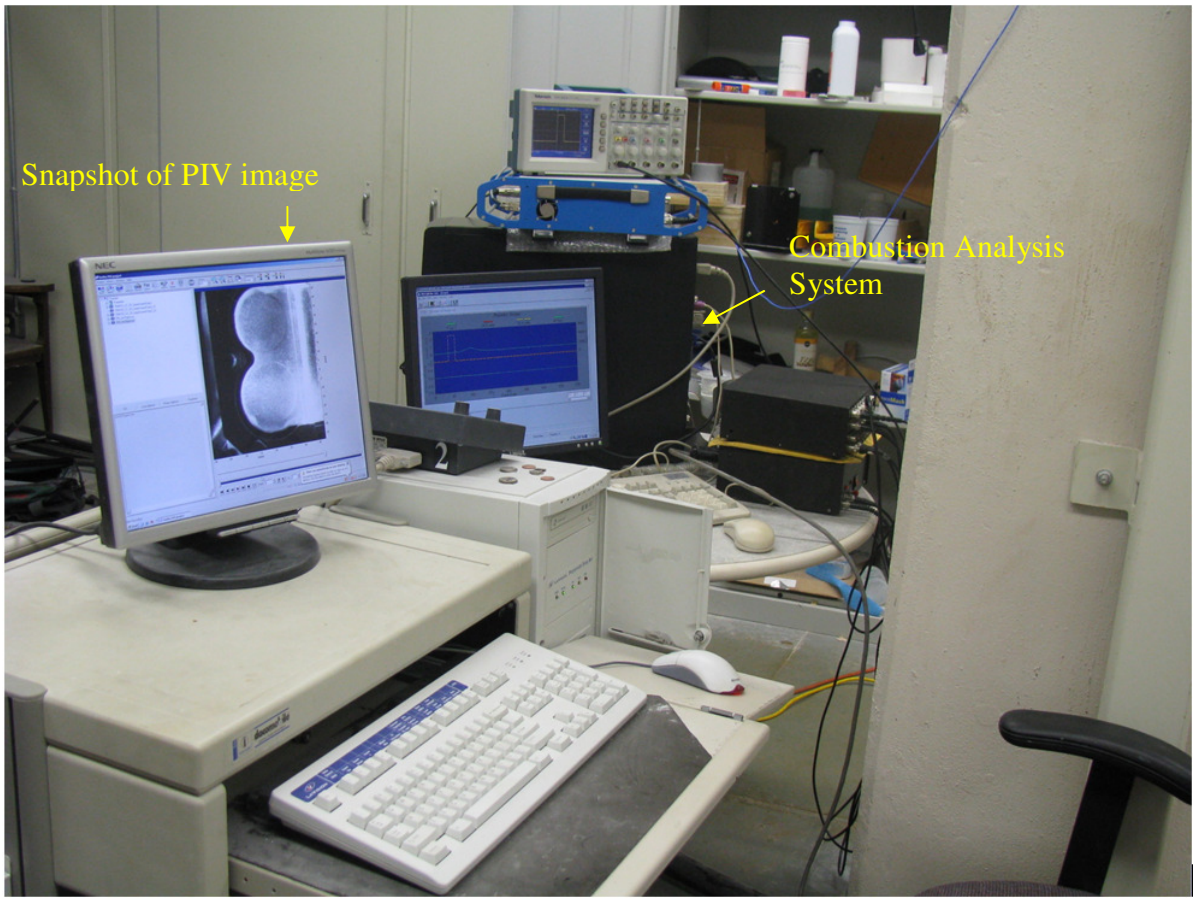

Figure 39: Snapshot of PIV image and cylinder pressure measurement.

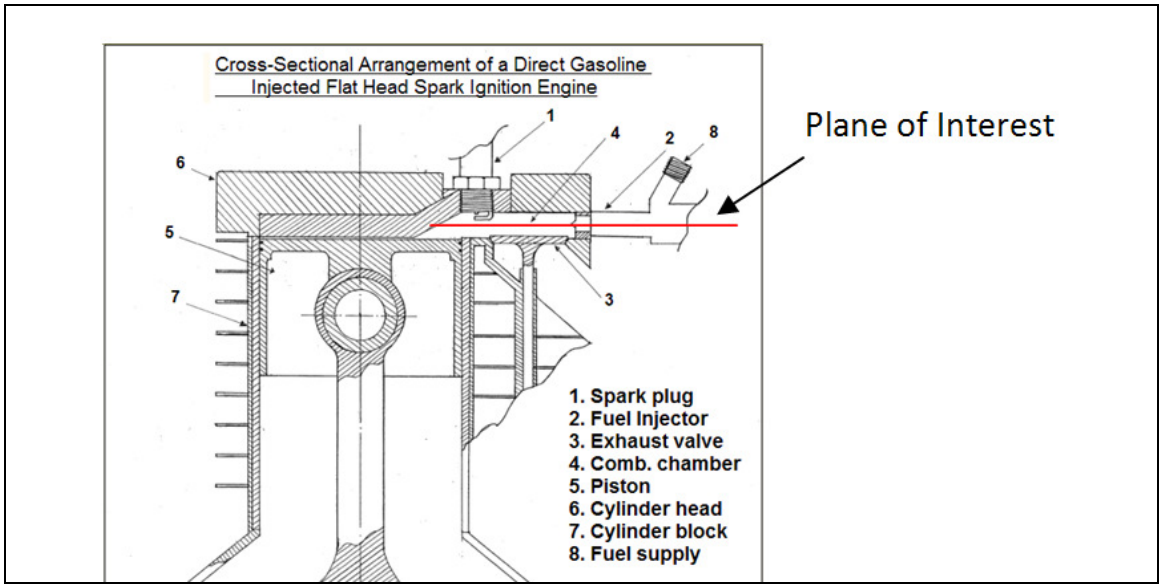

Figure 40: Plane of interest at which PIV measurements are made.

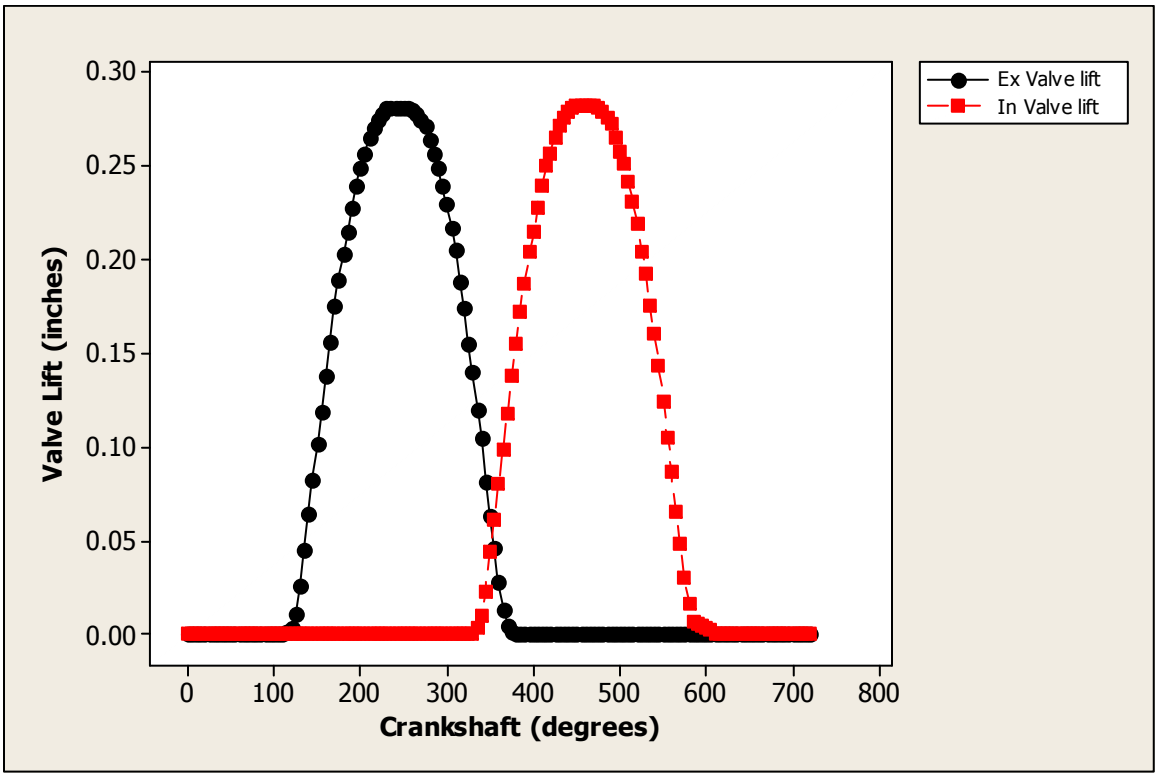

Figure 41: DIFH engine valve lift profile.

This particular valve timing has an overlap of 40 crank angle degrees (CAD); defined as the period during which both the intake and exhaust valves are open. In this study only the general flow characteristics inside the combustion chamber over the intake and compression stroke is of interest. The knowledge of the in-cylinder flow is essential not only to decide the location of the fuel injector and the spark plug, but also the combustion performance of the engine can be analyzed based on the mean air motion during fuel injection and spark ignition process. The fluid flow in the compression stroke is of interest because the squish event is initiated during this stroke, which is thought to be responsible for the turbulence generation in the combustion chamber of the DIFH engine.

Engine Performance Measurements:

The DIFH engine is based on a SV Briggs & Stratton engine platform. The majority of the modifications were made to the engine cylinder head. A special cylinder head was machined out of a wrought aluminum slab. The basic combustion chamber shape of the OEM engine was retained and the design frozen for one compression ratio. Any changes to the compression ratio were accomplished by using cylinder head gaskets of different thicknesses, machined out of annealed copper sheets. The engine performance was evaluated at two fuel injector locations, one on the intake valve side and the other on the exhaust valve side. The spray direction of the injectors in both locations were aimed at the opposite valve pocket from either injector. A fan spray fuel injector was used in this study based on the combustion chamber shape. One of the most important attributes of the fan spray is its sheet like spray pattern. The combustion chamber is shaped like a bread slice that has a thickness far smaller than the breadth and

width. Conventional fuel injectors have a conical spray pattern. Using a conventional fuel injector with this type of combustion chamber would result in excessive fuel-wall wetting. To alleviate this problem, the fan spray fuel injector is used with the plane of the spray parallel to the cylinder head deck. The cylinder head of a SV engine also gives ample flexibility in placing the spark plug. From the PIV analysis presented in the previous section the formation of coherent flow structure in both the valve pockets is clearly visible, although the timing of their formation with respect to crank angle is different. By placing the spark plug over the intake valve, exhaust valve, or in between the two valves, the engine performance can be studied to evaluate the effect of spark plug location on combustion performance. Another lever that has significant effect on engine performance is fuel pressure. A high-pressure fuel pump is independently operated to provide the high pressure fuel supply to the injector. The required fuel pressure is adjusted by a pressure relief valve located in the high pressure circuit and the fuel pressure is measured as well as logged using a Kistler 4763B5 pressure transducer with the help of the data acquisition system. Other parameters that were perturbed to operate the engine were injection timing, ignition timing, and fuel pulse width. Table 8 lists the parameters (factors) used in the optimization study of the DIFH engine, and the levels considered for creating a design of experiment (DOE) test matrix. Since the number of levels for all the factors are not the same, a general full factorial design was created with the seven factors. The exhaust valve side and the intake valve side were fixed as the two levels for the injector location. With reference to Figure 34, the fuel injectors were placed in the valve pockets such that the centerline of fuel spray of both injectors intersected with the centerline Z-Z' of the combustion chamber. The three levels of spark plug

locations were fixed at locations E, F and D as shown in Figure 34. One of the main advantages of gasoline direct injection lies in the possibility of reducing engine knock by late injection of fuel into the compression stroke, which allows engine operation at higher compression ratios.

Table 8: Factors and levels for DOE.

Factors	Levels
Injector Location	2 (Hi, Low)
Spark Plug Location	3 (Hi, Middle, Low)
Compression Ratio	2 (Hi, Low)
Fuel Pressure	2 (Hi, Low)
Ignition Timing	2 (Hi, Low)
Injection Timing	2 (Hi, Low)
Fuel pulse width	2 (Hi, Low)

The stock Briggs & Stratton engine runs on a compression ratio of about 6.5:1. Compression ratios of 8:1 and 10:1 were tested as the two levels of the DOE in a bid to improve thermal efficiency. The operating range of the DIFH engine was never established before and therefore at a fixed engine configuration consisting of fuel injector location, spark plug location and ignition timing, the DIFH engine was run at a lower and a higher fueling value to establish the low and the high levels for the DOE. The low fueling corresponded to 40 CAD duration injection pulse width whereas; the high fueling was set at 50 CAD duration injection pulse width. After fixing the fueling levels, the engine was run over a spark sweep at these fueling conditions at two different fuel

injection timings. Retarded ignition timings beyond TDC compression resulted in misfire while advancing timing beyond 25° BTDC resulted in very rough engine operation associated with engine knocking. The two fuel injection timings were fixed at BDC compression and 90° BTDC compression. At BDC compression stroke, the in-cylinder airflow reversal into the combustion chamber begins, as shown in Figure 46. At this location maximum fuel spray penetration can occur, wetting the combustion chamber walls. At 90° BTDC compression, the in-cylinder airflow structure develops into a swirling motion that can help in reducing the fuel spray penetration as well as air fuel mixing, as shown in Figure 48. Although a more structured airflow pattern is developed at 45° BTDC during the compression stroke as shown in Figure 49, than at 90° BTDC, the former location was not desirable because it caused spark plug wetting leading to engine misfire. With the factors and levels defined appropriately the resulting general full factorial design required 192 engine operating points. The results of these experiments are discussed in the following section.

Results and Discussion

The main focus of this experimental effort is to investigate the factors that play a significant role in the operation of the DIFH engine rather than to optimize for best engine performance. As explained in the previous experimental procedure section, there are seven main factors that need to be investigated to optimize the DIFH engine performance. The choice of the stock SV Briggs & Stratton engine platform was none more than a limitation than judicious choice of combustion chamber shape based on analysis. The first investigation into the effect of the combustion chamber shape on

in-cylinder air motion was accomplished using PIV techniques. Figures 42 – 50 show the velocity vector plots generated by the PIV measurements over the intake and compression strokes. In Figure 42, at TDC during the intake stroke, the combustion chamber is an open control volume experiencing the valve overlap period. There is some gas flow back through the exhaust valve but the bulk of the air rushes into the combustion chamber through the intake valve. This is evident by the large velocity magnitude over the intake valve. In Figure 43, at 45° ATDC during the intake stroke the exhaust valve is already closed, drawing all the airflow through the intake valve. The average velocity of the intake air increases by about 4% and the centroid of the largest average velocity vectors are shifted towards the exhaust valve side. In Figure 44, at 90° ATDC during intake stroke, the magnitude of the average velocity vectors start decreasing although the centroid of the largest average velocity vectors continue shifting towards the exhaust valve side. In Figure 45 at 135° ATDC during the intake stroke, the average velocity of the intake air drops significantly. Until this time no significant mean air motion pattern is developed in the combustion chamber and any fuel injected during this period will be carried into the cylinder volume.

In Figure 46 at bottom dead center (BDC) into the intake stroke, the average airflow velocity decreases to the lowest value and flow reversal into the combustion chamber takes place. Even though the intake valve is still open, no evidence of airflow through the intake valve is evident. A definite pattern of swirling air motion starts to develop in both the pockets holding the intake and exhaust valves, although the magnitude of the average velocity is higher on the intake valve side. At this moment the direction of swirl in both pockets of the combustion chamber is same.

In Figure 47 at 45° ABDC during the compression stroke, the average air velocity in the combustion chamber starts increasing and strong swirling motion sets up in the intake valve pocket. The weak initial swirling motion that was evident in the exhaust valve pocket at BDC is replaced by higher velocity air rushing into the pocket. In Figure 48 at 90° ABDC during the compression stroke, developing swirling motions are evident in both valve pockets of the combustion chamber. The direction of swirl in both valve pockets is opposite to each other. In Figure 49 at 135° ABDC during the compression stroke, well developed swirling air motions in opposite rotational directions are formed in the intake and the exhaust valve pockets. The unique design of the combustion chamber splits the incoming airflow into the two pockets to set up two distinctive swirling motions. Such a coherent flow structure formation late during the compression stroke is evidence of the large contribution of squish as a turbulence generating mechanism. In Figure 50 at TDC in the compression stroke, the swirling air motion has weakened significantly in both of the valve pockets. This is caused by turbulence decay due to viscous dissipation.

The DOE described above in the experimental section is based on the understanding of the airflow pattern over the intake and compression stroke. Figures 51-63 show the results of the experiments carried out as per the combinations of the DOE parameters. Figure 51 shows the plot of COV NIMEP versus compression ratio, injector location and, spark plug location. These three parameters are fixed hardware parameters that once frozen in design cannot be varied to study engine performance. The points shown in the figure also contain data that are representative of fueling quantity, injection timing, ignition timing and, fuel injection pressure. The combinations shown in the plot that do

not contain data are the ones that had all misfiring cycles. It can be seen that only the cases of compression ratio 8:1 with the injector located at the intake valve side and spark plug located at either the intake or exhaust valve pocket have the lowest COV NIMEP. Figure 52 helps to extend the understanding of the variation of COV NIMEP at the different engine operating conditions. It shows the plot for 0-10% burn duration, which is an indicator of the flame initiation stage of spark ignited combustion. It is evident from this plot that the same combination of engine parameters that showed the least COV NIMEP also show the lowest 0-10% burn duration. Compression ratio of 10:1 is not considered for further analysis because at this compression ratio the combustion chamber under consideration shows very limited optimization opportunities. Figure 53 shows the main effects plots that explain the influence of the engine parameters on engine power. The fuel injector located at the intake valve side yields more power output than that at the exhaust valve side. The location of the spark plug has a more profound effect on engine power with the spark plug located at the exhaust valve side showing the highest power output. Although higher fuel injection pressure has only a slight negative impact on engine power, it might have a significant effect on engine out emissions. Fuel injection timing also has very little impact on the engine out power. Consistent with conventional understanding, the engine power output increases both with ignition timing as well as higher fueling.

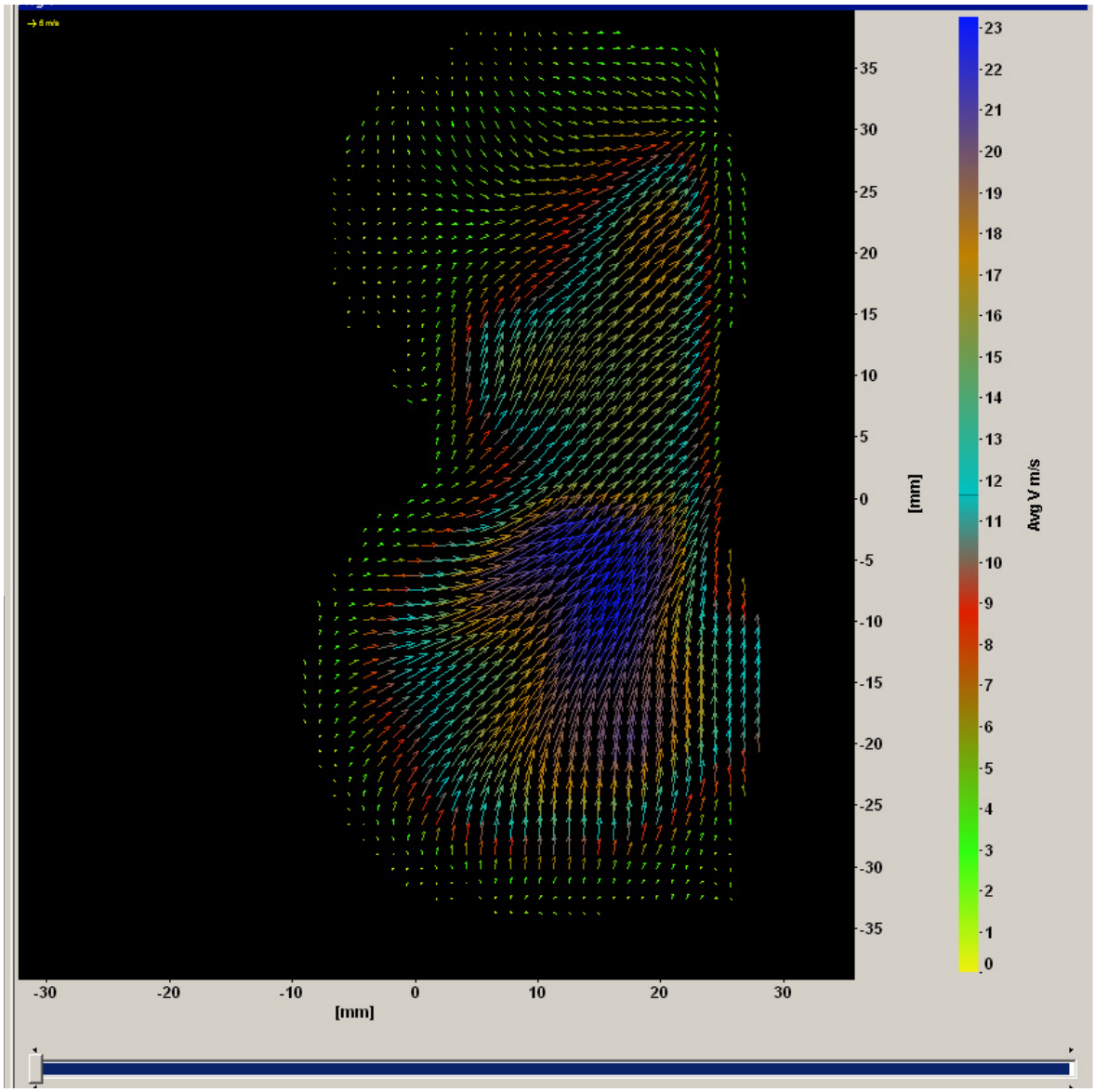

Figure 42: Velocity vector plot of 0^{o} ATDC intake stroke.

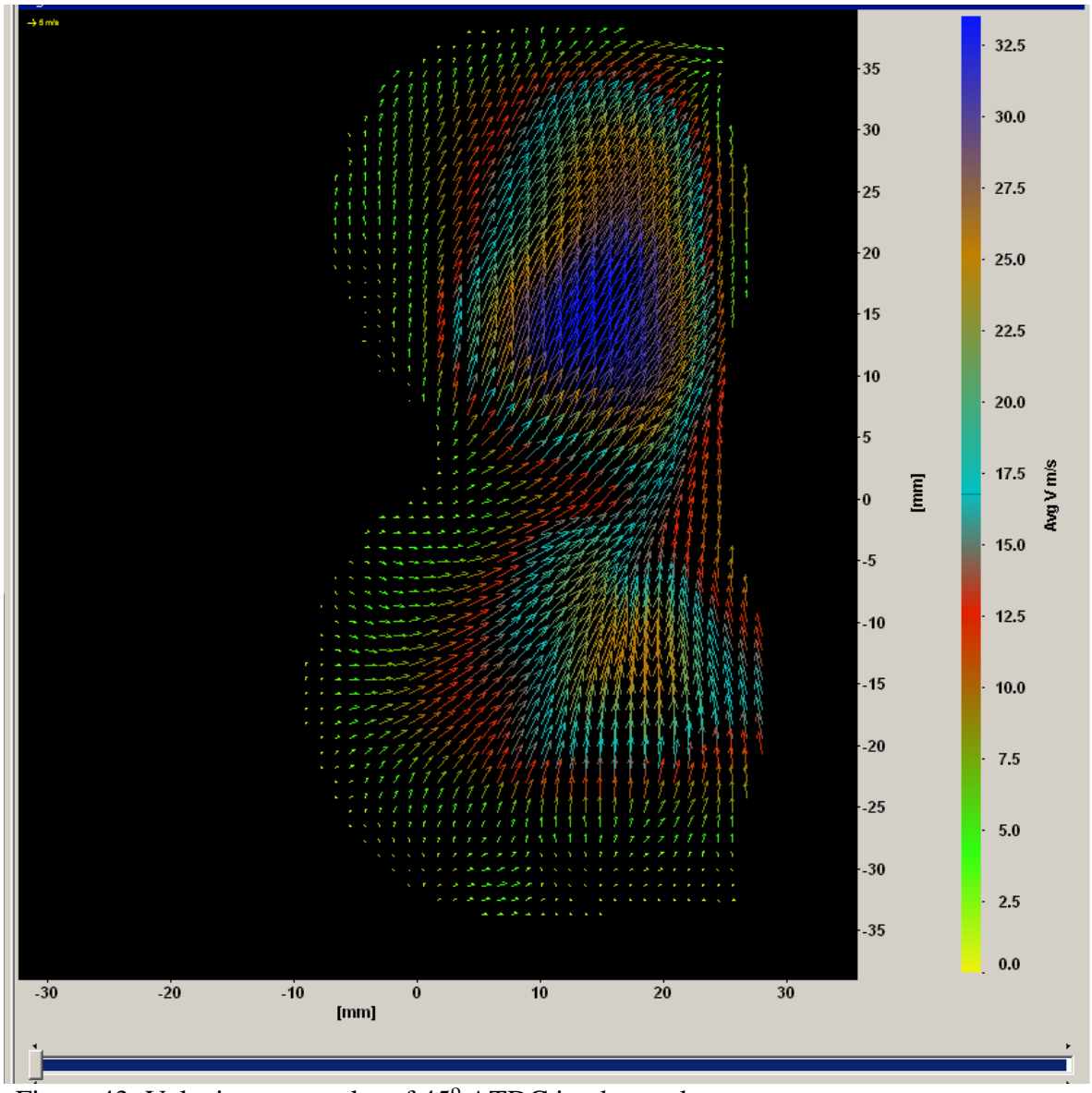

Figure 43: Velocity vector plot of 45^{o} ATDC intake stroke.

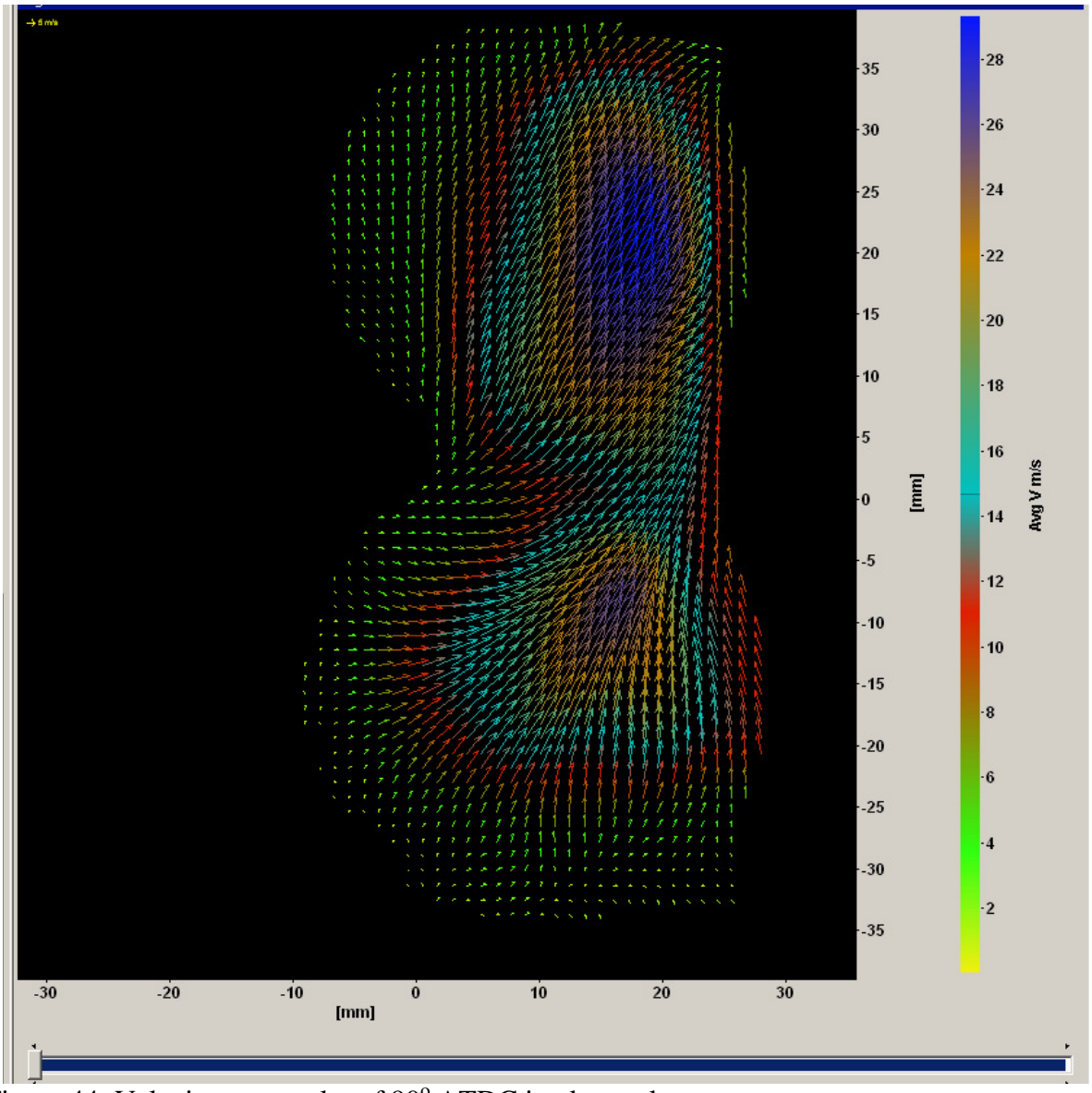

Figure 44: Velocity vector plot of 90^{o} ATDC intake stroke.

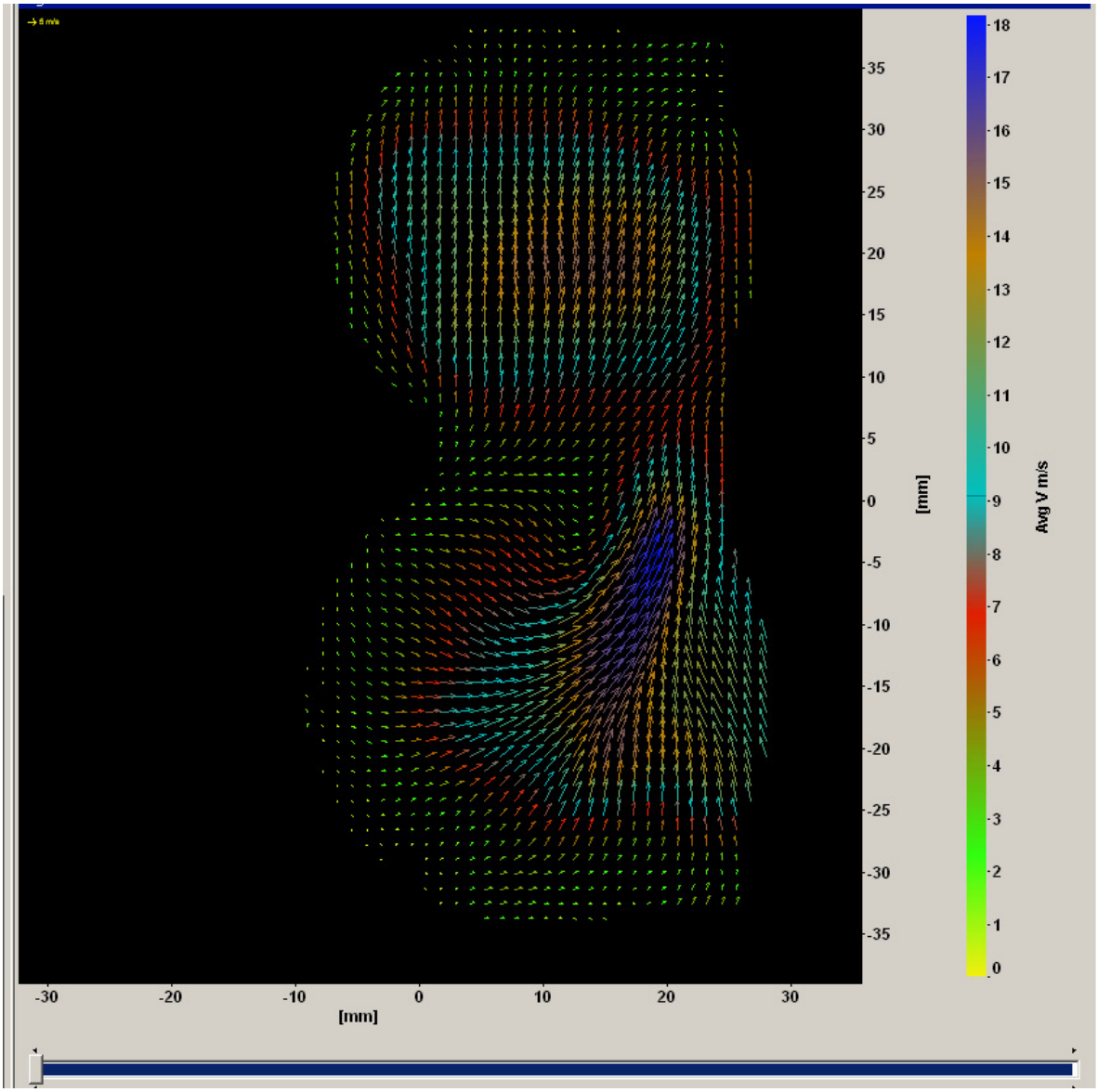

Figure 45: Velocity vector plot of 135^{o} ATDC intake stroke.

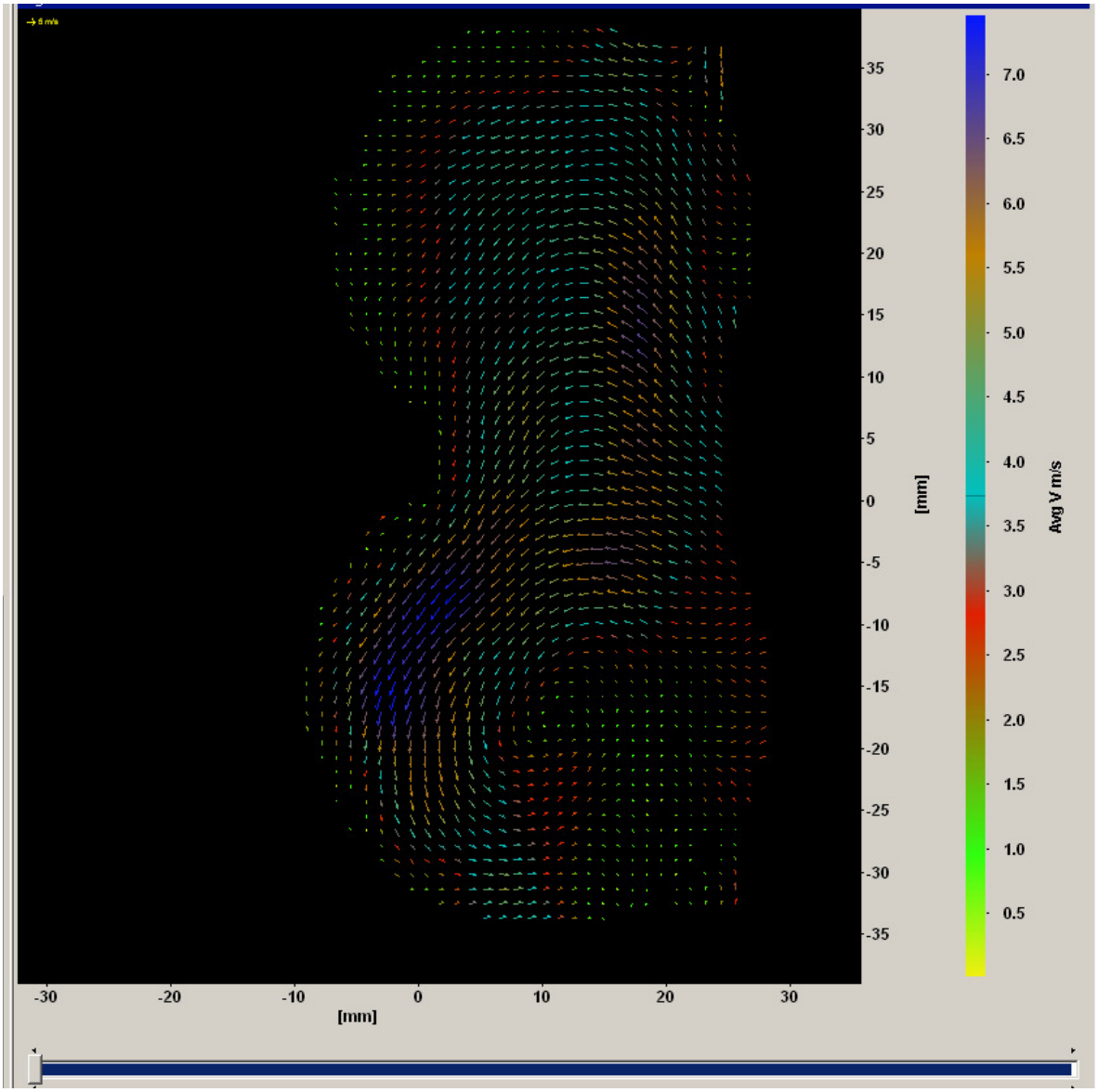

Figure 46: Velocity vector plot of 180^{o} ATDC intake stroke (BDC compression).

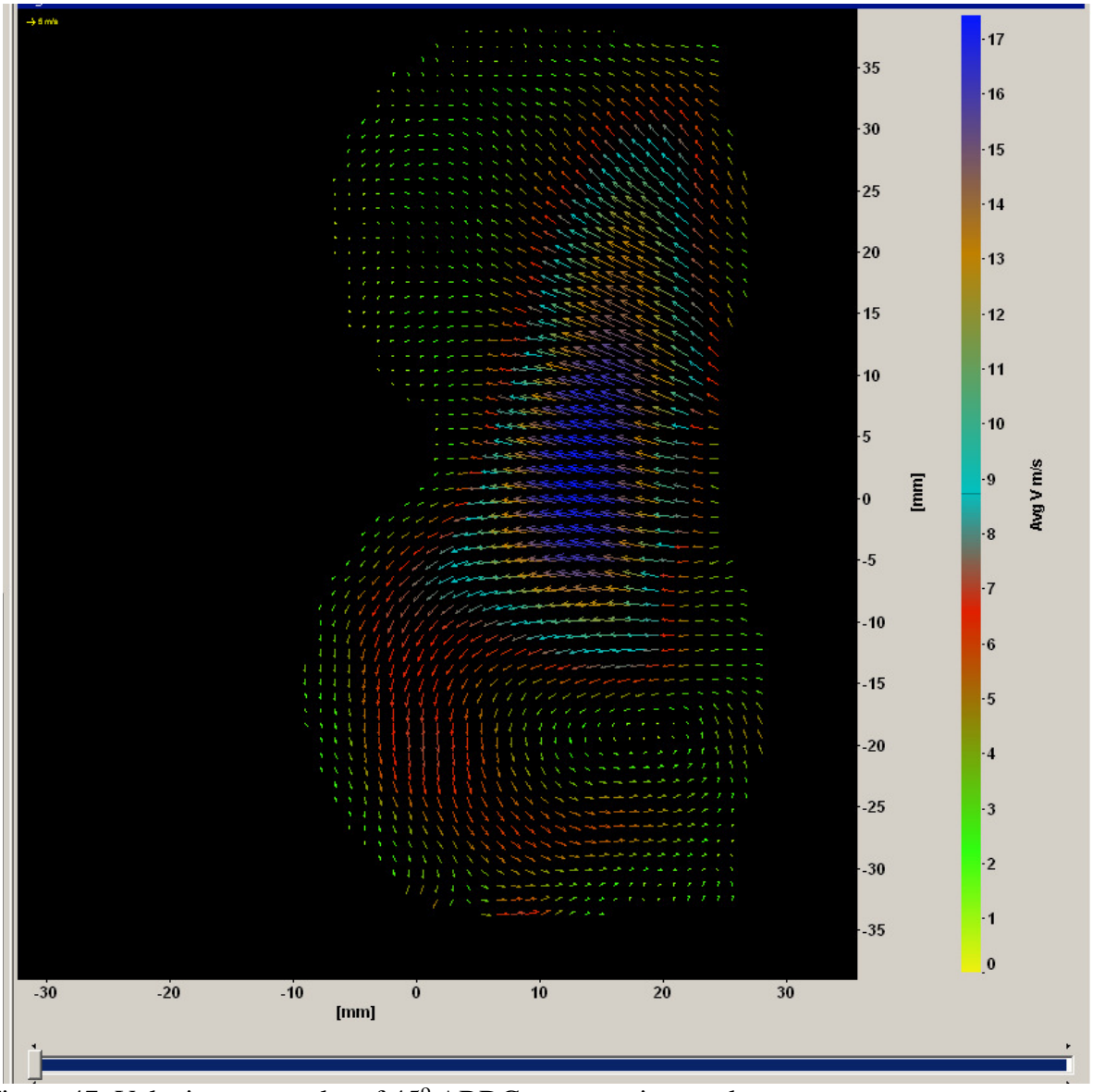

Figure 47: Velocity vector plot of 45^{o} ABDC compression stroke.

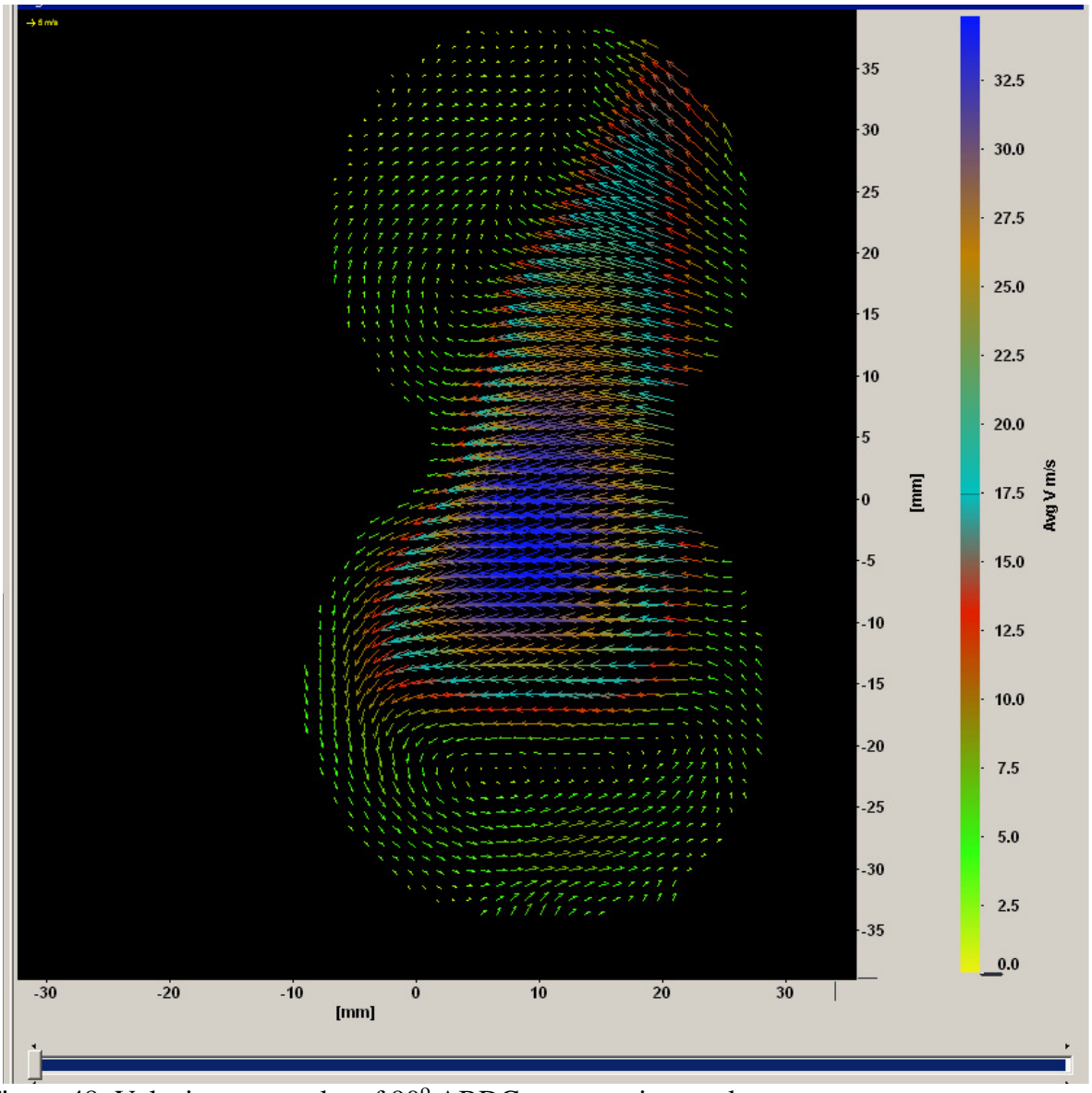

Figure 48: Velocity vector plot of 90^{o} ABDC compression stroke.

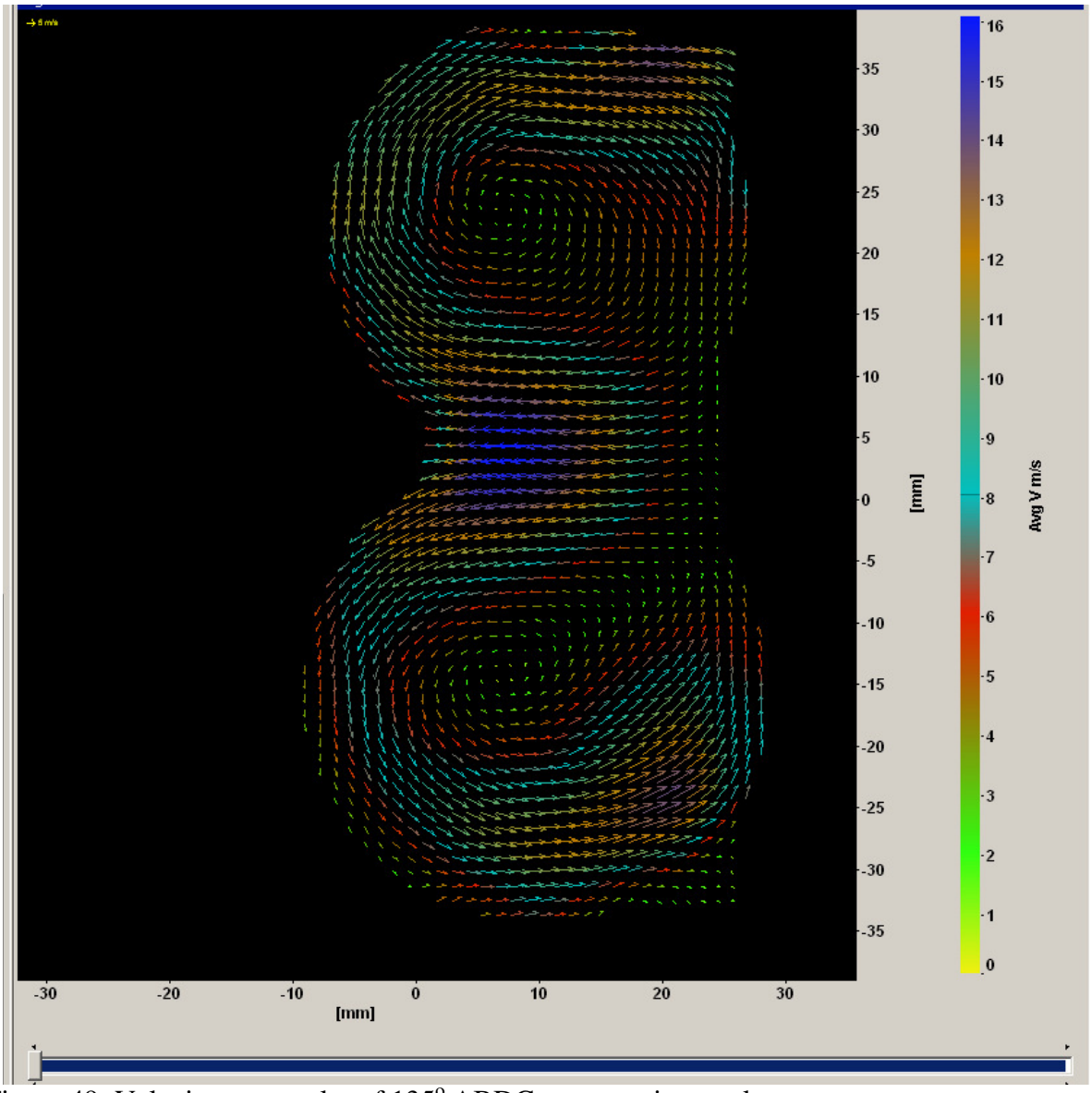

Figure 49: Velocity vector plot of 135^{o} ABDC compression stroke.

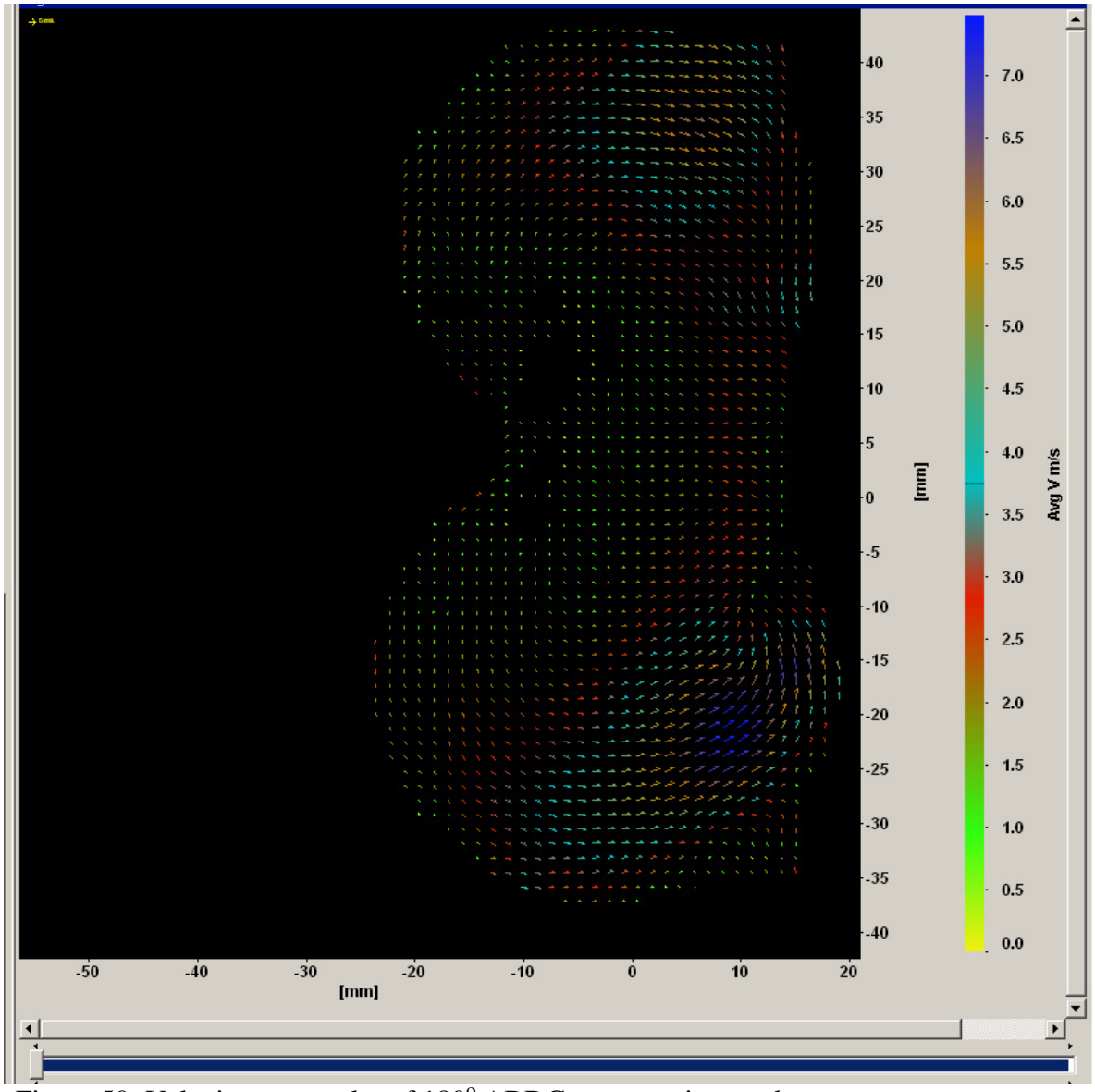

Figure 50: Velocity vector plot of 180^{o} ABDC compression stroke.

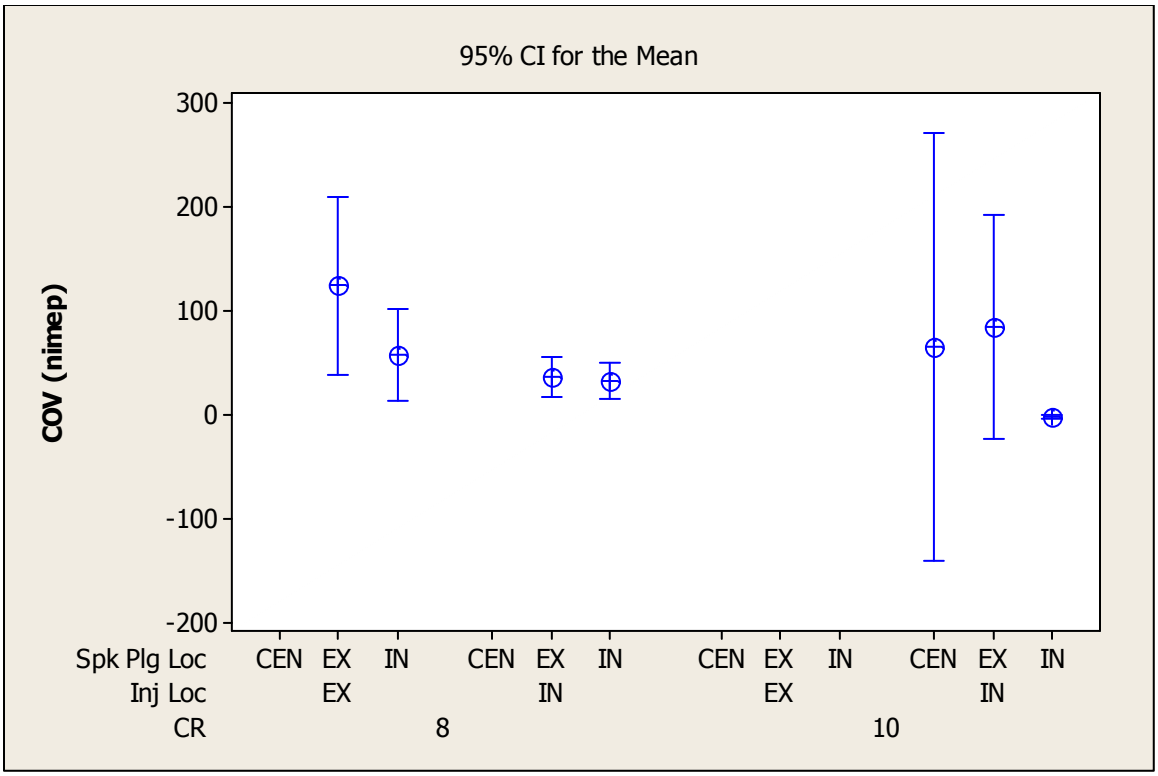

Figure 51: Interval plot of cov (nimep) vs. compression ratio, injector location, spark plug location.

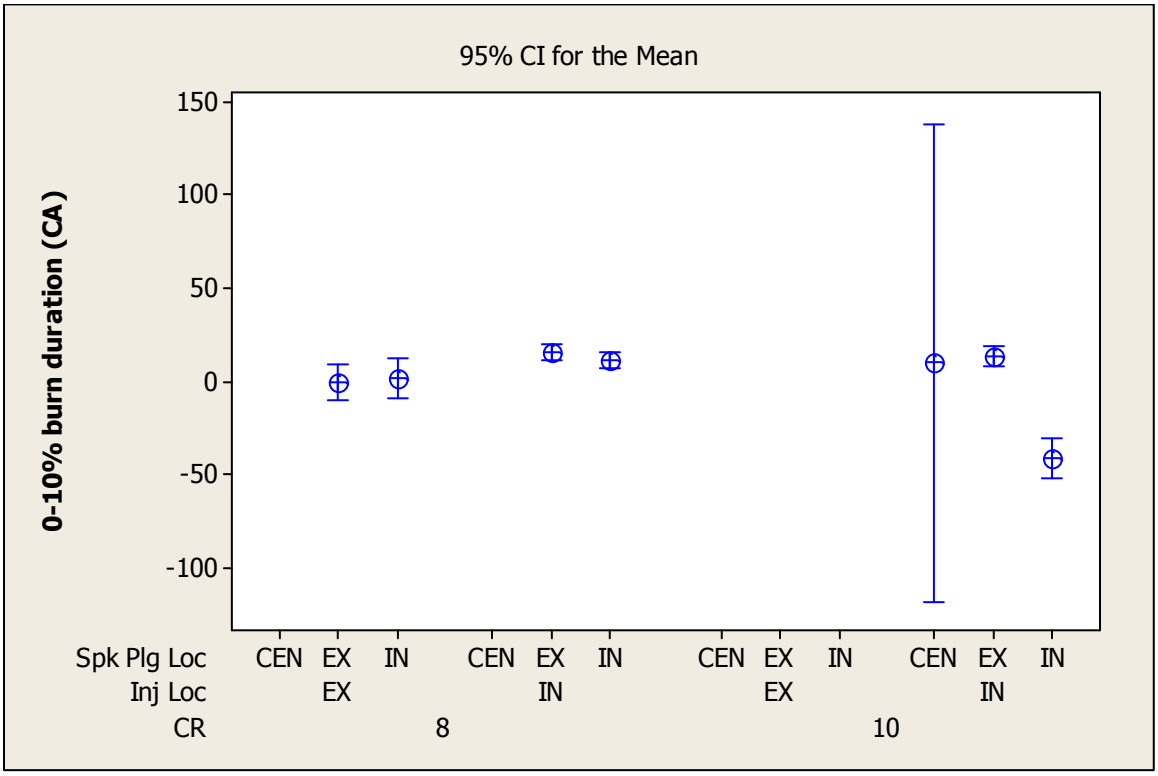

Figure 52: Interval plot of 0-10% burn duration vs. compression ratio, injector location, spark plug location.

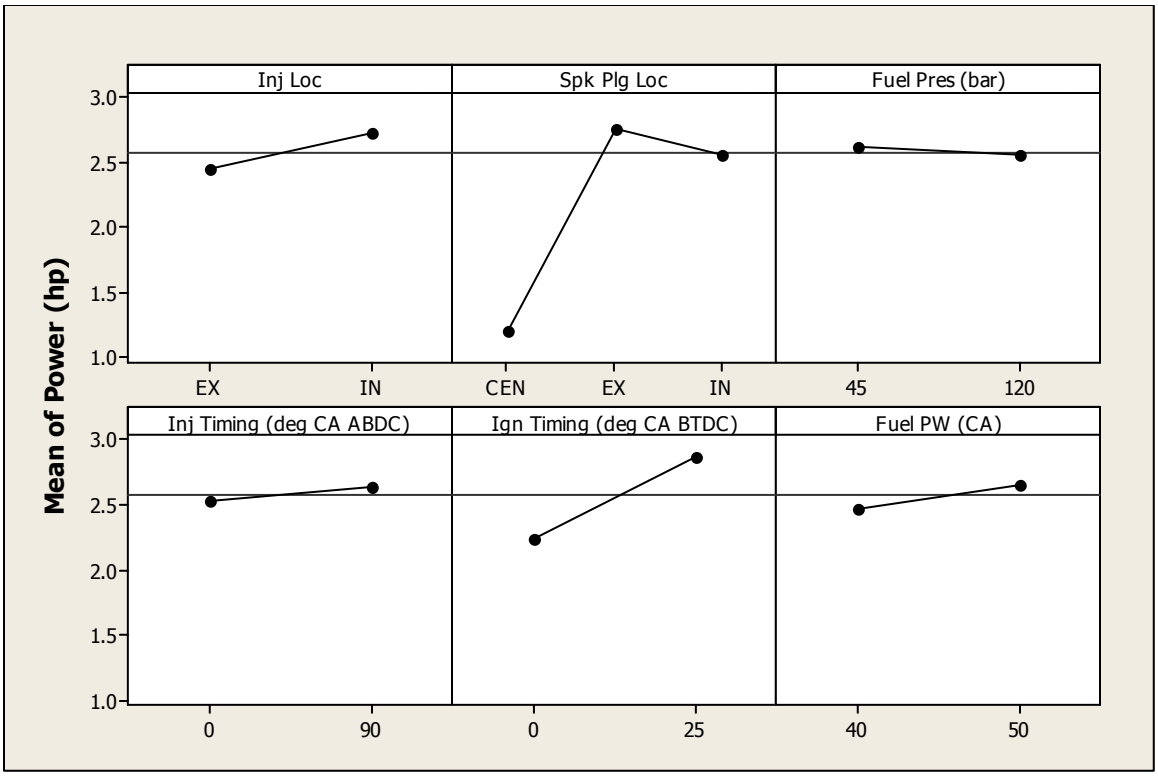

Figure 53: Main effects plot (data means) for power, 8:1 compression ratio.

What is so easily visible in the main effects plot may not always be the case as engine parameters may have complex interactions with each other. This is more clearly understood from the interaction plots for power, as shown in Figure 54. It can be clearly seen that ignition timing has almost negligible interaction with fuel injection pressure and injection timing and has only slight interaction with injector location and spark plug location. Similarly, injection timing has very little interaction with fuel pulse width, but all other engine parameters have very significant interaction with each other. This makes the combustion chamber a very complex system and could be a very difficult task for performance optimization.

One of the critical challenges facing the DIFH engine design is controlling unburned hydrocarbon (UHC) emissions. Because of the very compact combustion

chamber design, it is difficult to prevent fuel over spraying on to the combustion chamber walls, a major source of UHC for the DIFH engine. The optimum arrangement of the engine parameters as per the levels defined by the DOE for minimizing UHC emissions is shown in Figure 55. It suggests the location of the injector at the intake valve side, the spark plug to be located also at the intake valve side, fuel pressure at 45 bar, fuel injection timing at BDC compression, ignition timing at 25° BTDC and, fuel pulse width at 50 CAD duration. From point of view of the in-cylinder air motion, at 45° after BDC compression as shown in Figure 47, a swirling air motion is already setup in the intake valve side of the combustion chamber, which grows stronger as the piston travels towards TDC. By having the injector and spark plug placed at the intake valve side along with a low fuel pressure to reduce fuel spray penetration towards the exhaust valve side, most of the fuel is trapped in the intake valve side of the combustion chamber and therefore, igniting the charge at the intake valve side should produce the lowest amount of UHC emissions. But it should be kept in mind that at BDC compression, the cylinder pressure is almost ambient pressure and, therefore, a fuel pressure of 45 bar is high enough for the fuel spray to penetrate to the far end of the combustion chamber, producing UHC emissions. This is evident from Figure 55 where, with the same injector location, the spark plug at the exhaust valve side produces higher UHC emissions than the spark plug located at the intake valve side because more fuel is trapped into the intake valve pocket. The UHC emissions are highest with the spark plug located at the centerline Z-Z' of the combustion chamber. At this location the velocity of the in-cylinder air flowing into the combustion chamber due to squish from the piston top is very high, possibly causing the

flame initiated at the spark plug to be convected away from the electrodes. This may result in very high cyclic variability in combustion and even flame extinction.

A similar plot in Figure 56 shows the engine parameters for low NOx emissions. The combination of arrangement of the engine parameters for low NOx emissions is reversed to those for low UHC emissions. In this particular case of the DIFH engine combustion chamber, the UHC emissions are an order of magnitude higher than NOx emissions and therefore, the location of engine parameters for optimized NOx emissions can be discounted at this time. Figure 57 shows the best combination of engine parameters for minimum brake specific ($HC+NO_x$), as can be obtained with the DIFH combustion chamber. The CO emissions at various combinations of the engine parameters are shown in Figure 58. It is interesting to note that CO emissions can be reduced by placing the injector on the exhaust valve side as opposed to the intake valve side for lowest UHC emissions. Similarly the location of the spark plug on the exhaust valve side has more potential to reduce CO emissions rather than on the intake valve side required to reduce UHC emissions.

The discussion in the paragraph above was focused to capture the behavior of the DIFH engine combustion chamber performance. At the onset, the DIFH engine was proposed as an engine design that could alleviate the engine out emission issues faced by conventional OHV engines and, at the same time have high diesel like efficiency.

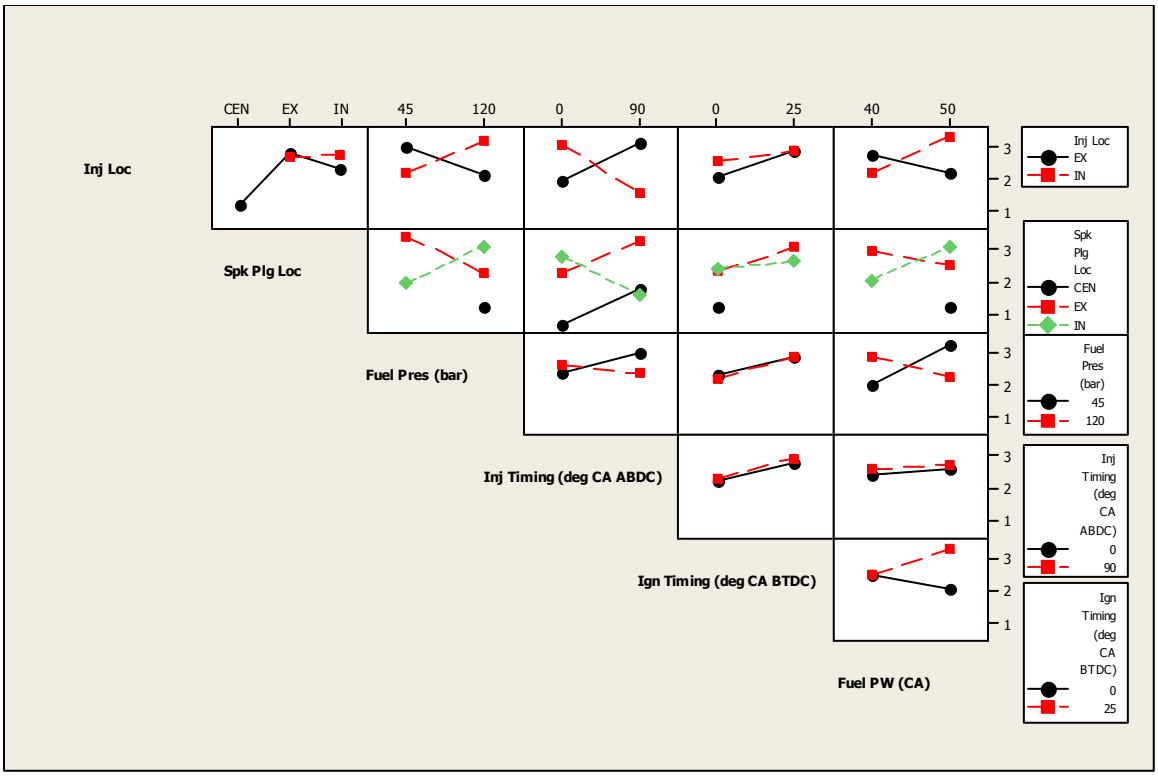

Figure 54: Interaction plot (data means) for power, 8:1 compression ratio.

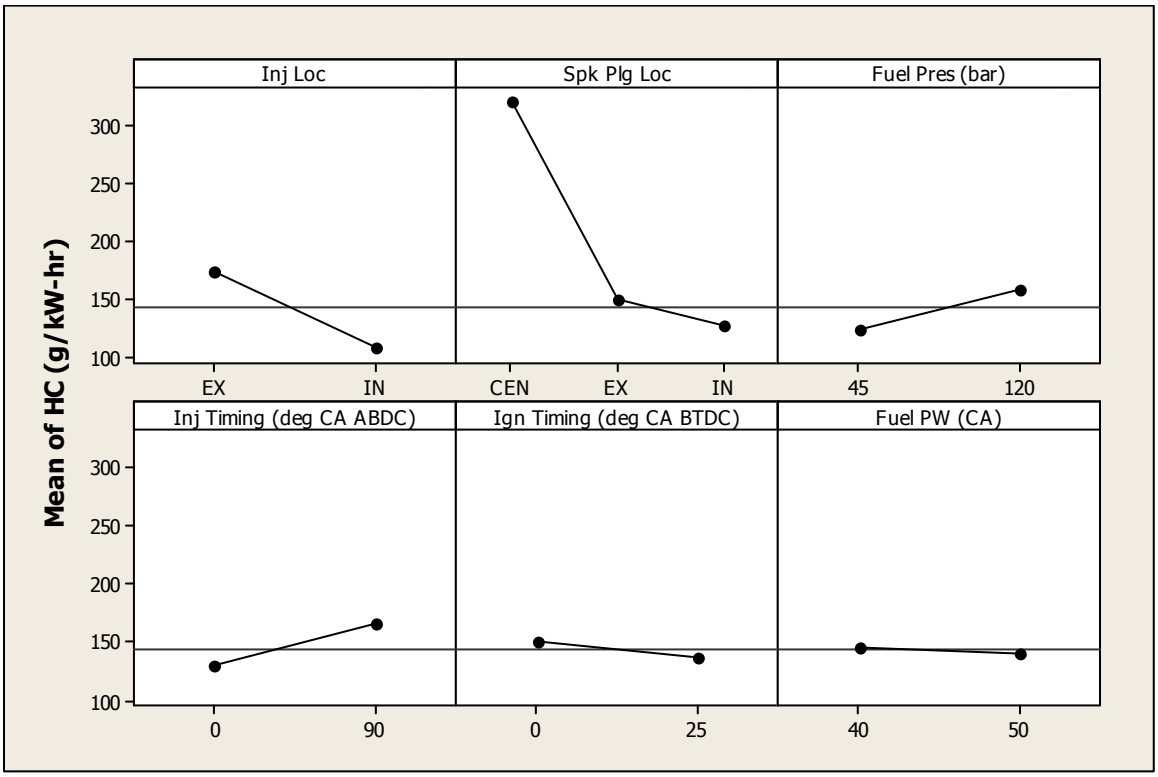

Figure 55: Main effects plot (data means) for HC, 8:1 compression ratio.

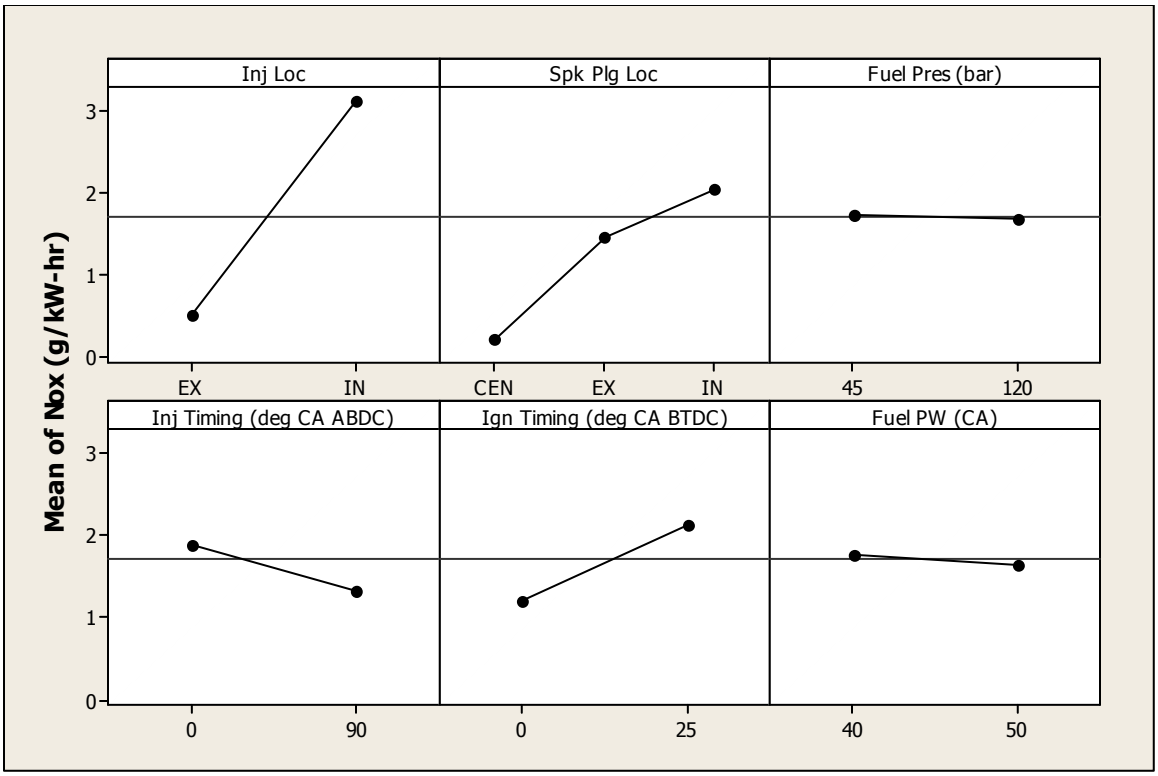

Figure 56: Main effects plot (data means) for NO_x, 8:1 compression ratio.

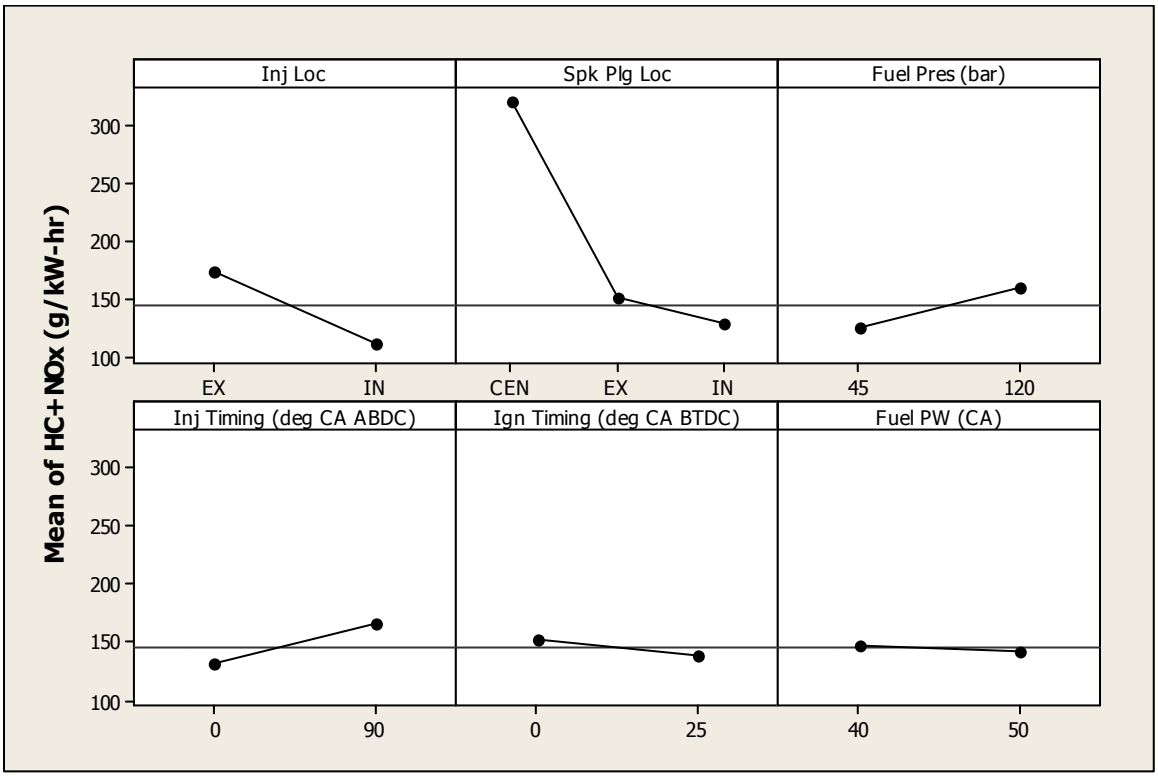

Figure 57: Main effects plot (data means) for $(HC+NO_x)$.

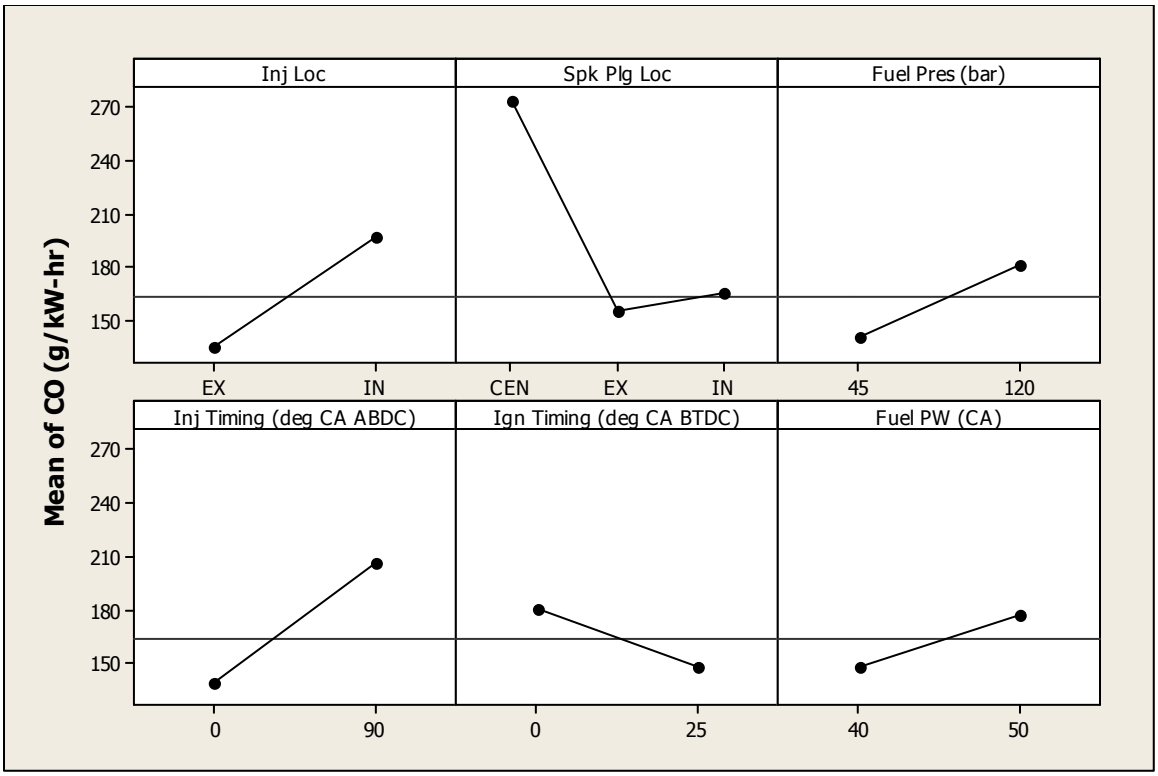

Figure 58: Main effects plot (data means) for CO.

One of the main advantages presented by the DIFH engine design is the ability to manipulate the placement of key engine performance hardware, which is definitely an advantage over conventional gasoline direct injection engines that suffer from hardware packaging issues and complex cylinder head design. The outcome of the initial set of experiments conducted with the stock Briggs & Stratton SV engine combustion chamber design showed extensive interaction between the various engine parameters as discussed above.

The unacceptably high engine out UHC emissions is a result of fuel wall wetting and engine knocking caused by end gas auto ignition. The effect of fuel wall wetting on UHC emissions can be seen in Figure 59 where the engine out UHC emissions were reduced by lowering the fuel injection pressure from 120 bar to 45 bar. The other major

issue with the current DIFH combustion chamber is its design. At this moment it would be worthwhile to individually study the effect of injector location and spark plug location on engine power as affected by the combustion chamber design. In Figure 60, both the injector and the spark plug are located on the exhaust valve side. Several interesting findings can be pointed out from the results. In one case, at the same fuel injection pressure of 120 bar, a fueling value of 50 CAD duration at BDC compression fuel injection timing and TDC ignition timing produces less than 0.3 hp whereas a lower fueling value of 40 CAD duration produces about 3.2 hp at 25° BTDC ignition timing and 90° BTDC fuel injection timing. This is a good example of how charge stratification near the spark plug due to reduced mixing time can cause a lower air-fuel ratio in the vicinity of the spark plug, which leads to high combustion efficiency. However, allowing the fuel and air to mix can cause an overall lean air-fuel mixture and, hence, poor combustion efficiency. In another case, at a lower fueling of 40 CAD duration at 45 bar fuel injection pressure, 90° BTDC injection timing and 25° BTDC ignition timing the engine produced 4.8 hp as compared to a fueling of 50 CAD duration at 120 bar fuel injection pressure, BDC compression injection timing, and TDC ignition timing, where the engine produced 0.3 hp. This is further evidence of the positive effect of charge stratification on engine power output because the higher injection pressure caused the fuel spray to penetrate further into the combustion chamber towards the intake valve side rather than be distributed near the spark plug located at the exhaust valve side.

Figure 61 investigates another aspect of the engine hardware combination. Here the fuel injector is located at the exhaust valve side whereas the spark plug is located at the intake valve side. In one case, at a fuel injection pressure of 45 bar, fueling duration

of 40 CAD, BDC compression injection timing and, 25° BTDC ignition timing, the engine produces 1.8 hp as compared to 2.8 hp at a fuel injection pressure of 120 bar with all other engine parameters remaining same. This is evidence of the fact that at a lower injection pressure insufficient fuel was able to penetrate towards the intake valve side from the injector located at the exhaust valve side. From the in-cylinder air motion studies, it can be recalled that during this time frame a swirling mean air motion is generated in the intake valve pocket, while the combustion air is pushed into the exhaust valve pocket in a direction opposing the direction of the fuel spray. Therefore, a higher quantity of fuel is required to create a stratified charge near the spark plug for better combustion. In this case the higher quantity of fuel is supplied by the higher fuel injection pressure.

Figure 62 shows the results for the case where the fuel injector is located at the intake valve side whereas the spark plug is located at the exhaust valve side. At a fuel injection pressure of 45 bar, BDC compression injection timing, 25° BTDC ignition timing and 40 CAD duration fueling, the engine produces 1.4 hp as compared to 4 hp with 50 CAD duration fueling. At the same engine conditions except 120 bar fuel injection pressure, the engine produces about 3.4 hp at both 40 CAD and 50 CAD duration fueling. From this we learn that at this configuration of the injector and spark plug location, lower injection pressure is not sufficient to transport enough fuel from the intake valve side to the exhaust valve side to facilitate good combustion. At higher injection pressure, both 40 CAD and 50 CAD duration fueling produced similar power output. In this fuel injector-spark plug location combination, the swirl generated in the

intake valve pocket traps most of the fuel in its motion, therefore, for fuel spray to penetrate into the exhaust valve pocket a higher fuel pressure is required.

The last combination to be considered is for the fuel injector and spark plug both located on the intake valve side, as shown in Figure 63. With this configuration at both, 45 bar and 120 bar fuel injection pressure, the engine produces less power when fuel is injected at 90° BTDC as compared to fuel injection at BDC compression. This suggests that with the fuel injector located at the intake valve side, homogeneous mixing of the fuel and air forms the dominant mechanism that supports good combustion rather than a stratified charge. A comparison of Figures 60 and 63, which have the fuel injector and the spark plug both on the exhaust valve side and intake valve side, respectively, shows different mechanisms supporting combustion. In Figure 60, stratified charge combustion seems to control combustion at higher efficiency because more power is produced as the injection timing is delayed and ignition timing is advanced. Whereas in Figure 63, engine power increases with injection timing advanced to BDC compression, which allows more time for fuel and air mixing.

A comparative engine performance study was conducted between the DIFH engine, OEM OHV carbureted engine and OEM SV carbureted engine of similar engine displacements. All three of the engines were compared at similar power output levels as shown in Figure 64. The DIFH engine had the worst engine out brake specific ($HC+NO_x$) emissions of about 110 g/kW-hr, followed by the SV engine with about 46 g/kW-hr and the OHV engine with about 14 g/kW-hr, as shown in Figure 65. The DIFH engine had the least engine out bsCO emissions of about 124 g/kW-hr followed by the OHV engine with about 579 g/kW-hr and the SV engine with about 530 g/kW-hr, as shown in Figure 66.

The DIFH engine had a fuel consumption of about 1.42 lb/hp-hr followed by the OHV engine with about 1.43 lb/hp-hr and the SV engine with about 1.88 lb/hp-hr, as shown in Figure 67.

The outcome of this study clearly shows that the DIFH engine with the current combustion chamber design fails to deliver a cleaner emission solution as compared to conventional OHV engines. It also fails to match the power output of conventional OHV engines of comparable displacements due to severe engine knocking at high engine loads. The main cause of this poor performance is attributed to the combustion chamber design. The combustion chamber seems to behave like two sub-systems within a single volume having different optimization characteristics. One way to overcome this issue will be to simplify the combustion chamber design so that fewer engine parameters play a role in engine optimization. The sketch shown in Figure 68 is a proposed combustion chamber design for consideration. In this design the spark plug is located at the center of the combustion chamber. Another important engine parameter is the fuel injector. In the current study an OEM automotive fuel injector was used. In direct injection engines the flow characteristics of the injector nozzle is very important in shaping the combustion behavior. For low power density engines like the one used in this study, an injector with lower flow rate is preferred to alleviate the problem of fuel wall wetting that causes high UHC emissions.

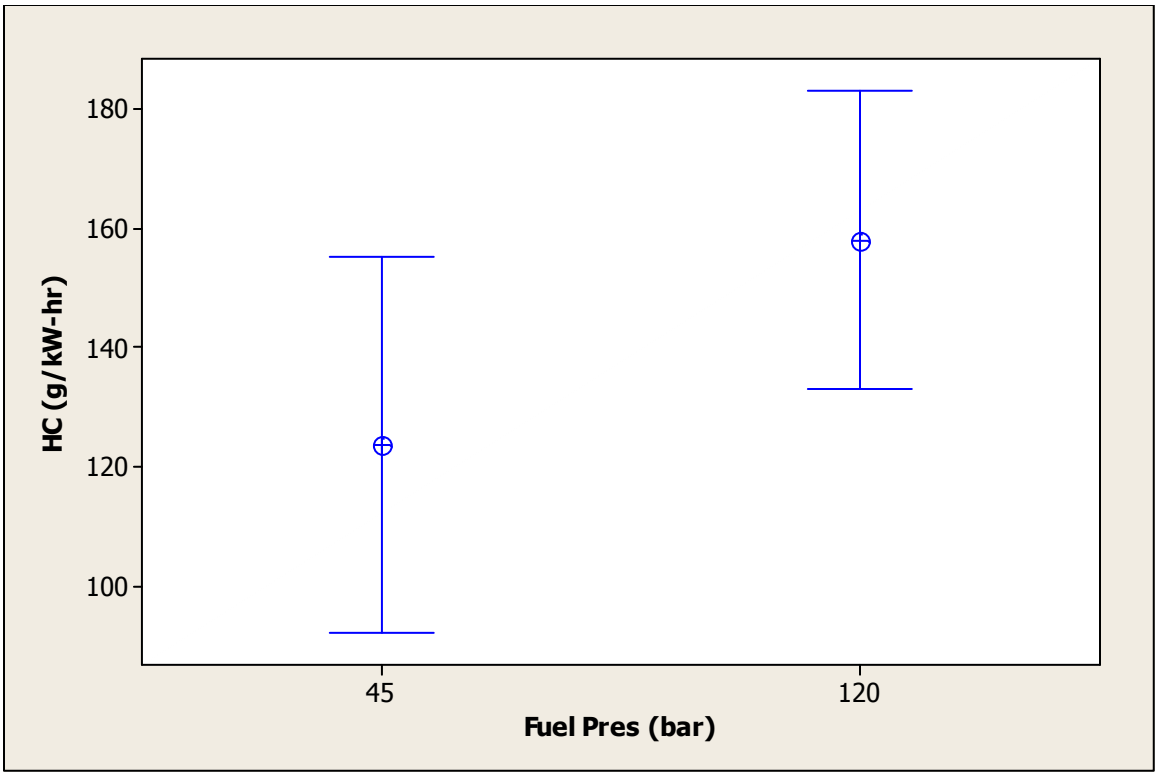

Figure 59: Interval plot of HC vs fuel pressure. Error bars are one standard error from the mean.

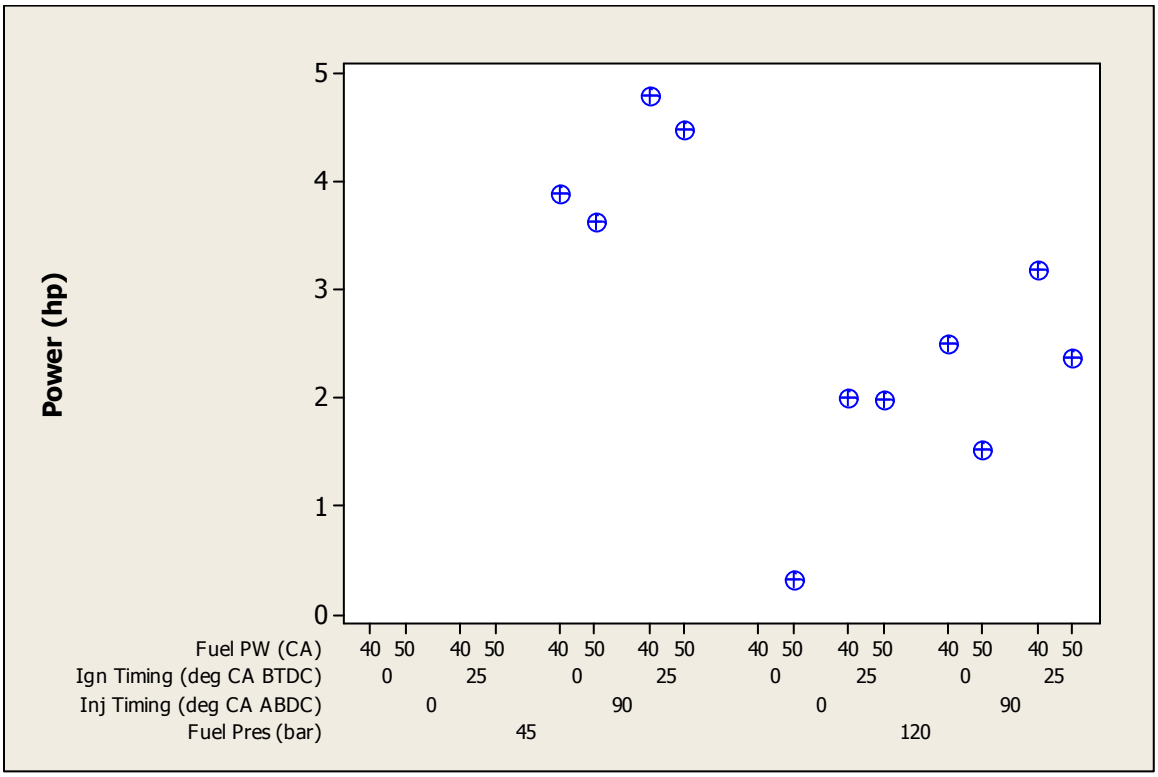

Figure 60: Interval plot of power, injector location over exhaust valve, spark plug location over exhaust valve.

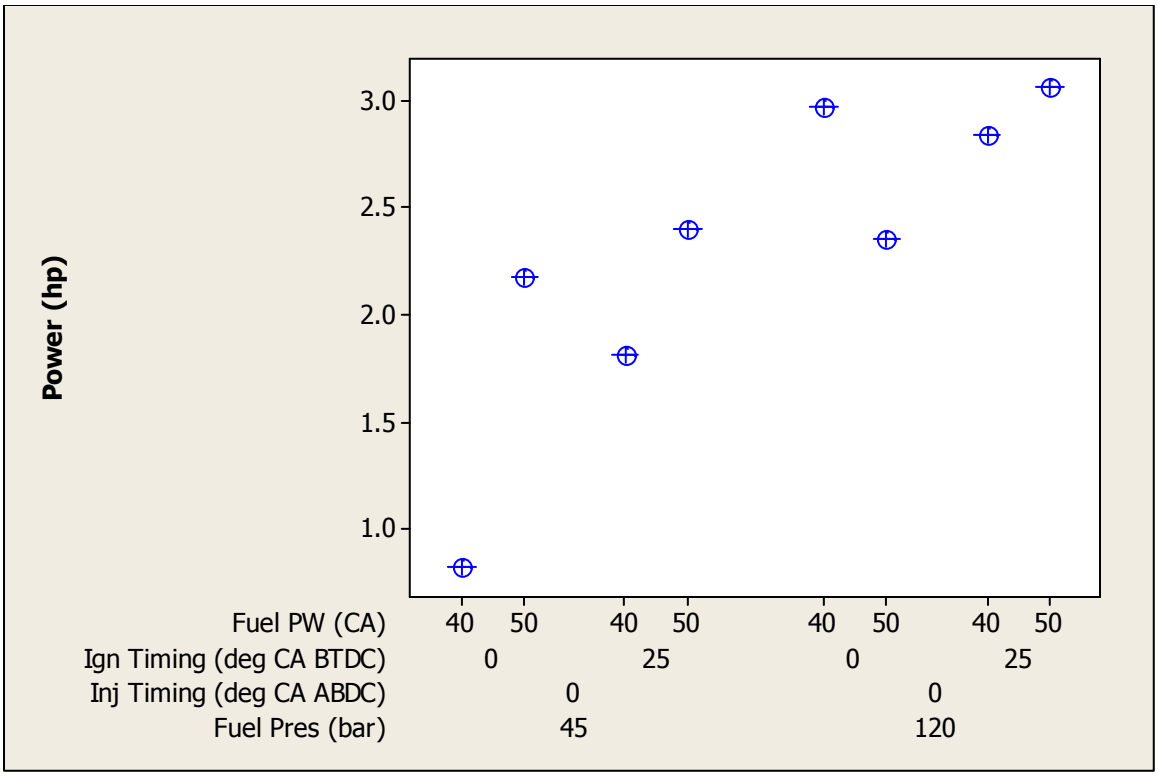

Figure 61: Interval plot of power, injector location over exhaust valve, spark plug location over intake valve.

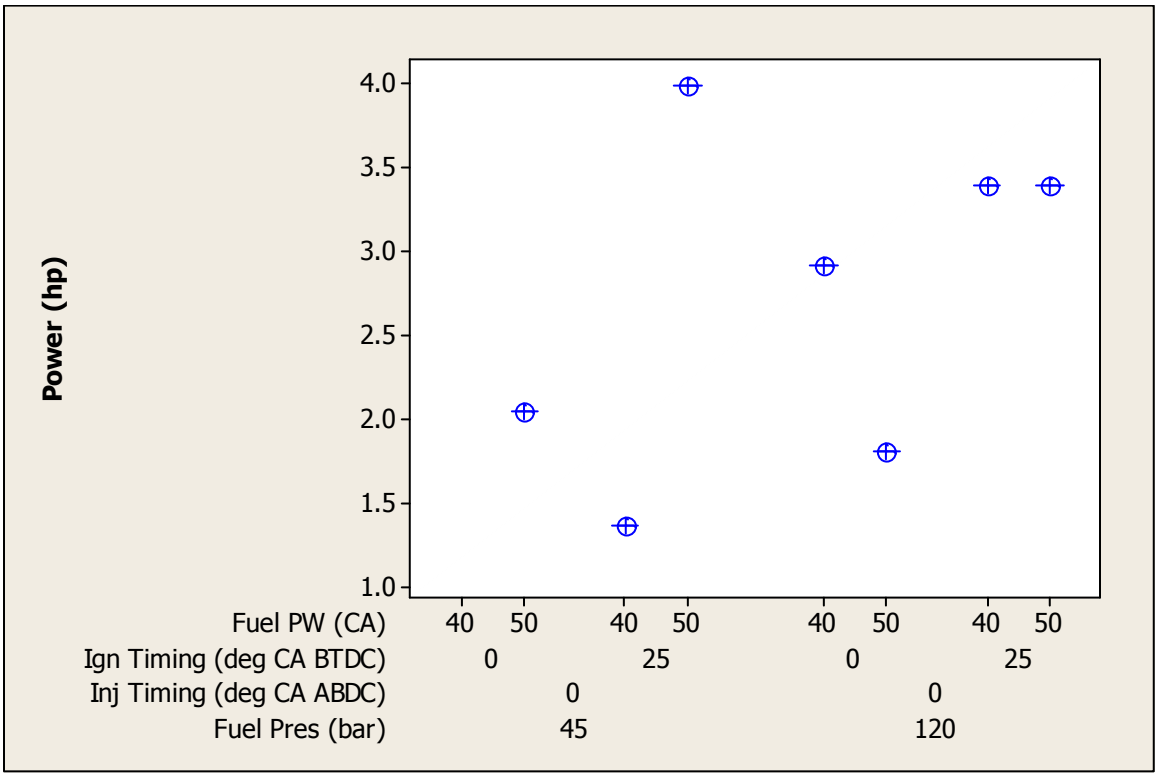

Figure 62: Interval plot of power, injector location over intake valve, spark plug location over exhaust valve.

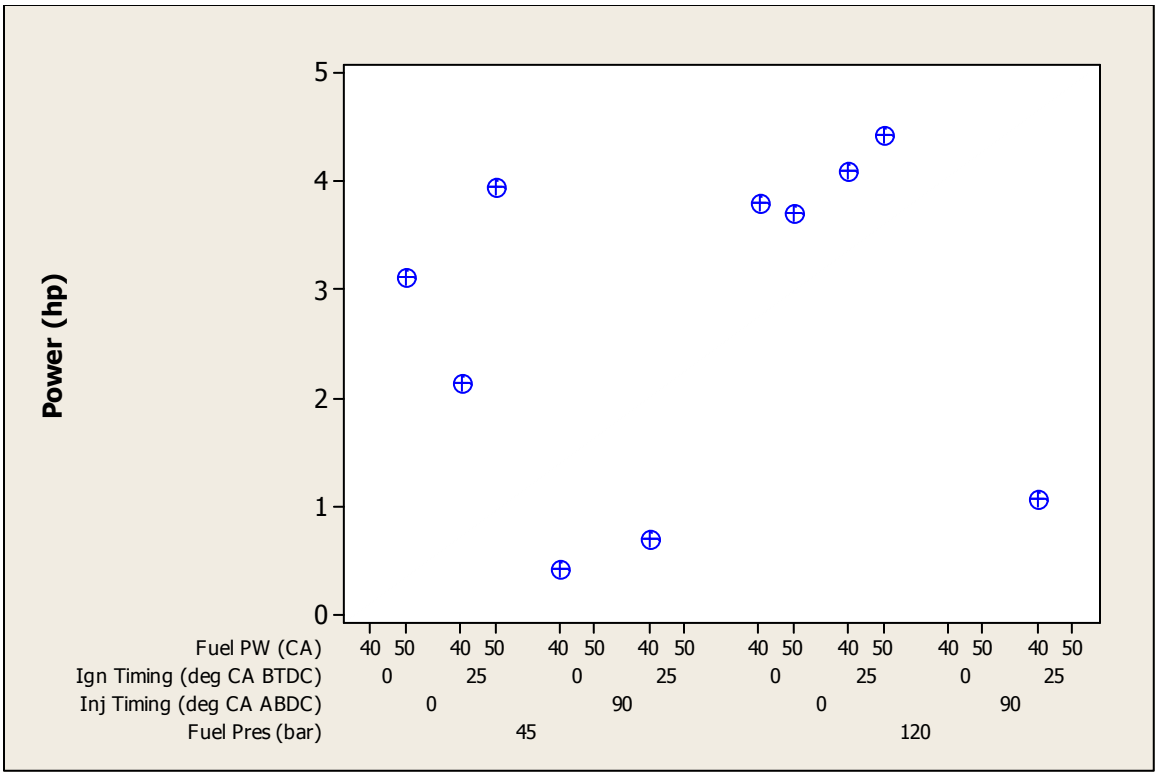

Figure 63: Interval plot of power, injector location over intake valve, spark plug location over intake valve.

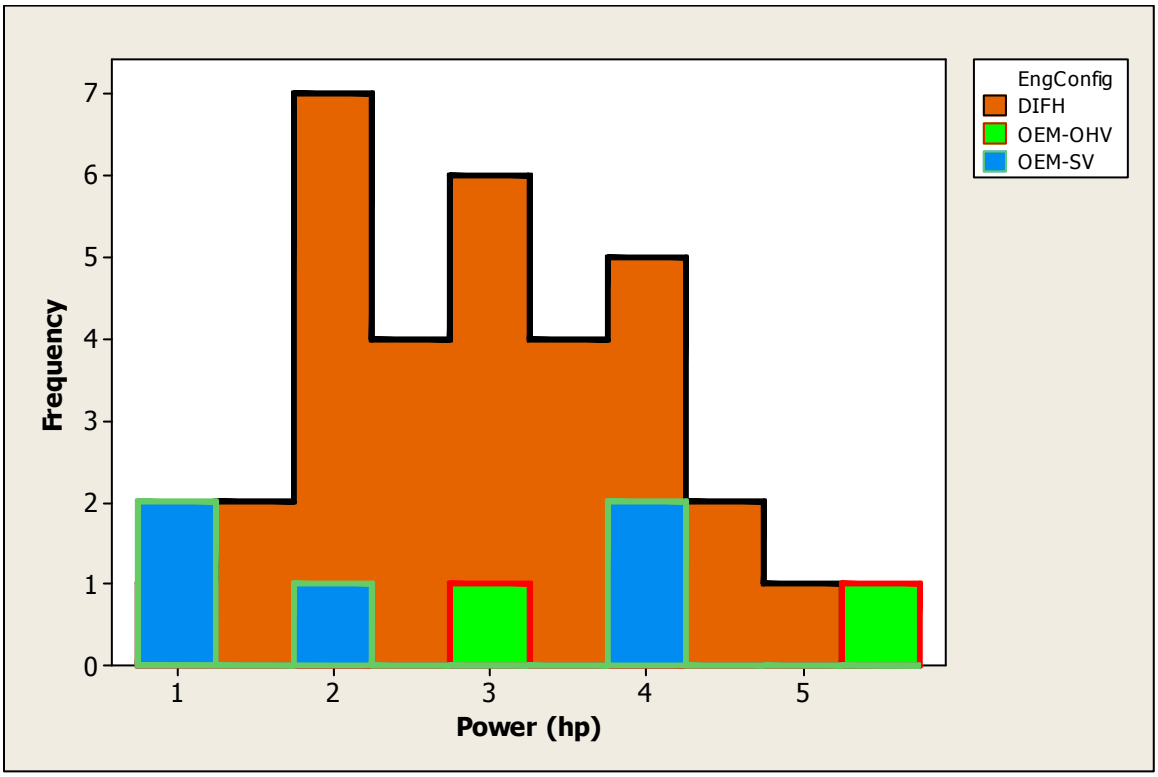

Figure 64: Histogram of power.

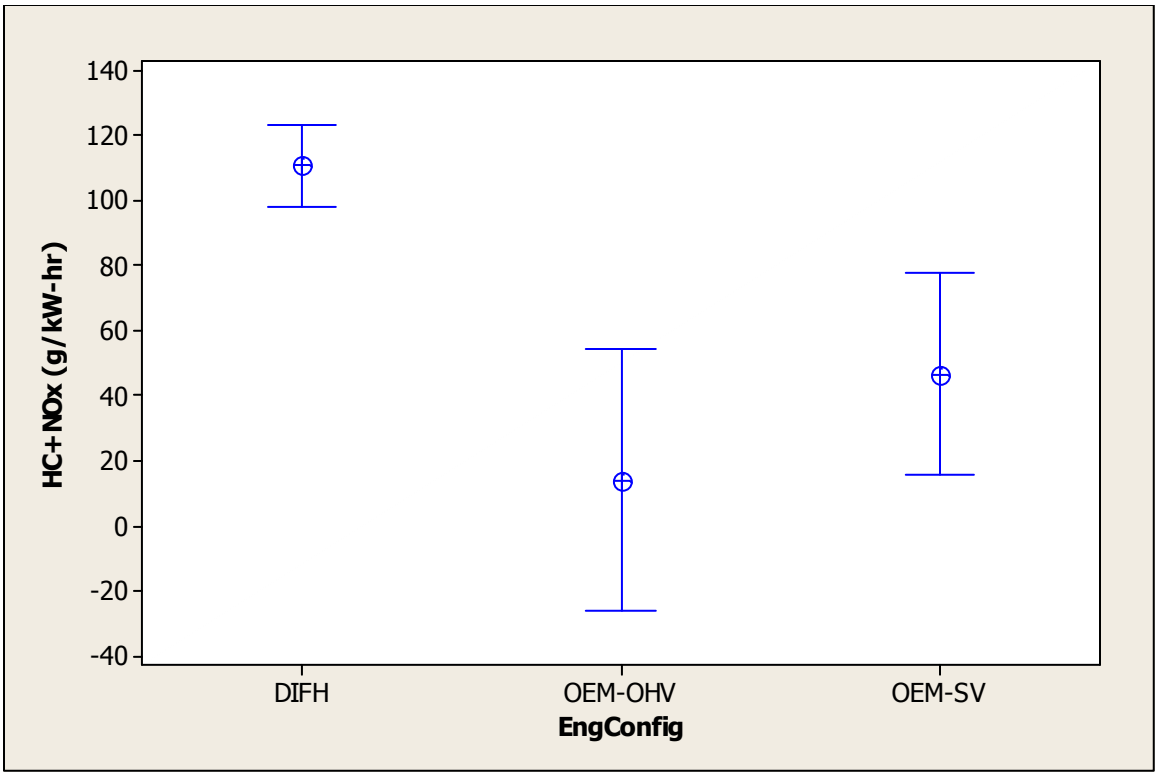

Figure 65: Interval plot of ($HC+NO_x$) vs engine configuration, optimized at modes 3, 4, and 5 power levels. Error bars are one standard error from the mean.

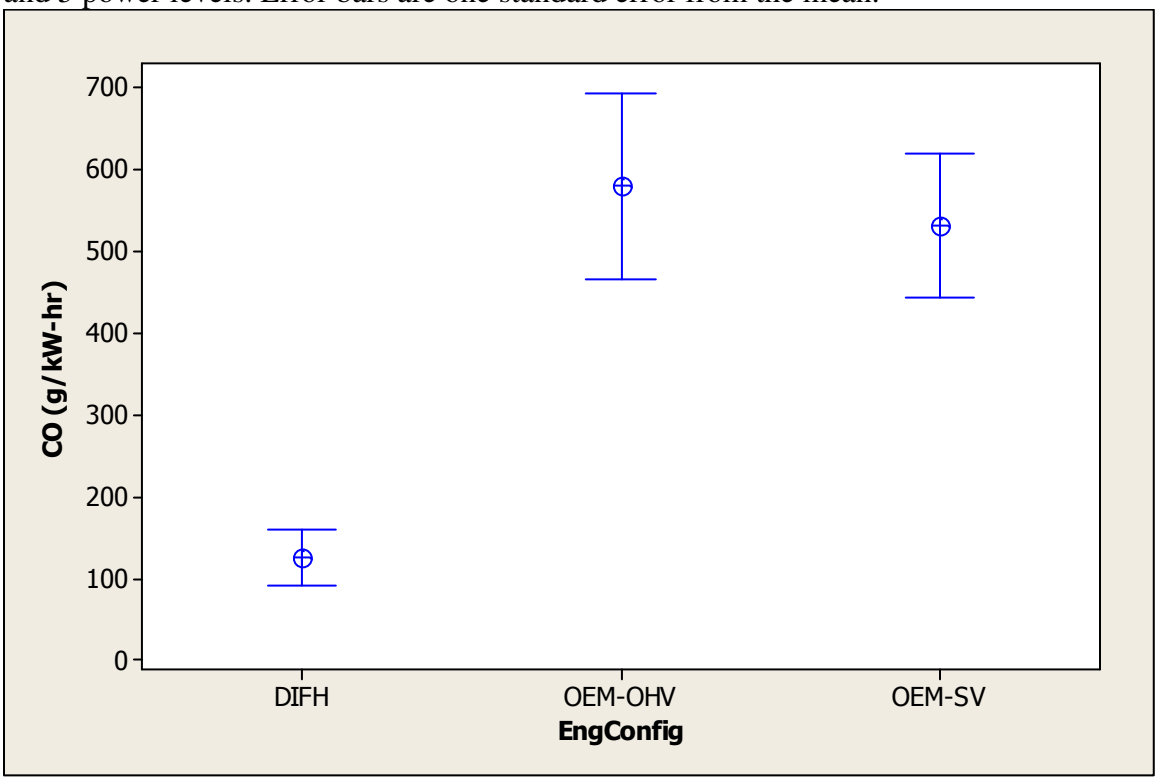

Figure 66: Interval plot of CO vs engine configuration, optimized at modes 3, 4, and 5 power levels. Error bars are one standard error from the mean.

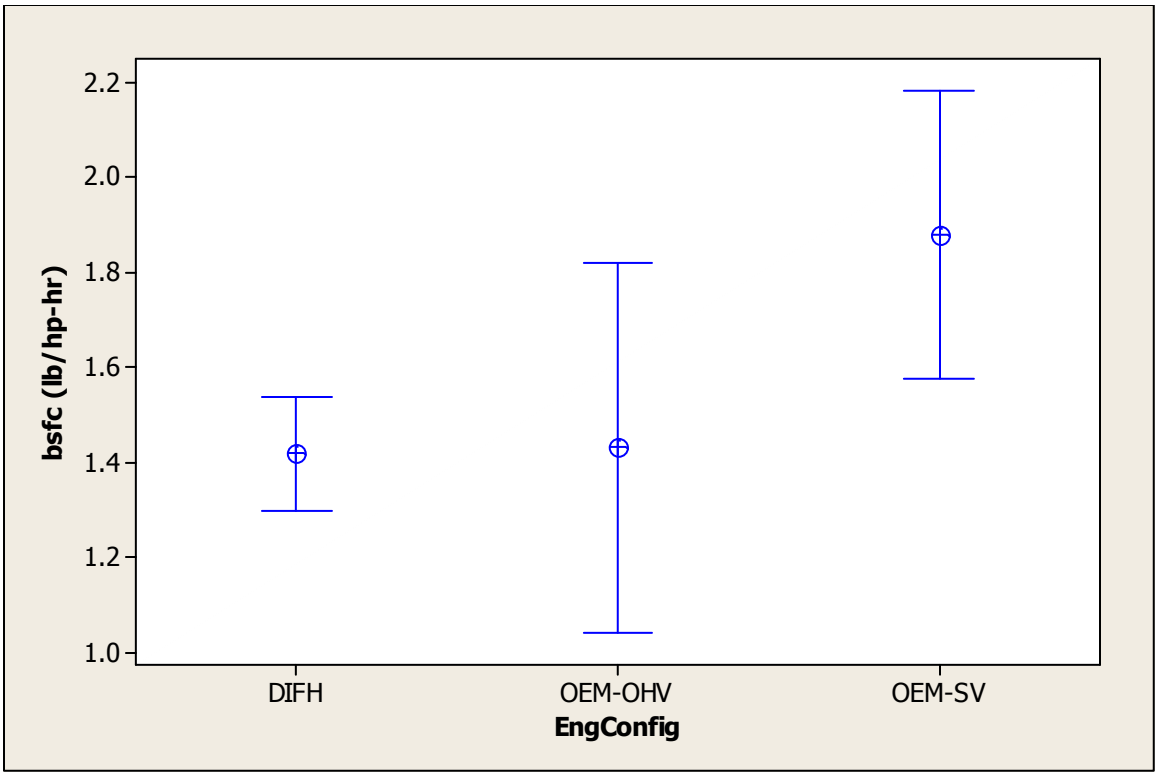

Figure 67: Interval plot of bsfc vs engine configuration, optimized at modes 3, 4, and 5 power levels. Error bars are one standard error from the mean.

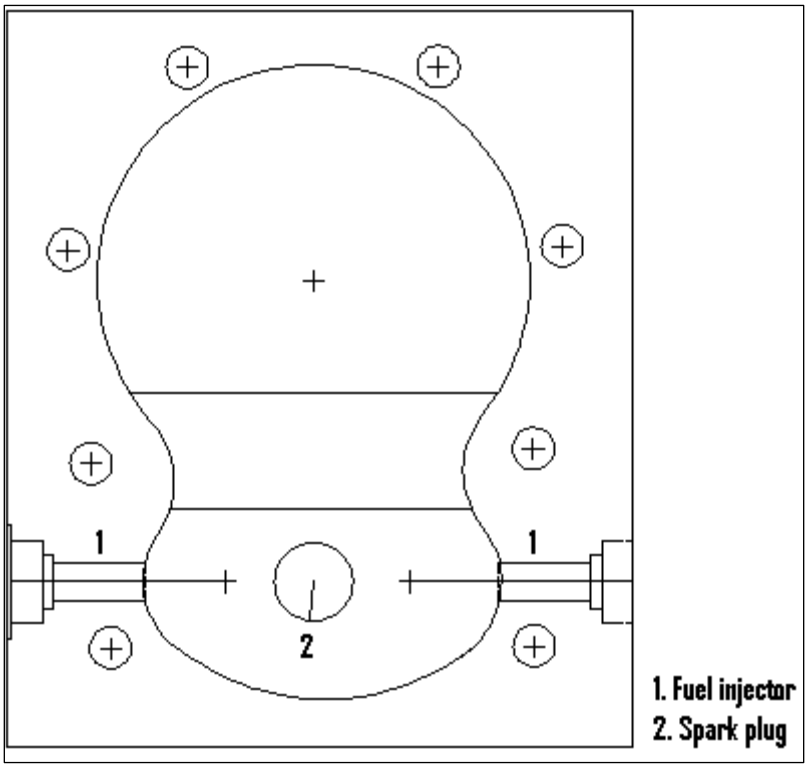

Figure 68: Proposed DIFH combustion chamber design.

Conclusion

A novel concept of a direct gasoline injection in flat head engine has been proposed. The engine could be successfully operated under power, and performance measurements were made to compare the performance of the DIFH engine to that of conventional spark ignited OHV engines. The findings of the study are summarized as follows.

- The DIFH engine concept offers more flexibility in the placement of the fuel injector and the spark plug, which are the key engine performance parameters.

This flexibility of hardware optimization is limited in conventional OHV GDI engines.

- PIV studies of in-cylinder air motion show that squish generated by the moving piston towards TDC in the compression stroke is the primary source of energy for developing the swirling mean air motion in the combustion chamber.
- A general full factorial DOE with seven factors was designed to investigate engine performance. The maximum power produced by the DIFH engine was about 4.8 hp at an improved bsfc of 0.62 lb/hp-hr compared to an OEM OHV engine of comparable displacement making 5.4 hp at a bsfc of 0.74 lb/hp-hr.
- The stock combustion chamber of the DIFH engine provided evidence that when both the fuel injector and the spark plug are located on the exhaust valve side of the combustion chamber; the engine performance was dependent on charge stratification. When the fuel injector and the spark plug are located on the intake valve side of the combustion chamber, the engine showed stronger performance when more time was allowed between fuel injection and ignition for the fuel and air to mix more homogeneously.
- The DIFH engine produces about eight times more brake specific ($HC+NO_x$) emissions than the OEM OHV engine and about 2.5 times more than that of the OEM SV engine, at the same power levels.
- The brake specific CO emissions of a DIFH engine are about 4.7 times lower than those of the OEM OHV engine and about 4.3 times lower than those of the OEM SV engine.

- The higher UHC emission of the DIFH engine is attributed to the poor combustion chamber design that causes complex interactions between key engine performance parameters. A combustion chamber design is proposed with a central location of the spark plug to promote better flame engulfment of the fuel-air mixture.

CHAPTER 5

SUMMARY AND CONCLUSIONS

Overview

Newer stringent emissions regulations are aimed at not only on-highway applications of IC engines but also off-highway applications. Application of expensive after treatment devices is one way to address the issue of reducing engine out emissions especially from non road small engines. Lean combustion strategies are also viable emissions reduction options. Lean combustion as applied to a small OHV SI engine used in utility devices is one part of the research. The other part proposes and investigates a novel engine design based on direct gasoline injection to obtain lean combustion.

Summary

Chapter 2 explores the possibility of applying lean combustion to small SI engines to reduce engine out emissions. Within the scope of study, spark plug related parameters, fuel injection system and air-fuel ratio strategies were identified as subjects of investigation to study cyclic variability in combustion and reduce emissions. J type spark plugs with two different electrode thicknesses of 2.5mm and 0.4mm and three different spark gaps of 0.5mm, 0.75mm and 1.0mm were used as ignition system parameters in the experimentation. The voltage and current during spark discharge were measured to calculate the ignition energy delivered to the spark plug. The carburetor was replaced

with a fuel injection system controlled by an engine management system. Two different fuel injectors were tested, one with a low flow characteristics and the other with a higher flow. The operating points of the engine for the experimentation were identified as per the EPA phase III B-cycle test procedure. The leanest AFR at each engine operating point was identified within the limits of COV of torque as compared to the baseline engine performance. The main findings showed that the spark discharge energy had a major influence on the engine performance. By the use of fuel injection it is possible to operate the engine at a very lean AFR at 75% and 50% load while maintaining a high volumetric efficiency. This helped to improve the thermal efficiency of the engine. The results suggest that small engines can be operated at leaner AFR to reduce engine out emissions and minimize the use of expensive after treatment devices.

Chapter 3 presents a novel engine design based on a direct fuel injected flat head (DIFH) engine. The main attributes of this design are simplicity in design, lower manufacturing costs and lower engine weight and height. Since the fuel spray has minimal direct contact with the cylinder liner in a DIFH engine as opposed to that in a conventional OHV GDI engine, the problem of engine lubricating oil contamination with gasoline can be reduced, which is another important characteristic of the DIFH engine.

The results of the DIFH engine performance is discussed in chapter 4. The DIFH combustion chamber was adopted from a stock Briggs & Stratton SV engine platform. The current combustion chamber had a twin pocket design, one over the intake valve and the other over the exhaust valve. This design caused complex interactions between key engine performance parameters. With the fuel injector and the spark plug both located on the exhaust valve side, the engine performance showed evidence of stratified charge

combustion, whereas, with the fuel injector and spark plug both located on the intake valve side the engine performance was strong when allowing more fuel-air mixing to occur. The performance of the DIFH engine was severely knocking limited at higher loads and produced very high levels of UHC emissions at all engine operating points although, the CO emissions were lower than both the OEM OHV and OEM SV engines. The DIFH engine also showed lower brake specific fuel consumption values when compared to both the OEM engine platforms. The problem of engine knocking and high UHC emissions was attributed to the stock combustion chamber design. A new combustion chamber design is proposed that is aimed at reducing the interactions between the key engine parameters.

Conclusions

This central theme of this research was based on lean combustion strategies to reduce engine out emissions. Chapter 2 is based on engine experimentations carried out on a OHV small engine whereas, chapter 4 investigates the performance of the DIFH engine design proposed in chapter 3. The specific conclusions from chapter 2 are summarized below;

- Minimum ignition energy requirements depend on the spark plug type. Although only one type of ignition system (TCI) was used in the current study, it was evident that thicker electrode spark plug had higher minimum energy requirements as compared to thin electrode spark plug.
- The COV of torque varied significantly as a function of spark plug electrode diameter. The thick electrode spark plug had a higher variation in COV of torque as a function of electrode gap than the thin electrode spark plug. Both types of

spark plug showed lower COV of torque at 0.75 mm electrode gap as compared to 0.5 mm and 1.0 mm electrode gap.

- The minimum ignition energy is a function of the gas pressure as verified by the decreasing ignition energy requirements with decreasing engine load for both spark plug types.
- The 0-10% burn duration increases with decreasing load, increasing the COV of torque and suggesting that initiating a stable flame gets more difficult with decreasing charge density.
- Although the burn duration for complete combustion increases with increasing AFR, it is still possible to achieve an acceptable COV of torque at higher engine loads by increasing the volumetric efficiency of the engine.
- Charge stratification can be achieved by injecting fuel over a shorter crank angle duration with the help of high flow fuel injectors. Although no effect was noticed on the 0-10% burn duration, a significant reduction in the 10-90% burn duration was observed, indicating a faster burn cycle. This also translated into a reduction of COV of torque.
- An engine derating strategy was applied in which mode 1 power (highest load) was reduced by about 9.5%. By doing this the engine could be operated at lower AFR as compared to baseline engine configuration at mode 1. With this approach not only the cylinder head temperature could be controlled within limits while running at higher AFR, but also the engine-out CO emissions were reduced by 85% at mode 1.

- An engine operation optimization study showed that EPA phase III limits of 8.0 g/kW-hr for ($HC+NO_x$) for class II small non-road engines can be achieved without the use of catalytic converters to reduce engine-out emissions. It was also shown that a reduction of about 97% in engine-out CO can be achieved with the application of a lean strategy and an overall fuel economy gain of about 6% can be obtained.

The conclusions drawn from the DIFH engine study in chapter 4 are as listed below;

- The DIFH engine concept offers more flexibility in the placement of the fuel injector and the spark plug which are the key engine performance parameters. This flexibility of hardware optimization is limited in conventional OHV GDI engines.
- PIV studies of in-cylinder air motion show that squish generated by the moving piston towards TDC in the compression stroke is the primary source of energy for developing the swirling mean air motion in the combustion chamber.
- A general full factorial DOE with seven factors was designed to investigate engine performance. The maximum power produced by the DIFH engine was about 4.8 hp at a bsfc of 0.62 lb/hp-hr compared to that of an OEM OHV engine of comparable displacement making 5.4 hp at a bsfc of 0.74 lb/hp-hr.
- The stock combustion chamber of the DIFH engine provided evidence that when both, the fuel injector and the spark plug are located on the exhaust valve side of the combustion chamber; the engine performance was dependent on charge stratification. When the fuel injector and the spark plug are located on the intake valve side of the combustion chamber, the engine showed stronger performance

when more time was allowed between fuel injection and ignition for the fuel and air to mix more homogeneously.

- The DIFH engine produces about 8 times more brake specific HC+(NOx) emissions than the OEM OHV engine and about 2.5 times more than that of the OEM SV engine, at the same power levels.
- The brake specific CO emissions of a DIFH engine is about 4.7 times lower than that of the OEM OHV engine and about 4.3 times lower than that of the OEM SV engine.
- The higher UHC emissions of the DIFH engine is attributed to the poor combustion chamber design that causes complex interactions between key engine performance parameters. A combustion chamber design is proposed with central location of the spark plug to promote better flame engulfment of the fuel-air mixture.

Future Work

The experimentations conducted in chapter 2 have shown the practical feasibility of application of lean combustion to small engines. It is worthwhile to carry out more experimentation to further optimize the engine performance for reduced engine out emissions with the following recommendations;

- Conduct ignition system studies with higher energy ignition systems and multispark capabilities on engine performance especially at low load lean engine operation.
- Conduct a study of effect of fuel injector flow characteristics on charge stratification and combustion duration at all engine operating loads.

The high engine out UHC emissions is the biggest disadvantage of the DIFH engine that prevents it from being a viable alternative to conventional OHV GDI engines. Further work needs to be done to alleviate this issue. The following recommendations are made for further investigations;

- Conduct experimentation with the proposed combustion chamber design with central spark plug location, as shown in figure 66.
- Conduct optimization studies of the fan spray fuel injector to determine the optimum nozzle cup flow and fuel injection pressure to reduce engine out UHC emissions.
- Conduct a valve optimization study to maximize the expansion ratio during the power stroke of the DIFH engine to maximize work output.
- Explore the possibility of the use of an oxidation catalyst to reduce engine out UHC emissions.

References

1. http://www.econogics.com/en/smallpol.htm

2. Ozdor, N. et al., Cyclic variability in spark ignition engines-A literature survey, SAE 940987.

3. Heywood, J. B., Internal Combustion Engine Fundamentals, McGraw-Hill, 1988.

4. Sher, E., Hacohen, Y., Ignition delay and combustion duration in H_2 enriched gasoline engines, Combust. Sci. and Tech., vol 65, pp 263-275, 1989.

5. Maly, R. R., and Vogel, M., Initiation and propagation of flame fronts in lean CH_4-Air mixtures by the three modes of the ignition spark, Seventeen symposium (international) on combustion, The combustion institute, pp 821-831, (1978).

6. Shen, E. and Jiang, D., Investigation on the flame initiation and early development in a spark ignition engine, SAE 922239.

7. Kalghatgi, G.T., Spark ignition, early flame development and cyclic variation in I.C. engines, SAE 870163.

8. Bianco, Y., et al., The effect of initial flame kernel conditions on the flame development in SI engines, SAE 912402.

9. Tagalian, J. and Heywood, J. B., Flame initiation in a spark ignition engine, Combustion and flame, vol. 64, pp 243-246, 1986.

10. Poulos, S. G., The effect of combustion chamber geometry on S.I. engine combustion rates : a modeling study, Masters Thesis, 1980.

11. Young, M. B., Cyclic dispersion in the homogeneous charge spark ignition engine-A literature survey, SAE 810020.

12. Heywood, J. B. and Vilchis, F. R., Comparison of flame development in a spark ignition engine fueled with propane and hydrogen, Comb. Sci. and Tech., vol. 38, pp 313-324, 1984.

13. Matsui, K., et al., Measurement of local mixture strength at the spark gap of S.I. engines, SAE 790483.

14. Sher, E., and Keck, J. C., Spark ignition of combustible gas mixture, Combustion and flame, vol. 66, pp 17-25, 1986.

15. Kalghatgi, G. T., Early flame development in a spark ignition engine, Combustion and flame, vol. 60, pp 299-308, 1985.

16. Patterson, D. J., Pressure variations, A fundamental combustion problem, SAE 660129.

17. Matthes, W.R. and McGill, R.N., Effects of the degree of fuel atomization on single cylinder engine performance, SAE 760117.

18. Hamal, K., et al. Combustion fluctuation mechanism involving cycle to cycle spark ignition variation due to flow motion in SI engines, 21st symposium (International) on combustion, 1986.

19. Johansson, B., Influence of the velocity near the spark plug on early flame development, SAE 930481.

20. Namazian, M., et al., Schlieren visualization of the flow and density fields in the cylinder of a spark ignition engine, SAE 800044.

21. Pischinger, S., and Heywood, J. B., How heat losses to the spark plug affect flame kernel development in an SI engine, SAE 900012.

22. Peters, N., Laminar flamelet concepts in turbulent combustion, 21st symposium (international) on combustion, Combustion Institute, 1986.

23. Viswanath R. K., et al., Examination of laminar-flamelet concept using vortex/flame interactions, Proceedings of the combustion institute, Article in Press.

24. Meneveau, C. and Poinsot, T., Stretching and quenching of flamelets in premixed turbulent combustion, Combustion flame, 86, pp 311-332, 1991.

25. Ho, C. M., and Santavicca, D. A., Turbulence effects on early flame kernel growth, SAE 872100.

26. Witze, P. O., et al., Conditionally sampled velocity and turbulence measurements in a spark ignition engine, Combustion science and technology, vol. 36, pp 301-317, 1984.

27. Pundir, B. P., et al., Effect of charge non-homogeneity on cycle-by-cycle variation in combustion in SI engines, SAE 810774.

28. Whitelaw, J. H., and Xu, H. M., Cyclic variations in a lean-burn spark ignition engine without and with swirl, SAE 950683.

29. Pischinger, S., and Heywood, J.B., A study of flame development and engine performance with breakdown ignition systems in a visualization engine, SAE 880518.

30. Ziegler, G. F. W.,Maly, R.R., Wagner, E. P., Effect of ignition system design on flammability requirements in ultra-lean turbulent mixtures, Combustion in engineering, vol.1, pp 81-92, 1983.

31. Witze, P.O., The effect of spark location on combustion in a variable swirl engine, SAE 820044.

32. Nakamura, M., et al., Multipoint spark ignition for lean combustion, SAE 852092.

33. http://www.cdc.gov/co/faqs.htm#how

34. http://www.scorecard.org/health-effects/references.tcl?short_hazard_name=resp

35. http://mtsu32.mtsu.edu:11233/Smog-Atm1.htm

36. The Effect of Lean Burn on Emission Reduction in a Small Utility 4-Stroke Spark Ignition Engine, SAE 978486.

37. Swamy, K. R. et al., Study and Development of Lean Burn Systems on Small 4-Stroke Gasoline Engines, SAE 2001 01 1801/4222.

38. Yamamoto, H., Investigation on Relationship Between Thermal Efficiency and NO_x Formation in Ultra-Lean Combustion, SAE 1999-01-3328.

39. Wataru, I., Application of Air-Fuel Mixture Injection to Lean-Burn Engines for Small Motorcycles, SAE 2004-32-0052/JSAE 20044339.

40. Bresenham, D., The Effect of High Ethanol Blends on Emissions from Small Utility Engines, SAE 1999-01-3345/JSAE 9938100.

41. Pundir, B. P., Emission Reduction in Small SI Engine Generator Sets, SAE 2004-01-1089.

42. Ayala, F. A., et. al., Effects of combustion phasing, relative air-fuel ratio, compression ratio, and load on SI engine efficiency, SAE 2006-01-0229.

43. Lumley, J. L., Engines an Introduction, Cambridge University Press, 1999.

44. Ziegler, G.E.W., et.al., The influence of spark plug orientation on Flame kernel formation in flowing mixtures, SAE 865031.

45. Lee, M. J., Hall, M., Ezekoye, O. A., and Matthews R., Voltage, and Energy Deposition Characteristics of Spark Ignition Systems, SAE 2005-01-0231.

46. Zhao, F., Harrington, D. L., and Lai, M., Automotive Gasoline-Direct Injection Engines, Society of Automotive Engineers, Inc., Warrendale, PA, 2002.

47. Ricardo, H. R., and Hempson, J. G. G., The High-Speed Internal Combustion Engine, Blackie & Son Limited, London and Glasgow, 2004.

48. Mahato, C., Midkiff, K. C., and Puzinauskas, P. V., Direct Injection Panhead Engine, U.S. Provisional Patent Application Filed February 13, 2007., Serial No. 60/889,678.

49. Srinivasan, K. K., Quantification of in-cylinder flow in a motored four valve spark ignition using two dimensional particle image velocimetry, Masters Thesis, 2002.

50. Bottom, K. E., PIV measurements of in-cylinder flow and correlation with engine performance, PhD dissertation, 2003.

51. Choi, W., and Guezennec, Y. G., Study of the flow field development during the intake stroke in an IC engine using 2-D PIV and 3-D PTV, SAE 1999-01-0957.

52. LAVISION Flow Master product-manual; Item-number: 1105011-4.

53. Raffel, M., et. al., Particle Image Velocimetry- A Practical Guide, Springer-Verlag Berlin Heidelberg, 1998.